**UNIVERSITY OF ALBERTA**

# THE ROLE OF RHO GTPASES, RAC1 AND RAC2, IN REGULATING MAST CELL EXOCYTOSIS

BY

ALICIA BAIER

A THESIS SUBMITTED TO THE FACULTY OF GRADUATE STUDIES AND RESEARCH
IN PARTIAL FULFILLMENT OF THE REQUIREMENTS FOR THE DEGREE OF

MASTER OF SCIENCE

CELL BIOLOGY



SPRING 2012
EDMONTON, ALBERTA

**Abstract**

Mast cells are tissue-resident immune cells that undergo exocytosis upon activation, releasing potent immunoregulatory molecules that initiate inflammatory responses. Here, I investigated the role of the hematopoietic specific Rho GTPase, Rac2, and the ubiquitous, Rac1, on mast cell exocytosis. Our hypothesis is that FcεRI-mediated mast cell exocytosis is differentially regulated by Rac1 and Rac2 GTPases. Three experimental systems were used to investigate their roles in mast cell function; Rac2 knockout mice, Rac1 and Rac2 siRNA knockdown, and treatment with the Rac inhibitor, EHT-1864. My results suggest that Rac1 and Rac2 regulate multiple stages of FcεRI-mediated response in mast cells. I found that calcium flux and exocytosis were Rac1 and Rac2-dependent processes. My data suggests that Rac1 and Rac2 regulate exocytosis through a convergent pathway but regulate calcium flux through alternate pathways. Moreover, I found that Rac2 does not regulate actin remodelling, thereby suggesting this may be a Rac1-mediated process.

# TABLE OF CONTENTS

## CHAPTER 2 MATERIALS AND METHODS

**CHAPTER 3 RESULTS**



**CHAPTER 4 DISCUSSION**

## LIST OF TABLES

## LIST OF FIGURES

# CHAPTER 1

# INTRODUCTION

## 1.1 Mast cells

Mast cells are immune cells that are known to amplify adaptive immune responses and they are best known for their pathological roles in initiating inflammatory responses in disease (reviewed in Kalesnikoff and Galli, 2008). Propagation of immunological responses in inflammatory diseases such as asthma and allergic inflammation are triggered by improper activation of mast cells, resulting in the aberrant exocytosis of immunoregulatory molecules (Kitamura, 1989). These effects are elicited through antigen-induced cross linking of IgE-bound FcεRI surface receptors, which initiate a complex signaling cascade (Figure 1.1). Activation of the FcεRI-mediated cascade results in several events; influx of calcium, activation of exocytosis resulting in the release of preformed mediators contained within intracellular granules (referred to as degranulation in immune cells), generation of lipid derived mediators and the synthesis and secretion of cytokines and chemokines (reviewed in Metcalfe et al., 1997).

### 1.1.1 Mast cell biology

Mast cells are tissue-resident and densely granulated immune cells that originate from pluripotential myeloid progenitor cells located in the bone marrow (Kirshenbaum et al., 1991). Unlike other immune cells that are differentiated upon departure from the bone marrow, mast cells remain undifferentiated in the bone marrow and circulate in blood as hematopoietic progenitor mast cell precursors (reviewed in Metcalfe et al., 1997). Mast cells undergo differentiation only upon arrival at specific tissue sites. They subsequently undergo maturation and

specialization of morphological and functional characteristics in response to the growth and differentiation factors present at the resident tissue (reviewed in Metcalfe et al., 1997).

Mast cells typically reside in tissues that interface the external environment, to function as immunological sentinels (Galli et al., 1999). Since mast cells populate a variety of tissues, they exhibit some heterogeneity both in their structure and function (reviewed in Kitamura, 1989; Metcalfe et al. 1997). Two general sub-populations of mast cells exist; connective tissue mast cells (CTMCs) and mucosal mast cells (MMCs). CTMCs reside in tissues such as the epithelium and sub-mucosal and muscle layers of the peritoneal cavity, whereas MMCs reside in tissues of the lung and lamina propria of the intestinal lining (Lee et al., 1985). These two sub-populations of mast cells also exhibit structural and functional differences. CTMCs are 10-20 μm in size, contain 10-20 pg of histamine/cell, do not synthesize leukotriene C4 and are activated by polybasic compounds such as substance-P and compound 48/80 (reviewed in Kitamura, 1989). In contrast, MMCs are 5-10 μm in size, contain 1 pg of histamine/cell, synthesize leukotriene C4 and are not activated by polybasic compounds such as substance-P and compound 48/80 (reviewed in Kitamura, 1989). Both subsets of mast cells are activated via IgE binding of FcεRI and undergo FcεRI-mediated exocytosis, however to different extents.

A defining morphological feature of mast cells is the presence of numerous densely packed granules in the cytoplasm (reviewed in Kitamura, 1989). Activation of mast cells results in the mobilization of granules and

exocytosis of immunoregulatory molecules present in the granules, a process known as degranulation. Mast cell secretory granules are more accurately classified as secretory lysosomes. Conventional secretory cells possess two distinct organelles for degradation and storage of proteins, lysosomes and secretory granules, respectively. However, cells of hematopoietic origin possess one organelle with dual function, the secretory lysosome, which is a lysosome that is capable of storage and regulated exocytosis (Blott and Griffiths, 2002).

Secretory lysosomes of mast cells contain hydrolases (mast cell protease, tryptases and β-hexosaminidase) and membrane proteins (LAMP -1, LAMP-2 and CD63) that are highly characteristic of lysosomes (Metcalfe et al., 1997; Puri and Roche, 2008; Williams et al., 1999; Grutzkau et al., 2004; Williams and Web; 2000), in addition to a diverse array of pro-inflammatory molecules (histamine, heparin, chondroitin sulphate E and serotonin) (Metcalfe et al., 1997). Mast cell secretory lysosomes are fully functional in that they actively degrade proteins in addition to storing newly synthesized immunoregulatory molecules. Exocytosis of secretory lysosomes is highly regulated and requires the typical components of exocytic machinery such as SNAREs and Rabs (reviewed in Blott and Griffiths, 2002). Regulation of mast cell exocytosis is further reviewed in ***Section 1.2***.

Mast cell granule composition has been shown to exhibit heterogeneity between animal cells (human vs. mouse vs. rat), degree of maturity (immature vs. mature), mast cell sub-populations (CTMCs vs MMCs) and site of tissue residence (reviewed in Kitamura, 1989). Moreover, individual mast cells also exhibit heterogeneity as there are several subsets of granules that contain different

mediators (Puri and Roche, 2008; Williams et al., 1999; Grutzkau et al., 2004; Vincent-Schneider et al., 2001; Hibi et al., 2000; Williams and Web; 2000).

### 1.1.2 Mast Cell Function

**Biological function**

The specialized location of mast cells in tissues at the interface of the external environment is important for their role as the primary immune cells that initiate immune responses. Mast cells express a variety of cell-surface receptors that can be activated by an array of ligands, resulting in the synthesis and secretion of a multitude of immunoregulatory molecules that in turn can activate numerous different cell types. A growing body of literature suggests that the biological functions of mast cells contribute to the regulation of numerous immunological and physiological processes. Mast cells contribute to acquired immunity (Kambayashi et al., 2008; Gaudenzio et al., 2009), innate immunity (Marshall et al.,2004; Galli et al., 1999) and wound healing (Noli and Miolo, 2001).

**Pathological function**

Propagation of immunological responses in inflammatory diseases such as asthma and allergic inflammation are triggered by improper activation of mast cells resulting in the aberrant exocytosis of immunoregulatory molecules (Kitamura, 1989). These effects are elicited through antigen-induced cross linking of IgE-bound FcεRI surface receptors, which initiate a complex signaling

cascade (Figure 1.1), that culminates in exocytosis and the secretion of immunoregulatory molecules.

Activation of the FcεRI-mediated cascade results in a bi-phasic response. The early initiation phase occurs in seconds to minutes after activation and the late phase occurs hours after activation (reviewed in Metcalfe et al., 1997). The early initiation phase is characterized by the influx of extracellular calcium and secretion of preformed mediators contained within intracellular granules (e.g. histamine, heparin, chondroitin sulphate E and mast cell protease) (Metcalfe et al., 1997). These early events result in localized physiological changes in the surrounding vascular tissue, such as vasodilation and smooth muscle constriction, thereby increasing vascular permeability and flow of circulating immune cells to the site of activation (Stevens and Austen, 1989). The late phase response is characterized by the generation of lipid derived mediators (e.g. leukotrienes and prostaglandin $D_2$) and the synthesis and secretion of cytokines and chemokines (e.g. TNF-α, IFN-γ, IL-1, IL-3, IL-4, IL-5, IL-6, IL-10, IL-13) (Kalensikoff and Galli, 2008; Metcalfe et al., 1997). These late events result in the recruitment of other immune cells to the site of activation (Tsicopoulos et al., 1994) and extravascular fibrin deposition (Mekori et al., 1990).

### 1.1.3 Mast Cell Activation

Mast cells can be activated through FcεRI-dependent and FcεRI-independent pathways, which often result in differential release of immune mediators based on the activating substance or ligand.

**FcεRI-dependent**

FcεRI is the primary receptor on mast cells responsible for granule exocytosis upon antigen challenge. FcεRI is a trimeric protein composed of an α chain, which is responsible for binding IgE with high affinity, a membrane tetra-spanning β chain, which amplifies receptor signaling via immunoreceptor tyrosine-based activation motifs (ITAMs), and a γ chain, which provides the receptor with its signaling competence via disulfide-linked homodimers of the ITAMs (Blank et al., 1989, Blank and Rivera, 2004). IgE binding to FcεRI, sensitizes the mast cell. Cross-linking of IgE-bound FcεRI receptors by specific antigen initiates the signaling cascade which culminates in exocytosis of granules (Pfeiffer et al. 1985; Kinet, 1999).

**FcεRI- independent**

In addition to the expression of the FcεRI receptor, mast cells also express several surface receptors that can be activated by an array of small molecule ligands and pro-inflammatory molecules. Additional mast cell receptors include c-kit receptors, complement receptors, TLRs, and G-protein coupled receptors (GPCRs) which, upon activation, generate distinct responses that are specific to the receptor activated. Stem cell factor (SCF) is a ligand that binds to and activates the c-kit (CD117) receptor to regulate proliferation and survival pathways in addition to exocytosis and transcription in mast cells (Kitamura et al., 1989; Gu et al., 2002; Yang et al., 2000). Complement fragments C3a, C4a and C5a are locally produced upon activation of the complement system, which is part of the innate immune system. These complement fragments then bind to and

activate specific mast cell complement receptors resulting in an anaphylactic response (reviewed in Erdei et al., 2004).

Mast cells also express toll-like receptors (TLRs), which are activated by pathogenic ligands of viruses, bacteria or fungi. Activation of the TLRs results in secretion of lipid mediators and transcriptional activation of inflammatory cytokines and chemokines (reviewed in Marshall, 2004). Polybasic molecules such as substance-P and compound 48/80 also activate mast cells (Lagunoff et al., 1983). While there have been no specific receptors identified for these proteins, it is suspected that they activate mast cells by either acting in a non-specific manner on existing receptors or through GPCRs. Regardless of the mechanism, it is known that these substances elicit exocytosis in mast cells (Repke and Beinert, 1987).

### 1.1.4 FcεRI signaling pathway

The FcεRI signaling pathway regulates a multitude of physiological responses in mast cells (Figure 1.1). Numerous studies over the last few decades have investigated the regulatory mechanisms of the FcεRI signaling pathway in mast cells. Our most current understanding of the FcεRI signaling pathway is depicted in Figure 1.1 (Kalensikoff and Galli 2008; Blank and Rivera 2004). FcεRI crosslinking by antigen aggregates receptors and induces cross-phosphorylation of ITAMs encoded in the γ and β chains via Lyn kinase. Phosphorylated ITAMs recruit and activate several key signaling molecules, such as Fyn and Syk kinases. Syk activation recruits and promotes the formation of the

LAT adaptor protein signaling complex, composed of several key molecules on the plasma membrane. PLC-γ is recruited to this signaling complex and is subsequently activated to cleave phosphatidylinositol-4,5-bisphosphate (PIP2) to produce inositol triphosphate (IP3) and diacylglycerol (DAG). IP3 binds to receptors on the ER membrane to induce calcium flux from ER stores. Upon depletion of calcium from ER stores, prolonged calcium flux can be induced through plasma membrane calcium release-activated calcium (CRAC) channels. PKC is activated by both DAG and calcium resulting in the regulation of exocytosis through an unknown mechanism. Concurrently, Rac is activated by the GEF Vav, which is also a component of the LAT adaptor signaling complex. Rac then activates signaling molecules that may be involved in transcriptional regulation, exocytosis and calcium mobilization (Gu et al., 2002; Song et al., 1999; Hong-Geller and Cerione, 2000).

**1.2 Mechanism and regulation of exocytosis**

Exocytosis is an essential eukaryotic cellular process, whereby intracellular vesicles are transported to the plasma membrane where they dock and undergo membrane fusion, resulting in the extracellular secretion of vesicle contents. Several regulatory mechanisms are coordinated to drive multiple stages of exocytosis including lipid metabolism, calcium flux, cytoskeletal remodelling and protein-protein interactions (reviewed in Jahn and Sudhof, 1999). F-actin remodelling (de-polymerization and re-polymerization) facilitate several exocytosis steps, from the initial events of vesicular transport to the plasma

membrane, to the final events of membrane fusion of docked granule-plasma membrane complexes (reviewed in Malacombe et al., 2006; Eitzen, 2003; *see* ***Section 1.3***).

The general mechanism for exocytosis is highly conserved and the molecular machinery for many steps has been described. Secretory vesicle formation is initiated at the trans-Golgi where the assembly of coat proteins drives vesicle budding (Chavrier and Goud, 1999). Unique Rab GTPases are incorporated onto vesicle surfaces, which spatially regulate their mobilization along actin cables and target them to the plasma membrane (Zerial and McBride, 2001; Advani et al., 1998). When activated, Rab GTPases recruit effector complexes that tether secretory vesicles/granules to the plasma membrane (Pfeffer, 1999). Once properly tethered, v-SNARE proteins from the docked vesicle and t-SNARE proteins from the plasma membrane are primed by NSF and form trans-SNARE coiled-coil complexes across the two membranes which drives their fusion (Ungermann et al., 1998). Final membrane fusion is triggered by a calcium flux, which stimulates opening and expansion of a fusion pore (Ungermann et al., 1998; Wickner, 2001; Klenchin and Martin, 2000).

Transient increase in intracellular calcium has been shown to be a requirement for multiple stages of exocytosis including signaling cascade activation, granule mobilization, actin rearrangement and the final granule-plasma membrane fusion (Nishizuka, 1995; Mellor and Parker, 1998; Beckers and Balch, 1989; Heidelberger, 1994; Peters and Mayer, 1998; Baram et al., 2001). The exact mechanism by which calcium regulates these events is still debated. Intracellular

calcium influx has been shown to regulate multiple aspects of the fusion machinery. Synaptotagmins are membrane bound calcium sensor proteins found on both the plasma membrane and vesicular membranes. Upon binding of calcium, they interact with SNAREs to promote calcium dependent trans-SNARE assembly and membrane fusion (Chapman, 2002; Baram et al., 2001).

Rho GTPases, specifically Rac, RhoA and Cdc42, have been shown to regulate various exocytosis events including actin remodelling, exocytic complex formation and calcium flux across a variety of cell models such as neuroendocrine cells and immune cells (Hong-Geller and Cerione, 2000; Abdel-Latif et al., 2004; Symons and Rusk, 2003; Ory and Gasman, 2011). Although their exact mechanism of regulation may vary between cells, it appears that the Rho GTPases are predominantly responsible for regulating actin remodelling for various stages of the exocytic process (reviewed in Etienne-Manneville and Hall, 2002; Symons and Rusk, 2003; Ory and Gasman, 2011; Eitzen, 2003; *see **Section 1.4** for more detailed information on Rho GTPase function*).

## 1.3 Actin

### 1.3.1 Actin remodelling

Actin remodelling is an essential cellular process that is required for nearly every aspect of cellular organization and function including cell division, cell migration and exocytosis (Pfeiffer et al., 1985). In cells that undergo regulated exocytosis, actin filaments prevent granules from prematurely accessing the plasma membrane during the resting state (Gasman et al., 2004; Ehre et al.,

2005). Upon stimulation, calcium influx and activated Rho GTPases induces F-actin cleavage and the polymerization of new actin filaments which act to translocate granules to the plasma membrane (Giner et al., 2005; Etienne-Manneville and Hall, 2002). Concurrently, depolymerization of the branched actin network at the cell cortex allows granules to access the plasma membrane for the final docking and fusion steps (Norman et al., 1996). Actin polymerization is also required to facilitate the formation of the docking complex that is formed between the granule and the plasma membrane (Ory and Gasman, 2011; Munson and Novick, 2006).

### 1.3.2 Actin modifying proteins

Actin remodelling is regulated by three different subsets of actin modifying proteins: actin-related protein 2/3 (Arp2/3), cofilin and formins (reviewed in Jaffe and Hall, 2005). Arp2/3 binds to the sides of polymerized actin, mediating branched-actin polymerization and is regulated by Cdc42 and Rac GTPase binding of WASP and WAVE, respectively (Millard et al., 2004; Kurisu and Takenawa, 2009). Formins bind to the barbed (growing) end of actin filaments to promote filament elongation and are regulated by Cdc42 and RhoA (Zigmond et al., 2004). Cofilin is regulated by Rac and severs F-actin filaments, which promotes both the formation of uncapped barbed ends as sites for new actin polymerization and filament formation (Ghosh et al., 2004) as well as actin depolymerization (Pollard and Borisy, 2003).

While all three actin modifying proteins are required for actin remodelling, actin polymerization is predominantly regulated by Arp2/3-mediated actin nucleation by creating sites with free barbed ends which act as a nucleation core for de-novo polymerization (reviewed in Campellone and Welch, 2010). The Arp2/3 complex binds to the side of an existing actin filament and together with nucleation promoting factors (NPFs), initiates assembly of a new filament in a branched manner (Goley and Welch, 2006). NPFs can be subdivided into four subgroups, WASP, N-WASP, WASP-family verprolin homologue (WAVE or SCAR) and the WASP and SCAR homologue (WASH) (Campellone and Welch, 2010). The predominant function of the WAVE NFPs is to activate Arp2/3 during plasma membrane protrusion and cell motility. Specifically, WAVE1 has been found to regulate dorsal membrane ruffling and slow migration (Suetsugu et al., 2003), whereas WAVE2 has been found to regulate peripheral membrane ruffling, lamellipodia formation and rapid motility (Yamazaki et al., 2003; Yan et al., 2003). As these actin remodelling events are known to be Rac-mediated, the NFPs WAVE1 and WAVE2 are of particular interest. Whether Rac1 and Rac2 differentially regulate activation of WAVE1 or WAVE2 remains to be elucidated.

### 1.3.3 Actin rich membrane ruffles are indicators of mast cell activation

Receptor activation induces membrane ruffles that are F-actin-dependent transient distortions of the plasma membrane. Several studies have investigated the function of these structures using fibroblast model systems and have found that they contribute to lamellipodia formation (Krueger et al., 2003),

internalization of ligand-bound receptors (Orth et al., 2006) and micropinocytosis (Dowrick et al., 1993). In contrast to work in fibroblasts, the function of membrane ruffles induced by antigen–dependent receptor activation in mast cells remains to be elucidated. Despite the uncertainty in the function attributed to these structures, the formation of membrane ruffles has become an established morphological indicator of a stimulated mast cell (Edgar and Bennett, 1997; Burwen and Satir, 1977; Pfeiffer et al., 1985). Within a mast cell model, it is well documented that exocytosis occurs in parallel with Rho GTPase dependent actin rich membrane ruffle formation, however, exactly how Rho GTPases contribute to this process is not understood.

## 1.4 Function of Rho GTPases

### 1.4.1 Rho GTPase family members

The Rho family of GTPases belong to the Ras superfamily, with RhoA, Cdc42 and Rac. as the best characterized members. Three Rac GTPase paralogs are currently known; Rac1 is ubiquitously expressed (Moll et al., 1991), Rac2 is expressed specifically in cells of hematopoietic origin (Didsbury et al., 1989) and Rac3, the less well understood paralog, is expressed primarily in the brain (Haataja et al., 1997). Rho GTPases act as molecular switches to mediate a multitude of intracellular signaling pathways including transcriptional regulation, cell division, actin remodelling and vesicular transport. Rho GTPases play an integral role in mediating signaling events, owing to their capacity to relay signals to a large array of downstream effectors (Ridley, 2001) and cross-talk with other

Rho GTPases (Ohta et al., 2006; Nimnual et al., 2003). Rho GTPases are best known for their regulation of actin-dependent membrane trafficking events in many cell types (reviewed in Etienne-Manneville and Hall, 2002; Symons and Rusk, 2003; Ory and Gasman, 2011; Eitzen, 2003).

Each Rho GTPase plays a unique role in mediating actin remodelling. RhoA stimulates the formation of stress fibres (Bader et al., 2004; Gasman et al., 1997) and negatively regulates Rac function (Ohta et al., 2006). In contrast, both Cdc42 and Rac are responsible for the formation of branched F-actin structures present in the leading edge of a migrating cell. Cdc42 plays a role in the formation of F-actin rich filopodia at the leading edge (Tapon and Hall, 1997). Additionally, Cdc42 facilitates exocytosis by regulating the formation of F-actin filaments near the plasma membrane (Guillemot et al., 1997; Hong-Geller and Cerione, 2000; Hong-Geller et al., 2001; Gasman et al., 2004). Rac is involved in the regulation of F-actin rich lamellipodia at the leading edge (Tapon and Hall, 1997; Kurokawa et al., 2004) and the formation of dorsal sub-plasma membrane actin rich membrane ruffles (Guillemot et al., 1997). Moreover, Rac is required for exocytosis (Hong-Geller and Cerione, 2000; Hong-Geller et al., 2001; Abdel-Latif et al., 2004).

The clearest evidence that Rho GTPases control vesicular trafficking and exocytosis has come from studies that examine bacterial toxins. For example, the intracellular pathogens *Salmonella*, *Yersinia* and *Leishmania* produce toxins that target Rho GTPases. Pathogens use these toxins to hijack cellular trafficking systems and evade elimination by blocking fusion of the phagocytosed pathogen

with degradative lysosomes (Boettner and Van Aelst, 2002; Brumell and Grinstein, 2004; Lerm et al., 2006; Pujol and Bliska, 2005). Moreover, extracellular pathogens such as *Clostridium* produce toxins (lethal toxin, toxins A and B) that glucosylate Rho proteins and inhibit exocytosis of neurosecretory signaling molecules in neurons, neuroendocrine cells and pancreatic beta cells (Doussau et al., 2000; Gasman et al., 1999; Kowluru et al., 1997).

While GTPases are known to be required for exocytosis and actin remodelling, the mechanisms underlying their regulatory functions in immune cells remains to be fully elucidated. Several studies have begun to elucidate their roles in neutrophils and mast cells (Abdel-Latif et al., 2004, Gu et al., 2002; Yang et al. 2000), however, the function of Rho GTPases in mast cells has been investigated to a much lesser extent.

### 1.4.2 Molecular regulation of Rho GTPases

Rho GTPase function is regulated by cyclical GTP/GDP exchange and hydrolysis, which is mediated by upstream guanine nucleotide exchange factors (GEFs) and GTPase activating proteins (GAPs) (Boguski et al., 1993). GEFs catalyze the exchange of GDP for GTP, thereby promoting Rho GTPase activation via GTP-binding. Conformational change induced by GTP-binding facilitates the interaction with effector proteins, thereby propagating downstream signaling events. GAPs promote GTP hydrolysis, leaving the Rho GTPase in a GDP-bound inactive state, thereby inactivating downstream effector functions. GDIs are a third group of Rho regulatory molecules that inhibit GDP

disassociation, rendering them unavailable to GEFs for GTP exchange. GDIs also extract GTPases from membranes and retain the GTPase in a cytosolic complex, inhibiting it from interacting with membranes. These molecular on/off switches are imperative for regulating the downstream components of the pathways in which the Rho GTPase is involved, and ultimately a broad array of cellular functions at the molecular level (reviewed in Etienne-Manneville and Hall, 2002).

While the general mechanism of Rho GTPase regulation is common to all Rho GTPases, regulatory GEFs and GAPs can either exhibit specificity for a specific Rho GTPase, or broadly regulate several Rho GTPases. For example, Vav1 is capable of binding Rac, RhoA and Cdc42, however it binds with highest affinity to Rac and has only been shown to regulate Rac *in vivo* (Bonnefoy-Bérard et al., 1996; Crespo, 1997; Chrencik et al., 2008). Vav1 is expressed exclusively in cells of hematopoietic origin (Bonnefoy-Bérard et al., 1996) and is required for exocytosis, calcium flux, cytokine production and PLCγ tyrosine phosphorylation in mast cells (Manetz, et al., 2001) in addition to actin polymerization and migration in neutrophils (Kim et al., 2003). Moreover, recent evidence suggests that Vav1 may also regulate Rac2 in neutrophils since it directly interacts with p-Rex1, a Rac2 specific GEF (Lawson et al., 2011). p-Rex1 has been identified as a Rac2-specific GEF in neutrophils, and is required for regulation of F-actin formation (Dong et al., 2005). Interestingly, Vav1 is currently the only Rac specific GEF identified in mast cells. See Table 1.1 for a complete list of known GEFs and GAPs for Rac1 and Rac2 across cell models.

### 1.4.3 Rac1 function in immune cells

Studies in neutrophils have revealed that Rac1 is required for actin-mediated processes vital to immune cell functions. Rac1-deficient neutrophils were defective in migration, actin assembly and inflammatory cell recruitment; however they did not exhibit defective superoxide production (Glogauer et al., 2003). Sun et al. (2004) further suggest that Rac1 is required for migration by specifically regulating chemotactic orientation of the cell, as Rac1 deficient neutrophils exhibited defective orientation towards a stimulus. Rac1 is also important for integrating signals for neutrophil recruitment into the lung tissue during an inflammatory response (Fillipi et al., 2007). Rac1 has been shown to regulate exocytosis and F-actin rich membrane ruffle formation in mast cells. Dominant negative Rac1 mutants (constitutively GDP-bound) exhibited decreased exocytosis, decreased calcium flux and failed to form membrane ruffles under stimulated conditions (Guillemot et al., 1997; Hong-Geller and Cerione, 2000). In contrast, constitutively active (constitutively GTP-bound) Rac1 mutants exhibited enhanced exocytosis and calcium flux (Hong-Geller and Cerione, 2000). Furthermore, Hong-Geller and Cerione (2000) have provided evidence to suggest that Rac1 may regulate components of the FcεRI signaling pathway, such as calcium flux, IP3 formation and PKC activation. However, the findings of Hong-Geller and Cerione (2000) were not fully convincing because expression of dominant negative Rac1 mutants did not correspond with a profound reduction in exocytosis or calcium flux.

### 1.4.4 Rac2 function in immune cells

The Rac2 Rho GTPase is of particular interest in immunological models since Rac2 is expressed exclusively in cells of hematopoietic origin (Didsbury et al., 1989). Utilizing a Rac2 knock-out mouse (Rac2 KO), Rac2 has been found to play a role in T-cell (Li et al., 2000), B-cell (Croker et al., 2002), neutrophil (Abdel-Latif et al., 2004) and mast cell (Gu et al., 2002) function. The specific cellular expression of Rac2 contrasts with the expression profile of Rac1, which is ubiquitously expressed in all cell lineages (Moll et al., 1991).

Rac1 and Rac2 share 92% amino acid sequence identity (Didsbury et al., 1989), with the C-terminus sharing the least sequence identity (Figure 1.2). The prevailing view in the field is that differences in amino acids at the C-terminus are largely responsible for the different intracellular location of Rac1 and Rac2 in neutrophils (Filippi et al., 2004; Magalhaes and Glogauer, 2010). It remains to be determined if differences in amino acids outside the C-terminus are also required for localization. The Rac1 C-terminus (KKRKRK) is more positively charged (+7), and therefore preferentially locates to the more negatively charged membrane such as the plasma membrane. The Rac2 C-terminus (RQQKRA) is less positively charged (+4), and therefore preferentially locates to more intermediately charged membranes such as intracellular granules (Filippi et al., 2004; Magalhaes and Glogauer, 2010). The differential localization of Rac1 and Rac2 to distinct membranes suggests that these GTPases have distinct intracellular roles.

Studies undertaken in neutrophils have suggested that Rac1 and Rac2 have specific roles in receptor-mediated actin remodelling (Sun et al., 2007). Rac2 was predominantly responsible for regulating actin polymerization via free barbed end assembly. Rac2 deficient neutrophils showed abrogated Arp2/3 mediated free-barbed end formation of polymerized actin, whereas Rac1 deficient neutrophils exhibited no significant defects (Sun et al., 2007). Moreover, it was observed that Rac2 was responsible for regulating 60% of the free barbed end assembly, while Rac1 was responsible for 15% (Sun et al., 2007).

Studies in neutrophils have revealed that Rac2 deficiency results in defective actin remodelling and the selective exocytosis of the predominant immunoregulatory granules (primary granules) (Abdel-Latif et al., 2004), drastically reduced F-actin formation and migration in response to stimulus (Li et al., 2002) and reduced NADPH superoxide production. (Glogauer et al., 2003). The specific function of Rac2 in mast cells remains largely uncharacterized. Work from the lab of Dr. D. Williams provides the only evidence to suggest Rac2 plays a role in mast cell function. Yang et al., (2000) demonstrated that Rac2 KO BMMCs exhibited defective c-kit receptor-mediated Akt activation, adhesion, migration and serotonin exocytosis. Moreover, Gu et al., (2002) demonstrated that Rac2 regulates c-kit mediated mast cell protease gene expression and JNK activity in BMMCs. However, the c-kit receptor is only one of several mast cell surface receptors. Signaling via this receptor regulates proliferation and survival pathways through a signal cascade that is distinct from the FcεRI signal cascade. The FcεRI receptor is the predominant receptor for mast cell activation in allergic

and asthmatic responses and plays an important role in mast cell exocytosis, possibly through the regulation of actin remodelling. Therefore, the function of Rac2 in regulating FcεRI-mediated exocytosis in mast cells remains to be elucidated.

### 1.5 Rationale and objectives

Mast cells are tissue-resident immune cells responsible for initiating inflammatory responses. Improper activation of mast cells results in the aberrant release of immunoregulatory molecules, which propagates inflammatory diseases such as asthmatic and allergic disorders. The secretion of immunoregulatory molecules is elicited through antigen-induced cross-linking of IgE-bound receptors, which triggers the exocytosis of pro-inflammatory molecules. Studies in neutrophils have demonstrated different roles for Rho GTPases, Rac1 and Rac2 in the regulation of actin remodelling events during exocytosis (Abdel-Latif et al., 2004; Li et al., 2002 and Sun et al., 2007). However, the function of Rac2 in regulating FcεRI-mediated exocytosis, calcium flux and actin remodelling in mast cells remains to be elucidated. Here, I have investigated the effect of the hematopoietic cell specific Rho GTPase, Rac2, and the highly similar ubiquitous, Rac1, on mast cell exocytosis. Our hypothesis is that FcεRI-mediated signaling transduction events that trigger exocytosis converge through a Rac GTPase-mediated pathway that is differentially regulated by Rac1 and Rac2.

The objective of this study was to determine if Rac1 and Rac2 differentially regulate exocytosis, calcium flux and actin remodelling in mast

cells. To investigate the roles of Rac1 and Rac2 in mast cell exocytosis, three experimental systems were used; a Rac2 knockout mouse, Rac1 and Rac2 siRNA knockdown in the RBL-2H3 mast cell line and the Rac inhibitor, EHT-1864. It was found that Rac1 and Rac2 regulate FcεRI-mediated exocytosis, calcium flux and actin remodelling in BMMC and RBL-2H3 mast cells. Further delineation and characterization of the roles that Rho GTPases Rac1 and Rac2 play in mast cell exocytosis is required to determine the exact mechanism by which they exert their regulation. This will not only increase the understanding of the biological process of exocytosis in mast cells, but also provide useful insight for future studies aimed at targeting regulatory molecules involved in eliciting allergic and asthmatic disease.

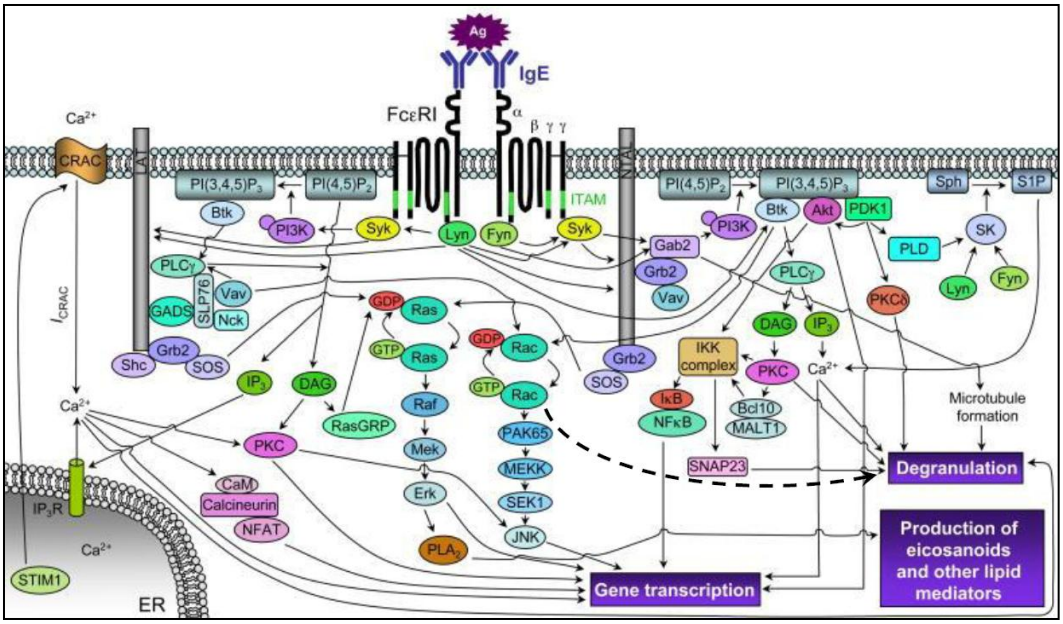


**Figure 1.1 FcεRI-mediated signaling pathways**

The FcεRI receptor binds IgE with high affinity, and requires cross linking of IgE-bound FcεRI receptors by specific antigen binding to propagate the signaling cascade which culminates in exocytosis of granules, (Pfeiffer et al. 1985; Kinet, 1999). FcεRI crosslinking by antigen recruits and activates several key signaling molecules, such as Lyn, Fyn and Syk kinases which mediate activation of all subsequent signaling molecules in the pathway. Syk activation promotes the formation of the LAT adaptor protein signaling complex, composed of several key molecules that activate a network of interconnected pathways. PLC-γ is recruited to this signaling complex resulting in the cleavage of PIP2 to produce IP3 and DAG. IP3 induces calcium flux from ER stores, and upon depletion of ER calcium stores, prolonged extracellular calcium flux is induced through activation of plasma membrane CRAC channels. DAG and calcium activate PKC which is involved in regulating exocytosis, however, PKC targets in this pathway are unknown. Concurrently, Rac is activated by the GEF Vav, which is also a component of the LAT adaptor signaling complex. Rac then activates signaling molecules involved in transcriptional regulation and exocytosis which is known as degranulation in specialized immune cells such as mast cells (reproduced from Kalesnikoff and Galli, 2008).


**Figure 1.2 Amino acid sequence alignment of Rac1 and Rac2**
ClustalW was used to align the amino acid sequences of Rac1 and Rac2 from *Homo sapiens, Rattus rattus and Mus musculus*. A s*ingle* a*sterisk* indicates positions of fully conserved amino acid, a *colon* indicates conservation between amino acids with similar properties and a *period* indicates conservation between amino acids with weakly similar properties. C-terminal tail differences are highlighted in the red box.

# CHAPTER 2

# METHODS AND MATERIALS

## 2.1 Preparation of bone marrow mast cells

### 2.1.1 Mice

Rac2 knockout (Rac2 KO) mice (a gift from Dr. Paige Lacy, Pulmonary Research Group, University of Alberta) were used to study the effect of Rac2 deficiency on mast cell function. The Rac2 KO mice were previously generated by targeted disruption of the *rac2* gene (Roberts et al., 1999). Rac2 KO mice were bred at the University of Alberta animal care facility and were backcrossed into C57Bl/6 mice for over 11 generations. Rac2 KO C57BL/6 mice were age-matched to wild-type C57Bl/6 mice obtained from Charles River, Canada (Saint-Constant, PQ). Animals were housed under specific pathogen-free conditions and were fed autoclaved water and food. Mice used in these experiments were 5 months old.

### 2.1.2 Bone marrow mast cell (BMMC) isolation, culture and maintenance

Bone marrow mast cells were prepared by cytokine differentiation of cells isolated from murine bone marrow as previously described (Jensen et al., 2006). Briefly, animals were sacrificed and the tibias and fibulas were isolated and washed with water. The isolated bones were then crushed with a mortar and pestle in Hanks Balanced Salt Solution (HBSS) supplemented with 1 mg/ml bovine serum albumin (BSA) and 0.1 mg/ml glucose. Cells were pelleted by centrifugation at 300*g* for 10 min at 4$^{o}$C and resuspended in 10 ml of warm RPMI 1640 (Roswell Park Memorial Institute) supplemented with cytokines (20 ng/ml

Interleukin-3 (IL-3) and 50 ng/ml Stem Cell Factor (SCF), as indicated), 1 X Non-Essential Amino Acids NEAA, 1 X mM sodium pyruvate, 10% heat-inactivated foetal bovine serum (HI-FBS), 100 units/ml penicillin and 100 μg/ml streptomycin.

Cells were incubated in T75 flasks for four days at 37$^{o}$C and 5% $CO_2$. After the fourth day post isolation, 10 ml of fresh supplemented RPMI 1640 was added to the original flask and incubated for an additional four days. Every four days thereafter, the media was hemi-depleted (50% removed) and the suspended cells were transferred to a new T75 flask to which 10 ml of fresh supplemented RPMI 1640 was added. BMMCs were maintained at concentrations ranging between 1 - 2 x $10^6$ cells/ml. Cells used in experimental assays were cultured in this way for four weeks prior to use in experiments. Cells were only used for experiments between weeks 4-6 of culture. Cells were used in assays three to four days after being cultured in fresh supplemented media so as to avoid cytokine-mediated responses.

Two separate culture conditions for the BMMCs were used (IL-3 alone, or IL-3 + SCF) due to discrepancies in the literature as to which condition yields the more responsive population of mast cells. It is widely accepted that IL-3 is essential to not only promote differentiation of mast cells from progenitor cells, but also for the proliferation of differentiated mast cells (Rottem et al., 1993; Yung et al., 1984). However, it is unclear whether additional cytokines enhance the responsiveness of the cells. When used in conjunction with IL-3, SCF maintains mast cell viability and promotes development (Rottem et al., 1993;

Galli et al., 1994). Moreover, SCF culturing conditions gives rise to populations of mast cells that most resemble connective tissue phenotypes (Tsai et al., 1991). It was found that the IL-3 + SCF culture condition produced a greater yield of mast cells (by almost two-fold), in comparison to the IL-3 culture condition (Figure 2.1 A). IL-3 and IL-3 + SCF cultured BMMCs appeared to have similar total β-hexosaminidase content (Figure 2.1 B). Moreover, comparable FcεRI surface density was observed between the two cultures (Figure 2.1 C). However, when compared for responsiveness to FcεRI-mediated stimulation, the IL-3 + SCF culture consistently exhibited near basal levels of exocytosis in response to stimulation. In contrast, the IL-3 culture exhibited robust levels of response to stimulation (Figure 2.1 D). Therefore, BMMCs cultured in IL-3 alone were selected for experimental use.

### 2.1.3 BMMC sensitization and stimulation for exocytosis

Anti-DNP-IgE (Bohn and Konig, 1982; Lui et al., 1980) and the multivalent ligand, bovine serum albumin (BSA) synthetically conjugated to multiple (~30) 2,4-dinitrophenyol groups ($DNP_{30}$-BSA) (Kohler and Milstein, 1976) were derived in the early 1980s as tools to activate mast cell cultures in vitro. Anti-DNP-IgE clone SPE-7 (Sigma-Aldrich) was used to sensitize mast cell cultures. $DNP_{30}$-BSA was used to crosslink anti-DNP-IgE bound FcεRI receptors. Cells were sensitized by incubation with 60 ng/ml of anti-DNP-IgE (clone SPE-7, Sigma-Aldrich) in cytokine free-RPMI media overnight. Following sensitization, cells were washed twice with 37$^{o}$C PBS and stimulated with 25 ng/ml of DNP-

BSA (Invitrogen) in HEPES Tyrodes Buffer (HTB) at 37$^{o}$C and 5% $CO_2$ for the indicated time. Anti–DNP-IgE and DNP-BSA concentrations were optimized to yield the highest activation response, assayed by level of exocytosis (data not shown). BMMCs cells were also stimulated with a non-physiological stimulus, 500 μM calcium ionophore (Sigma-Aldrich). Calcium ionophore is a mobile ion-carrier that forms stable complexes with divalent cations, thereby increasing intracellular calcium levels (Sahara et al., 1990). Calcium ionophore was used to bypass the FcεRI mediated activation, as a positive control (Sahara et al., 1990). Quantification of exocytosis is described in ***Section 2.3.1*.**

## 2.2 Rat basophilic leukemia-2H3 (RBL-2H3) cell line

Bone marrow-derived mast cells are an excellent model system in which to study mast cell function. However, despite their utility, bone marrow mast cell work is challenging. Propagation, differentiation and maturation of isolated bone marrow mast cells requires extensive propagation before the cells are ready to be used (Moon et al., 2010). Yield of cells after this period is limited. Moreover, once differentiated, cells are only experimentally viable for two weeks before they begin to lose responsiveness to antigen (Personal communications: Dr. Amanda Carroll-Portillo, University of New Mexico, USA; Dr. Juan Rivera, National Institute of Health, USA). To avoid these complications the rat basophilic leukemia cell line, RBL-2H3 was used. The RBL-2H3 cell line is a widely recognized and highly utilized model system for studying mast cell function

(Kulczycki et al. 1974; Passante and Frankish, 2009). RBL-2H3 cells are a particularly good model for exocytosis studies since they exhibit mast cell-like granular morphology and content (Seldin et al., 1985). Additionally, RBL-2H3 cells express high levels of surface FcεRI receptors that propagate the canonical exocytosis signaling pathway seen in mast cells (Barsumian et al., 1981). In light of these advantages, RBL-2H3 cells were used to overcome some of the issues associated with BMMCs.

### 2.2.1 RBL-2H3 cell culture maintenance

RBL-2H3 cells (a gift from Dr. Dean Befus, Pulmonary Research Group, University of Alberta) were maintained according to culturing protocols adapted from Jensen et al. (2006). Cells were grown in Minimal Essential Medium (MEM) supplemented with 10% HI-FBS and cultured in conditions of 37$^{o}$C and 5% $CO_2$. Cells were split every 2-3 d, or when 80% confluent. RBL-2H3 cells were used in experimental assays at the end of the 2-3 d culture to ensure similar growth conditions between experiments.

### 2.2.2 RBL-2H3 sensitization and stimulation for exocytosis

RBL-2H3 cells were sensitized and stimulated for exocytosis according to previous protocols (Naal et at., 2004). Briefly, cells were incubated with 60 ng/ml anti-DNP-IgE (SPE-7) in OptiMEM for 2 h, washed twice with Earle's balanced salt solution (EBSS) and subsequently incubated with 25 ng/ml $DNP_{30}$-BSA in EBSS for the required time of the assay. RBL-2H3 cells were also stimulated

with 500 μM calcium ionophore (A23187; Sigma –Aldrich), a non-physiological stimulus. Quantification of exocytosis is described in ***Section 2.3.1.***

### 2.2.3 siRNA treatment and RNA isolation of RBL-2H3 cells

Pre-validated siRNAs (Ambion) targeted to the non-conserved regions of Rac1 and Rac2 were used to transfect RBL-2H3 cells (Table 2.1). Two siRNAs, targeted to two different locations in the non-conserved regions of each mRNA, were used for each transfection. RBL-2H3 cells were transfected with an optimized amount of siRNA (5 nM total) (data not shown) using 5 μl Lipofectamine 2000 transfection reagent (Invitrogen) in 2 ml Optimem. After 6 h of incubation, the transfection media was replaced with MEM supplemented with FBS and incubated for 48 h before use in experimental assays. To ensure all pre-existing endogenous Rac1 and Rac2 protein and mRNA was degraded, 48 h was selected as the optimal time to wait before using the cells as it was the time point which showed the maximum reduction of Rac1 and Rac2 mRNA as determined by qPCR (data not shown).

48 h post incubation with siRNAs, RNA was isolated from $1x10^6$ RBL-2H3 cells using TRIZOL reagent (Invitrogen) according to manufacturer's instructions. Isolated RNA was subsequently treated with DNaseI (Invitrogen), according to manufacturer's specifications. Post DNaseI treatment, RNA was made into cDNA, via first strand synthesis using Super Script II (Invitrogen), according to manufacturer's instructions.

### 2.2.4 Quantification of Rac1 and Rac2 siRNA knockdown in RBL-2H3 cells

Quantitative polymerase chain reaction (qPCR) was used to determine the effectiveness of knockdown achieved by the siRNA transfection. 48 h post transfection, RNA was extracted from transfected cells using Trizol reagent, DNaseI treated and reversed transcribed into cDNA. The resulting cDNA was used in qPCR reactions to quantify the levels of endogenous mRNA. SyberGreen Super Mix Low ROX (BioSciences Quanta PerfeCTa ) was used to detect mRNA copies, according to manufacturer's instructions. Briefly, 10 μl of Syber green was added to 5μl cDNA (25 ng) and 5 μl (2.5 μM total) forward and reverse primers (Table 2.1). A Stratagene MxPro (Mx3005p) qPCR machine was used to detect cDNA transcripts. To calculate relative mRNA copy numbers, the ΔΔ Ct (ΔΔ= delta delta, Ct=threshold value) method was used (Livak and Schmittgen, 2001). The formula to calculate copy number is as follows:

$$\text{Relative transcript levels} = \frac{\text{PCR efficiency}^{\text{housekeeping gene Ct}}}{\text{PCR efficiency}^{\text{target gene Ct}}}$$

Values obtained were corrected to primer efficiencies (determined by standard curves for each primer) and then corrected to the cDNA values of a housekeeping gene, GAPDH. Values were subsequently normalized to expression of either Rac1 or Rac2 in cells treated with a control siRNA. Negative siRNA (Ambion) was used as a negative control as it exhibits non-targeting effects and has limited sequence similarity with known rat genes. Data was analyzed by ANOVA analysis to determine statistical significance. Non-Paired, two-tailed Student's T-

test at $\alpha$=0.05 were used to compare each treatment individually to the negative siRNA.

### 2.2.5 Transfection

Amaxa nucleofection was used to transfect both RBL-2H3 cells and BMMCs, as it was found to be the technique that yielded the highest transfection efficiency for both cell lines. The Amaxa Nucleofector was used according to manufacturer's instructions. The Amaxa cell line nucleofector Kit T and program X-001 were selected as optimized setting to transfect cells. $1.5x10^6$ cells were transfected with 5 μg of plasmid DNA and given 12- 24 h to recover before experimental assays were performed. Refer to Table 2.2 for complete details of plamsids used.

pEGFP-C1 plasmids (Clonetech) containing wild-type and mutant Rho GTPases were obtained for Rac1 and Rac2. Each Rho GTPase has a set comprising of a wild type (WT) clone and two mutant clones; a constitutively-active (GTP-bound) Q61L mutant and a dominant negative (GDP-bound) T17N mutant. All constructs used were obtained from Dr. Jennifer Stow (University of Queensland, Australia). All constructs were confirmed by sequencing. Each mutant Rho GTPase was N-terminally tagged with GFP followed by the linker sequence, Ser-Gly-His-Arg-Gly-Gly-Gly-Ser. Constructs were N-terminally tagged so as to avoid disruption of the C-terminal lipid modified tail. Moreover, the amino acid linker between GFP and the Rho GTPase was used to ensure GFP did not interfere with molecular interactions of the Rho proteins.

CD63-EGFP plasmid was obtained from Dr. Sanford Simon, Rockefeller University (Jaiswal et al., 2002). To study granule mobilization dynamics, CD63-EGFP was transfected by Amaxa nucleofection into RBL-2H3 cells and BMMCs. Lifeact m-Ruby, a live-cell F-actin probe was obtained from Dr. Michael Glogauer, University of Toronto (Riedl et al., 2008). To study the dynamic process of actin remodelling, live-cell imaging was performed using the Lifeact F-actin probe. BMMCs and RBL-2H3 cells were transfected by Amaxa Nucleofection with Lifeact m-Ruby F-actin probe. Lifeact binds to the sides of polymerized actin, and as a result, does not interfere with the functionality and dynamics of the actin monomers or polymerized actin (Riedl et al., 2008).

## 2.3 Biochemical assays

### 2.3.1 Exocytosis assay

Mast cells have numerous granules in their cytoplasm that contain a plethora of vasoactive and immunological mediators. The granules of mast cells are lysosomal in nature and as a result, are also termed secretory lysosomes (Andrews, 2000). Mast cell secretory lysosomes contain substantial amounts of β-hexosaminidase, a lysosomal enzyme that functions to hydrolyze hexosamines, in addition to glucosides, galactosides and oligosaccharides present in the cell (Aronson and Kuranda, 1989). Previous studies have established that β-hexosaminidase release correlates with the release of histamine, a substance known to be responsible for eliciting the pathological affects of activated mast

cells (Schwartz et al., 1979). Hence, β-hexosaminidase is a widely used as an indicator of exocytosis in mast cell studies (Blank and Rivera, 2006).

In accordance with other studies, β-hexosaminidase enzyme assays were performed on the supernatants of stimulated mast cells to assess exocytosis (Blank and Rivera, 2006). Mast cells were plated in 96-well microtitre dishes at 200,000 cells/well. After 24 h, cells were sensitized with anti-DNP-IgE and stimulated with DNP-BSA, as outlined in ***Section 2.2.2***. Plates were cooled on ice, centrifuged at 300*g* for 5 min and 50 µl of supernatant was mixed with 50 µl of 1.2 mM β-hexosaminidase substrate, 4-methylumbelliferyl-N-acetyl-β-D-glucosaminide (MUG, Sigma-Aldrich) dissolved in 50 mM sodium citrate pH 4.5. Reactions were incubated for 30 min at 37$^{o}$C, then terminated by the addition of 100 µl of 0.1 M glycine pH 11. Cleavage of the substrate releases the fluorescent product methylumbelliferrone, which was detected using a BioTek Synergy4 fluorimeter (360 nm excitation and 460 nm emission). Data was acquired with Gen5 V1.1 software. The amount of substrate cleaved, is directly proportional to the amount of enzyme present in the reaction and hence can be used to quantify exocytosis.

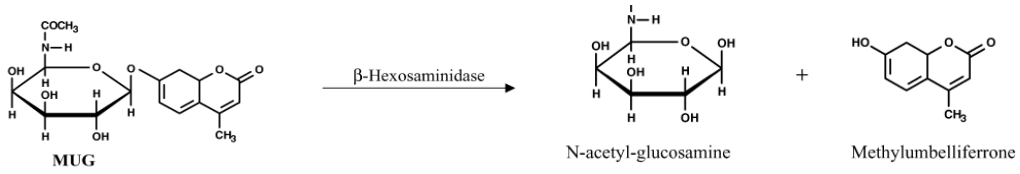

To account for variability of total cell count or granule density between cell populations, exocytosis was expressed a percent of total (Blank and Rivera, 2006). Moreover, to account for experimental variability in varying levels of basal exocytosis, all values were corrected for the basal levels of exocytosis of IgE-sensitized but unstimulated cells for each condition to provide the amount of spontaneous release. Therefore, % exocytosis values were calculated using the following formula (Blank and Rivera, 2006):

$$\% \text{ net specific release} = \frac{\text{release}_{\text{stimulated}} - \text{release}_{\text{spontaneous}}}{\text{total}_{\text{content}} - \text{release}_{\text{spontaneous}}} \times 100$$

Data was analyzed by non-paired two-tailed Student's T-test at $\alpha$=0.05.

### 2.3.2 Calcium flux assay

To observe the dynamics of calcium mobilization in BMMC and RBL-2H3 cells, the Fluo-3-AM calcium indicator was used (Invitrogen). Calcium flux assays were adapted from previous studies (Manetz et al., 2001). Cells were sensitized with anti-DNP-IgE, incubated with 1 μM Fluo-3-AM for 30 min and washed twice with sterile PBS. During this time, the cells took up and internalized the Fluo-3-AM dye. Fluo-3 exhibits a large fluorescence intensity increase upon binding of calcium, which is influxed into the cytoplasm following stimulation, which can then be detected and quantified. Cells were placed in a cuvette at a concentration of 500,000 cells/ml. A spectrophotometer (QM-SE4; Photon

Technology International) was used to detect fluorescence of the cells that occurred upon influx of extracellular calcium into the cell (excitation 506 nm and emission 526 nm). Readings were taken for 5 min as the sample was allowed to equilibrate prior to addition of stimulus. Data was acquired using Felix 32 ver1.0 software. Data was analyzed by non-paired, two-tailed Student's T-test at $\alpha$=0.05.

### 2.3.3 Western blot analysis

Cell lysates were prepared as follows: 2 - 5 x $10^6$ BMMC or RBL-2H3 cells were lysed by sonicating 2 min in lysis buffer (20 mM HEPES pH 7.5, 150 mM NaCl, 1% Triton X-100, 10 mM NaF, 1 mM sodium vanadate, 1 mM PMSF and 1 X Protease Inhibitor Cocktail (PIC)). Antibodies used for immunoblot analysis are listed in Table 2.3.

### 2.3.4 Flow cytometry

Post treatment, RBL-2H3 cells and BMMCs were placed on ice and prepared for flow cytometry. BMMCs and RBL-2H3 cells were labelled using the same protocol. For live-cell labelling, isolated cells were placed on ice, and then centrifuged at 1200*g* for 5 min at 4$^o$C. Cells were washed twice with ice cold PBS + 0.2% BSA and blocked with the same buffer for 15 min on ice. Cells were then analyzed if expressing GFP-tagged proteins, or were stained with conjugated antibodies for 45 min on ice. To analyze samples a FACS Canto II flow cytometer was used (Flow Cytometry Facility, University of Alberta). Facs Diva analysis program was used to analyze data.

To detect apoptosis in BMMCs, AnnexinV-488 (BD Biosciences) was used according to manufacturer's protocol. BMMCs were treated as indicated in the *Results* and incubated for 4 h, to allow sufficient time for apoptosis to be initiated, prior to staining with AnnexinV-488. As a positive control, cells were treated with 2.5 μM staurosporine and 5 μM cyclohexamide, which are well established inducers of apoptosis (Belmokhtar et al., 2001). Data was analyzed by non-paired two-tailed Student's T-test at $\alpha$=0.05.

## 2.4 Microscopy

### 2.4.1 Fixed-cell microscopy of BMMCs

Protocols for fixed-cell preparations of BMMCs for fluorescence microscopy were adapted from previous studies (Nishida et al., 2005; Zink et al., 2008). Briefly, BMMCs were subjected to various experimental treatments as indicated in the *Results*, placed on ice and fixed with 4% paraformaldehyde for 15 min. Cells were then cytospun onto non-charged glass slides at 300 rpm for 10 min, allowed to dry for 2 min and then stained with the appropriate antibodies. After washing the cells, Prolong Gold anti-fade mounting media (Invitrogen) was added and the coverslip applied.

Toluidine blue staining of BMMCs was performed to examine cell morphology. BMMCs were cytospun onto non-charged glass slides at 300 rpm for 10 min, fixed for 10 min in Mota's fixative and stained with Toluidine Blue

working solution for 30 min. After washing the cells, Cytoseal mounting media was added and the coverslip applied.

### 2.4.2 Fixed-cell microscopy of RBL-2H3 cells

Protocols for fixed-cell preparations of RBL-2H3 cells for fluorescence microscopy were adapted from previous studies (Edgar et al., 1997; Legg et al., 2007). Briefly, RBL-2H3 cells were grown on coverslips in a 6-well tissue culture plate and were subjected to various experimental treatments as indicated in the *Results*. Cells were placed on ice and fixed with 4% paraformaldehyde for 15 min. Cells were permeabilized and blocked with 0.5% saponin/PBS and stained with appropriate antibodies. After washing the cells, Prolong Gold anti-fade mounting media was added and the coverslip applied to a glass slide.

### 2.4.3 Live-cell microscopy of BMMCs

Actin reorganization and granule movement are dynamic processes and live-cell spinning disc confocal microscopy was required to capture these events. To accommodate to the environmental requirements of the cells, a temperature ($37^{o}$ C) and $CO_2$ (5%) controlled live-cell chamber was used to ensure ideal environmental conditions. Actin reorganization occurs dynamically in three dimensions and requires the three dimensional capacity of confocal microscopy to best capture these processes. Images were taken through the z-plane at distances of 0.26 μm, from just above the cell to just under the cell to ensure no information was missed. Depending on the thickness of the cell, the number of z-slices ranged

from 20-30, resulting in cells 5-8 μM thick having all intracellular structures being precisely captured. Maximum intensity projections (MIPs) were constructed which compiled all the information obtained in each of the z-slices. Fluorescence confocal microscopy images were obtained using a Perkin Elmer UltraVIEW VoX Confocal Imaging System equipped with Leica optics. Velocity 6.0 was used for image acquisition. Widefield microscopy images were obtained with a Zeiss Observer Z1 widefield system. AxioVision 4.8 for used for image acquisition. DIC microscopy images were obtained using a Quorum WAVE FX spinning disk confocal with a polariser. Velocity 6.1 was used for image acquisition.

Protocols for preparations of glass slides for live-cell imaging of BMMCs were adapted from previous studies (Zink et al., 2008; Deng et al., 2009). Live-cell plastic dishes with non-charged glass coverslip bottoms (33 mm glass bottom culture dishes No. 1; MatTek Corp) were incubated with a saturating concentration of DNP-BSA (20 μg/ml) in sterile PBS for 30 min at 37$^{o}$C. Post incubation, the dishes were rinsed five times with 3 ml of PBS and kept moist with 500 μl of PBS, and used within 1-2 h of incubation. PBS was replaced with 500 μl of HTB prior to use. BMMCs were imaged in a temperature (37$^{o}$C) and $CO_2$ (5%) controlled cell chamber.

### 2.4.4 Live-cell microscopy of RBL-2H3 cells

RBL-2H3 cells were incubated in MEM supplemented with FBS overnight in live-cell plastic dishes with poly-D-lysine coated glass coverslip

bottoms (33 mm glass bottom culture dishes No. 1; MatTek Corp). RBL-2H3 cells were observed to respond with a more homogenous, heightened morphological response when poly-D-lysine coated coverslips were used (data not shown). To ensure that any activation that may have occurred as a result of the poly-D-lysine coating, cells were incubated overnight in MEM before undergoing experimental manipulation. Moreover, it was found that cells incubated with poly-D-lysine coated surfaces exhibited functional FcεRI-mediated exocytosis similar to cells incubated with non-coated surfaces (data not shown). After overnight incubation, cells were sensitized for 2 h in MEM, washed 3X and incubated with 0.5 ml of EBSS. Cells were stabilized in the imaging chamber and then stimulated with 0.5 ml of 50 ng/ml DNP-BSA in EBSS. RBL-2H3 cells were imaged in a temperature ($37^{o}C$) and $CO_2$ (5%) controlled cell chamber.

A.

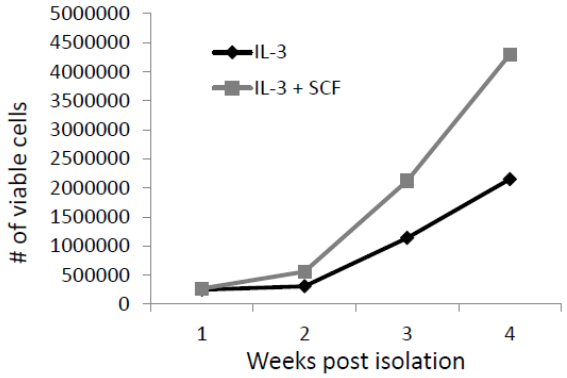
5000000
4500000
4000000
3500000
3000000
2500000
2000000
1500000
1000000
500000
0
# of viable cells
IL-3
IL-3 + SCF
1
2
3
4
Weeks post isolation

B.

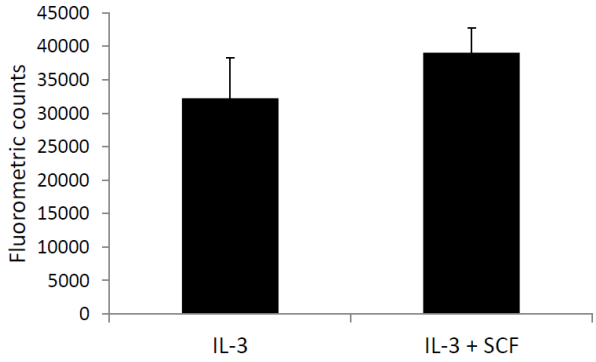
45000
40000
35000
30000
25000
20000
15000
10000
5000
0
Fluorometric counts
IL-3
IL-3 + SCF

C.

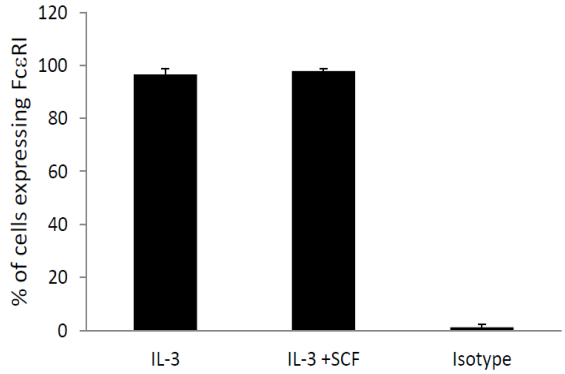
120
100
80
60
40
20
0
% of cells expressing FcεRI
IL-3
IL-3 +SCF
Isotype

D.

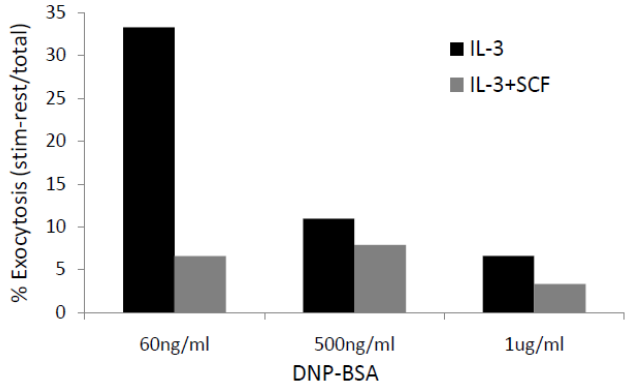
35
30
25
20
15
10
5
0
% Exocytosis (stim-rest/total)
IL-3
IL-3+SCF
60ng/ml
500ng/ml
1ug/ml
DNP-BSA

**Figure 2.1 Characterization of IL-3 and IL-3 + SCF cultured BMMCs**
(A) BMMCs from 1 - 4 weeks post isolation were stained with trypan blue. Viable cells were stained and counted with a hemacytometer. Values represent an average of 2 separate cultures. (B) BMMCs were live cell stained with 488-conjugated FcεRI antibody and FcεRI positive cells were detected by flow cytometry. Values represent an average of 5 independent experiments. (C) BMMCs were sensitized overnight with 60ng/ml of anti-DNP IgE and then stimulated with 25ng/ml of DNP-BSA for 30 min. (D) Exocytosis of IL-3 (black) and IL3+SCF (grey) cultured BMMCs was measured by fluorometric detection of β-hexosaminidase released from the cells into the supernatant. Exocytosis is expressed as a percentage calculated from values of resting cells (background) subtracted from stimulated cells and expressed as the percentage of total. BMMCs were treated with 0.1% TX-100 and total β-hexosaminidase content was measured by fluorometric detection of β-hexosaminidase in the supernatant. Values represent an average of 5 independent experiments.

**Table 2.1 Antibodies used for Western Blot applications for RBL-2H3 cells and BMMCs**

| Antibody | Commercial source | Host | Antibody type | Working dilution | Species reactivity |
|---|---|---|---|---|---|
| anti-Rac1 | UBI | mouse | monoclonal | 1 in 5000 | human, mouse, rat |
| anti-Rac1 | Santa Cruz | rabbit | polyclonal | 1 in 500 | human, mouse, rat |
| anti-Rac2 | Millipore (Dr. G. Bokotch) | rabbit | polyclonal | 1 in 4000 | human, mouse, rat |
| anti-Rac2 | Santa Cruz | rabbit | polyclonal | 1 in 500 | human, mouse, rat |
| anti-tubulin | Millipore | rabbit | monoclonal | 1 in 5000 | human, mouse, rat |

**Table 2.2 Primers used for siRNA knockdown and qPCR applications**
Primers used for siRNA knockdown are commercially constructed Ambion Silencer Select pre-designed primers. Primers used for qPCR were designed.

| Primer | ID | Company | Use | Target Nucleotide sequence (5'→3') | Target animal |
|---|---|---|---|---|---|
| Rac1 | S171174 | Ambion | siRNA | GGAUGAUAAGGACACGAUUtt | *Rattus* |
| Rac1 | S171175 | Ambion | siRNA | CAAACAGACGUGUUCUUAAtt | *Rattus* |
| Rac2 | S173008 | Ambion | siRNA | CAGACAGACGUGUUCCUCAtt | *Rattus* |
| Rac2 | S173010 | Ambion | siRNA | AUGUGAUGGUGGACAGUAAtt | *Rattus* |
| Rac1 *Fwd* | | IDT | qPCR | CGAAAGAGATCGGTGCTGTC | *Rattus* |
| Rac1 *Rev* | | IDT | | AACGGCTCGGATAGCTTCA | *Rattus* |
| Rac2 *Fwd* | | IDT | qPCR | TGGTGGACAGTAAACCTGTGAA | *Rattus* |
| Rac2 *Rev* | | IDT | | GCAGATGAGGAACACGTCTGT | *Rattus* |
| GAPDH *Fwd* | | IDT | qPCR | TGACTCTACCCACGGCAAGT | *Rattus* |
| GAPDH *Rev* | | | | GCTCCTGGAAGATGGTGATG | *Rattus* |

* IDT = Integrated DNA Technnology
** *Rattus* = *Rattus* norvegicus

**Table 2.3 Plasmids used for transfection of RBL-2H3 cells and BMMCs**

| Plasmid | Vector | Resistance* | Promoter | Company | Research lab obtained from** |
|---|---|---|---|---|---|
| Rac1WT-GFP | pcDNA 3.1+ | Neo/Amp | pCMV | Clonetech | Dr. Stow (U of Q, Australia) |
| Rac1 Q61L-GFP | pcDNA 3.1+ | Neo/Amp | pCMV | Clonetech | Dr. Stow (U of Q, Australia) |
| Rac1 T17N-GFP | pcDNA 3.1+ | Neo/Amp | pCMV | Clonetech | Dr. Stow (U of Q, Australia) |
| Rac2WT-GFP | pEGFP-C1 | Neo/Kan | pCMV | Clonetech | Dr. Stow (U of Q, Australia) |
| Rac2 Q61L-GFP | pEGFP-C1 | Neo/Kan | pCMV | Clonetech | Dr. Stow (U of Q, Australia) |
| Rac2 T17N-GFP | pEGFP-C1 | Neo/Kan | pCMV | Clonetech | Dr. Stow (U of Q, Australia) |
| CD63-EGFP | pEFGP-C1 | Neo/Kan | EF1 alpha | | Dr. Simon (Rockefeller) |
| Lifeact m-Ruby | pEGFP-N1 | Neo/Kan | pCMV | | Dr. Glogauer (U of T) |

*Neo = neomycin
Amp = ampicillin
Kan = kanamycin

**Dr. Jennifer Stow (University of Queensland, Australia)
Dr. Sanford Simon (Rockefeller University)
Dr. Michael Glogauer (University of Toronto)

# CHAPTER 3

# RESULTS

### 3.1 Exocytosis and calcium flux are Rac2 dependent processes in bone marrow-derived mast cells

To study the effect of Rac2 deficiency on mast cell morphology and function, primary bone marrow mast cells (BMMCs) were isolated and cultured from wild-type (WT) and Rac2 knockout (Rac2 KO) mice. Western blot analysis confirmed the absence of Rac2 protein and showed an upregulation of Rac1 protein expression in the Rac2 KO BMMCs (Figure 3.1 A). Phenotypically, Rac2 KO BMMCs appeared similar to WT mast cells, with similar growth rates (Figure 3.1, B) and similar density of FcεRI receptor expression on the plasma membrane (Figure 3.1, C). The granule content was comparable between Rac2 KO BMMCs and WT BMMC as they possessed comparable densities of toluidine blue stained granules (Figure 3.1, D) and comparable levels of total granular content of the lysosomal enzyme β-hexosaminidase (Figure 3.1, E).

Rac2 is required for functional exocytosis in neutrophils and c-kit mediated exocytosis in mast cells (Abdel-Latif et al., 2004; Yang et al., 2000). Therefore I sought to determine if the absence of Rac2 would have an effect on FcεRI-mediated mast cell exocytosis. Exocytosis was measured by assaying for the release of an intra-granular enzyme, β-hexosaminidase, into the cell supernatant. It was found that upon stimulation, Rac2 KO BMMCs had markedly reduced levels of β-hexosaminidase exocytosis (72%) (Figure 3.2, A) and retained more toluidine-blue positive granules (Figure 3.3), when compared to the WT BMMCs.

To determine if the exocytosis defect in Rac2 KO BMMCs was selective for the FcεRI signaling pathways, cells were stimulated with calcium ionophore. Calcium ionophore triggers exocytosis in a non-physiological manner through increased membrane permeability to calcium and therefore bypasses normal physiological signaling pathways (Piper and Seale, 1979). Upon stimulation with calcium ionophore, β-hexosaminidase levels were not significantly different in control versus Rac2 KO BMMCs (Figure 3.2 B).

FcεRI-dependent exocytosis in mast cells requires a concomitant increase in cytosolic calcium levels (Baba et al., 2008; Vig et al., 2008). To determine whether Rac2 deficiency affected this aspect of the FcεRI-dependent exocytosis signaling pathway, cytosolic calcium flux was analyzed. It was found that calcium flux was decreased by 63% in Rac2 KO cells (Figure 3.4, A and B). To determine if this defect in calcium flux was restricted to FcεRI dependent signaling, Rac2 KO cells were stimulated with calcium ionophore. No difference in calcium flux was observed upon treatment with calcium ionophore in Rac2 KO BMMCs versus the WT control (Figure 3.5, A and B).

### 3.2 FcεRI-mediated actin-rich membrane ruffling is not Rac2 dependent in BMMCs

In addition to secretion of inflammatory molecules, activated mast cells exhibit dramatic alterations in membrane morphology in response to antigen-mediated activation. Antigen-stimulated mast cells characteristically exhibit dorsal membrane ruffling and ventral membrane spreading, which are known to

be actin dependent processes (Burwen and Satir, 1977; Pfeiffer et al., 1985). These actin-rich membrane ruffles are distinctive indicators of mast cell activation, and are known to occur in parallel with secretion of inflammatory molecules, however, the mechanistic link between these two events is unknown. Therefore, I characterized the dynamics of actin remodelling in WT and Rac2 KO BMMCs. To qualitatively assess actin-rich membrane ruffle formation, confocal fluorescence and differential interference contrast (DIC) microscopy in both live cells and fixed cells was done to capture actin-rich membrane ruffling in response to antigen-mediated activation.

To assess the function of Rac2 on actin-rich membrane ruffle formation I first examined fixed cells via immunostaining. However, this method did not provide sufficient information about the dynamics of transient actin remodeling events. This was largely attributed to the fact that the membrane ruffling events that were observed in BMMCs were transient and highly dynamic. Live-cell microscopy was used to bypass this impediment, enabling the visualization of transient membrane ruffle formations. Lifeact-mRuby transfected BMMCs were used to visualize real-time actin dynamics in the cell. Lifeact-mRuby is a fluorescently tagged probe that binds to the sides of polymerized actin, thus allowing real-time observations of actin dynamics in the cell (Riedl et al., 2008). WT BMMCs exhibited characteristic actin-rich dorsal and peripheral membrane ruffling upon stimulation with DNP-BSA antigen (Figure 3.6, Supplementary Movie 1). Upon stimulation, WT BMMCs flattened and exhibited minor dorsal and prominent peripheral membrane ruffles (1-10 min), exhibited prominent

dorsal membrane ruffle formation (11-30 min) and eventually returned to resting state (40 + min) (Figure 3.6). No defect in the formation of actin-rich dorsal and peripheral membrane ruffles was observed in stimulated Rac2 KO cells. Stimulated Rac2 KO BMMCs exhibited comparable levels of membrane ruffling compared to WT BMMCs (Figure 3.6, Supplementary Movie 1).

### 3.3 Rac1 and Rac2 are required for calcium flux and exocytosis in the mast cell line, RBL-2H3

Deletion of Rac1 is embryonic lethal (Sugihara et al., 1998) and inducible knockout systems are not available for mast cells, therefore Rac1 KO mast cells were not available for experimental use (See ***Section 5.5***). To overcome this difficulty I used the mast cell line, RBL-2H3, and siRNA knock-down to examine the differential functions of Rac1 and Rac2. RBL-2H3 cells were treated with siRNA targeting Rac1, Rac2 or both mRNAs to study the effect of Rac1 and Rac2 deficiency on mast cell function. Pre-validated siRNAs (Ambion Inc.) designed specifically to non-conserved regions of Rac1 and Rac2 mRNA were used. These siRNAs exhibited excellent specificity for the appropriate Rac1 or Rac2 target RNA, as shown by quantitative real-time PCR (qRT-PCR) analysis (Figure 3.7 A). mRNA levels were depleted by 50% in siRNA treated cells (Figure 3.7 A), however, due to limitations in the availability of highly specific antibodies for individual Rac GTPases in RBL-2H3 cells, protein knock-down could not be confirmed (Figure 3.7 B).

To determine if siRNA knock-down of Rac1 or Rac2 affects FcεRI-mediated processes, exocytosis and calcium flux were investigated. siRNA knock-down of Rac1 and Rac2 resulted in a 60% and 56% decrease in exocytosis, respectively (Figure 3.8 A). When both Rac1 and Rac2 were simultaneously knocked-down, there was no additional reduction in exocytosis (Figure 3.8 A). Intracellular calcium flux was deceased by 50% and 60% in Rac1 and Rac2 siRNA knocked-down cells, respectively (Figure 3.8 B, C). However, when both Rac1 and Rac2 mRNA were simultaneously knocked down, calcium flux was reduced by 90%, in comparison to Negative siRNA treated cells (Figure 3.8 C).

### 3.4 Rac1 and Rac2 are required for actin-dependent membrane remodelling in the mast cell line, RBL-2H3

Confocal and widefield microscopy were used to characterize the effects of Rac1 and Rac2 deficiency on actin-dependent membrane remodelling. Similar to the experimental limitations in microscopy of the BMMCs, issues were encountered regarding the inability to capture the transient and dynamic nature of actin remodelling events when using fixed-cell microscopy. To overcome this limitation, the RBL-2H3 cell line was used for live-cell microscopy experiments. RBL-2H3 cells were transfected with Lifeact-mRuby to image actin dynamics in real-time. To adequately capture all of the morphological changes post stimulation, over 30 min of imaging time was required. It was found that the membrane ruffles were F-actin rich by fluorescent imaging of a limited number of

Lifeact-mRuby transfected cells using confocal microscopy (Figure 3.9; Supplementary Movie 2), However, to adequately capture the morphological events of a sufficient number of cells for quantification of morphological changes, images from 15 different locations (containing 10-15 cells each) were captured. Wide-field/bright-field microscopy was utilized to overcome the experimental limitations that occurred with confocal microscopy of Lifeact-mRuby, mainly laser toxicity of the cells and bleaching of the fluorophore. Using wide-field/bright-field microscopy, I was able to characterize the morphological changes that occurred when RBL-2H3 cells were stimulated (Figure 3.10, A *left panel;* Supplementary Movie 2). Upon stimulation, cells rapidly flattened (0 – 1 min), exhibited minor ruffling (1 - 15 min), formed prominent dorsal membrane ruffles (~15 min) that were highly transient and then returned to the resting state (45 - 60 min).

In Rac1 and Rac2 siRNA-treated cells, defects in actin-rich membrane remodelling were observed through live-cell imaging (Figure 3.10). In Rac1, Rac2 and Rac1 + Rac2 knockdown cells, the occurrence of minor ruffling, a partial response to stimulation, was not significantly affected. However, responses characteristic of fully stimulated cells, such as the formation of prominent ruffles and cell flattening, were significantly inhibited (Figure 3.10, B).

### 3.5 Characterization of a Rac-specific inhibitory drug, EHT-1864, in mast cell exocytosis, calcium flux and actin-dependent membrane remodeling

Considering inflammatory disease is exacerbated by the exocytosis of immunoregulatory molecules from mast cells (*e.g.* histamine), it is of great importance to investigate the potential for pharmacological inhibition of this cellular process. Through studies of two mast cell models, RBL-2H3 cells and BMMCs, I have shown that Rac1 and Rac2 regulate exocytosis in mast cells. Therefore, I next investigated whether the novel small molecule inhibitor of Rac, EHT-1864, could recapitulate the functional and morphological defects of exocytosis in knocked-down or deficient Rac1 and Rac2 cells.

EHT-1864 is a small-molecule that binds to both Rac1 and Rac2 with high affinity and not to other small GTPases (Shutes et al., 2007). Moreover, Shutes et al., (2007) deduced the mechanism by which EHT-1864 inhibits Rac by demonstrating that EHT-1864 not only prevented Rac GDP/GTP nucleotide exchange but also displaces bound nucleotide. Additionally, Rac-GTP formation and the interaction of Rac with its downstream effector, PAK, was also prevented (Shutes et al., 2007; Onesto et al., 2008). However, the exact location of the EHT-1864 binding site on Rac1 or Rac2 is not known. This will be studied by NMR spectroscopy in collaboration with Dr. Bryan Sykes (Department of Biochemistry, U of A), which will help resolve the exact mechanism of inhibition (See ***Section 5.6)***.

I sought to determine if EHT-1864 had an effect on mast cell function using both BMMCs as the primary cell model and the RBL-2H3 cell line as an

additional experimental model. EHT-1864 was found to work most optimally at 40μM final concentration (Figure 3.11 A). To ensure EHT-1864 was not toxic to cells, apoptosis and cell death was examined by Annexin V staining. At concentrations of EHT-1864 within the range used in this study (10 - 40 μM), I observed no significant increase in cell death. However, when EHT-1864 was used at concentrations higher than that used in our study (>80 μM) substantial cell death was induced

(Figure 3.11 B).

Pre-incubation of cells with EHT-1864 completely abrogated exocytosis in BMMCs (Figure 3.12), while the RBL-2H3 cell line exhibited only a 50% reduction (Figure 3.13, A). Moreover, when Rac1 and Rac2 knock-down RBL-2H3 cells were treated with EHT-1864, exocytosis could be further reduced (Figure 3.13, B). Additionally, intracellular calcium flux was completely inhibited in both BMMC and RBL-2H3 cells (Figure 3.14 A, B; 3.15 A, B).

I next examined the effect of EHT-1864 treatment on the morphological response of mast cells to stimulus. Cells that were pre-treated with EHT-1864 prior to stimulation exhibited morphology similar to that of untreated BMMCs (Figure 3.16 A). However, upon stimulation, EHT-1864-treated BMMCs failed to exhibit dorsal F-actin rich membrane ruffling and cell spreading (Figure 3.16, B) and instead remained morphologically similar to unstimulated BMMCs.

EHT-1864 treatment of RBL-2H3 cells also showed a profound effect on the morphological response to stimulus. Major membrane ruffling was completely blocked in EHT-1864-treated RBL-2H3 cells and cell spreading was greatly

inhibited, while minor membrane ruffling was not inhibited (Figure 3.17). This result was similar to that observed in the Rac1 and Rac2 knock-down RBL-2H3 cells (Figure 3.10).

To determine if the inhibitory effect on Rac was through the physiological signaling pathway, cells were stimulated with calcium ionophore to bypass FcεRI-mediated exocytosis. This approach resulted in a highly variable cellular response that could not be interpreted (Figure 3.14 C, D, E). Figure 3.14 C and D are representative of one experiment showing recovery of calcium flux with the addition of calcium ionophore in EHT-1864 treated cells. However, this response was not consistently repeatable. Figure 3.14 E is representative of an example of the variability of responses displayed by cells after calcium ionophore treatment to restore calcium flux in EHT-1864 treated cells.

### 3.6 Characterization of CD63, a lysosomal secretory granule marker, to visualize mast cell granules

An initial aim of this project was to characterize the link between actin remodelling and granule mobilization during mast cell exocytosis. To characterize the granule dynamics in mast cells, the utility of imaging CD63-GFP was explored. CD63 is a tetraspanin transmembrane protein expressed predominantly on the plasma membrane, lysosomes and lysosomal secretory granule membranes (Stipp et al., 2003). The rationale for selecting CD63 as a granule marker was derived from its use in previous neutrophil and mast cell studies to show granule movement to the plasma membrane (Mitchell et al., 2008, Nishida et al., 2005).

However, CD63 proved to be a poor marker for microscopic analysis of exocytosis in both the RBL-2H3 cell line and BMMCs.

Confocal microscopy of both fixed and live cells was used to observe granule-actin dynamics in RBL-2H3 cells. RBL-2H3 cells were co-transfected with CD63-GFP, as a marker for lysosomal secretory granule membranes, and Lifeact-mRuby as a marker for polymerized actin. Hundreds of cells were imaged using both fixed-cell and live-cell microscopy to analyze granule translocation to the membrane. CD63-GFP was distributed in a punctate fashion throughout the cytoplasm, correlating with secretory lysosomal granules (Figure 3.18). However, upon stimulation, the CD63-GFP granules did not exhibit a significant translocation to the plasma membrane (Figure 3.18; Supplementary movie 2; Supplementary movie 4).

In addition to CD63, RMCPII and Lamp1 were investigated for their utility as a granule maker and to visualize granule dynamics in RBL-2H3 cells (Figure 3.19). In both cases, these markers co-localized with CD63 and did not exhibit significant plasma membrane localization in stimulated cells. Other studies have investigated other markers including serotonin (5-HT; 5-hydroxytryptamine), Lamp-2, cathepsin D, histamine, MHCII, syntaxin-3 and VAMP-7 (Puri and Roche, 2008; Williams et al., 1999; Grutzkau et al., 2004; Vincent-Schneider et al., 2000; Hibi et al., 2000; Williams and Web; 2000). However, these studies were not examining the dynamics of granule markers, but rather, they were identifying distinct subpopulations of granules in RBL-2H3 cells and BMMCs.

## 3.7 Rac1 and Rac2 studies using constitutively-active or dominant-negative mutant proteins

### Localization analysis

Studies in neutrophils suggest that Rac1 and Rac2 localize to different membranes (Filippi et al., 2004; Magalhaes and Glogauer, 2010). Rac1 and Rac2 share 92% amino acid sequence identity (Didsbury et al., 1989), with the C-terminal tails sharing the least identity (Figure 1.2). The different amino acids at the C-terminus are largely responsible for the differential localization of Rac1 and Rac2 in neutrophils, as the C-terminus interacts with membranes. Studies in neutrophils have shown that Rac1 preferentially localizes to the plasma membrane and Rac2 preferentially localizes to the granular membranes (Filippi et al., 2004; Magalhaes and Glogauer, 2010). Therefore, we sought to determine if Rac1 and Rac2 exhibit differential localization to distinct membranes in mast cells. Because commercial antibodies are not available for fluorescent microscopy applications, RBL-2H3 cells were transfected with GFP-tagged versions of Rac1 and Rac2 to visualize localization of the proteins (Figure 3.20 A,B). It was found that there was no significant difference in the localization of Rac1 and Rac2, regardless of the level of protein expression observed by GFP fluorescence. Moreover, the GTPases appeared to be distributed ubiquitously throughout the cell (Figure 3.20 A, B).

### Morphological analysis

To determine if the constitutively-active (Q61L) or dominant-negative (T17N) mutations had an effect on cellular morphology, comparative analysis of RBL-2H3 cells transiently expressing WT-GFP, Q61L-GFP or T17N-GFP mutants of Rac1 or Rac2 was conducted. Cells showed varying levels of GFP expression in the population of transiently transfected cells, which we classified as very low, low and high expression levels (Figure 3.20 C, D). This classification was necessary, as only the 'high' levels of GFP expression showed significant changes in cell morphology. Moreover, the penetrance of morphological defects in high-expressing cells was not 100%, suggesting that there is heterogeneity in the cell population.

It was observed that 70% of cells expressing high levels of GFP-Rac1 Q61L exhibited a spread/flattened morphology in the absence of stimulus (Figure 3.20 C), and 50% of cells expressing high levels of GFP-Rac2 Q61L exhibited a spread/flattened morphology in the absence of stimulus (Figure 3.20 D). Moreover, 25% of cells expressing high levels of GFP-Rac1 T17N failed to exhibit a spread/flattened morphology upon addition of stimulus, however cells that did respond had an abnormal morphology is response to stimulus (Figure 3.20 C). The Rac2 T17N mutant could not be studied as the transfected cells did not express the protein at observable levels of GFP fluorescence.

**Functional analysis**

To analyze the effect of expressing mutant forms of Rac1 and Rac2 proteins on exocytosis, RBL-2H3 cells stably expressing GFP-tagged Rac wild-

type, constitutively active (Q61L) or dominant negative (T17N) mutants were prepared. Vectors were transiently transfected using the Amaxa Nucleofection system to obtain the highest level of transfection; in RBL-2H3 cells this proved to be 10-15% with this transfection method (data not shown). Therefore, if the mutants did exhibit defects in exocytosis, a 10-15% decrease in the total exocytosis of β-hexosaminidase would be expected. In contrast to our previous findings observed with Rac2 KO BMMCs and siRNA knock down of Rac1 and Rac2 in RBL-2H3 cells, no observable affect on β-hexosaminidase exocytosis was observed (Figure 3.21). The low transfection efficiency and variability in mutant protein expression may have been factors contributing to the inability to detect changes in β-hexosaminidase exocytosis between mutants.

To overcome the issue of low transfection efficiency and variability in mutant protein expression, stable cell lines were created using RBL-2H3 cells transfected with GFP tagged wild-type, Q61L or T17N mutant versions of either Rac1 or Rac2. After 2 weeks of growth using neomycin selection, and sorting GFP positive cells via flow cytometry, GFP positive cell populations ranging between 80-90% were obtained for all vectors (data not shown). There was no detectable difference in β-hexosaminidase exocytosis between the stable cultures of mutant and WT forms of Rac1 or Rac2 (Figure 3.22). It is of importance to note that RBL-2H3 cells stably expressing mutant forms of Rac did not exhibit any of the morphologies characteristic of the transiently transfected cells (data not shown).

**Supplementary Movie 1 Live cell DIC imaging of stimulated WT and Rac2 KO BMMCs**

Two fields of views are presented for both WT and Rac2 KO BMMCs, dorsal and ventral. The movie is made at 5 frames per second and spans 60 minutes over the course of stimulation of the BMMCs. DIC images were acquired using a 63X immersion oil lens (Quorum WAVE FX spinning disk confocal with a polariser). Movie can be found on supplementary DVD at back of thesis.

**Supplementary Movie 2 Live cell imaging of a stimulated RBL-2H3 cell**

Cells were double transfected with Lifeact-mRuby and CD63-GFP. Each frame in the movie is comprised of 40 Z slices, each of which is 0.26μm thick. Images were acquired using a 63X immersion lens on a spinning disk confocal microscope (Perkin Elmer UltraVIEW VoX Confocal Imaging System equipped with Leica optics). Movie can be found on supplementary DVD at back of thesis.

**Supplementary Movie 3 Live cell imaging of stimulated RBL-2H3 cells by brightfield microscopy**

The movie is made at 5 frames per second and spans 90 minutes over the course of stimulation of the RBL-2H3 cells. Images are acquired by widefield brightfield microscopy with a 40X oil immersion lens (Zeiss Observer Z1 widefield system). Movie can be found on supplementary DVD at back of thesis.

**Supplementary Movie 4 A, B Live cell imaging of a stimulated RBL-2H3 cell**

Cells were transfected with CD63-GFP. Each frame in the movie is comprised of 40 Z slices, each of which is 0.26μm thick. The movie is made at 5 frames per second and spans 15 minutes over the course of stimulation of the RBL-2H3 cells. Images were acquired using a 63X immersion lens on a spinning disk confocal microscope (Perkin Elmer UltraVIEW VoX Confocal Imaging System equipped with Leica optics). Movie can be found on supplementary DVD at back of thesis.

A.

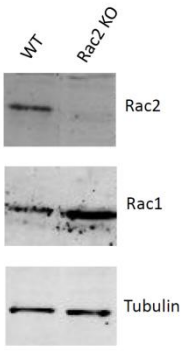
WT
Rac2 KO
Rac2
Rac1
Tubulin

B.

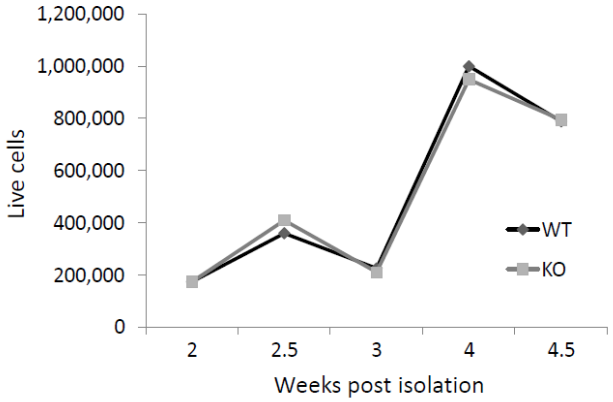
1,200,000
1,000,000
800,000
600,000
400,000
200,000
0
Live cells
2
2.5
3
4
4.5
Weeks post isolation
WT
KO

C.

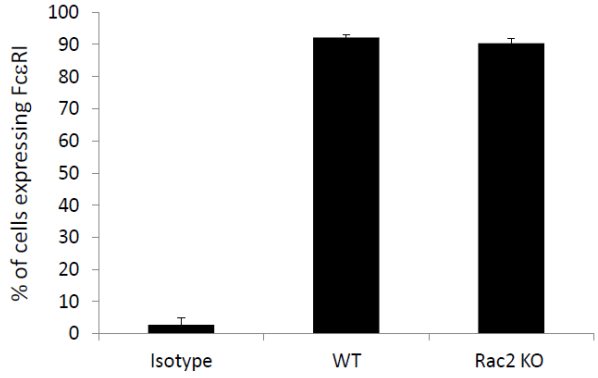
100
90
80
70
60
50
40
30
20
10
0
% of cells expressing FcεRI
Isotype
WT
Rac2 KO

D.

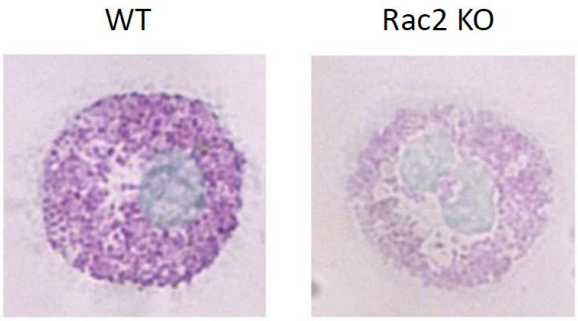
WT
Rac2 KO

E.

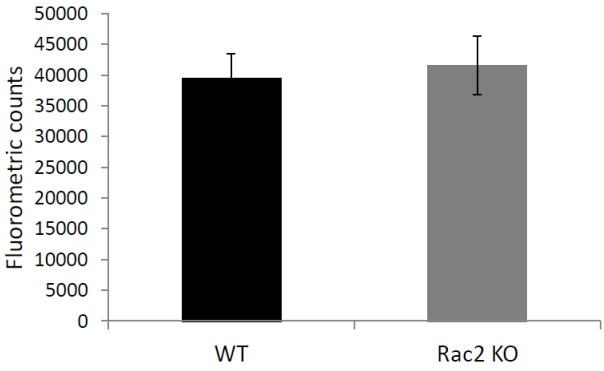
50000
45000
40000
35000
30000
25000
20000
15000
10000
5000
0
Fluorometric counts
WT
Rac2 KO

**Figure 3.1 Characterization of WT and Rac2 KO BMMCs**

Rac2 KO BMMCs are deficient in the Rac2 protein but otherwise exhibit comparable cell growth, FcεRI expression, toluidine blue staining and total β-hexosaminidase content. (A) Protein lysates were prepared from WT and Rac2 KO BMMCs and probed for Rac1, Rac2 and tubulin using anti-Rac1, anti-Rac2 and anti-β-tubulin antibodies. Protein expression was detected by immunoblot analysis. A representative image is displayed. (B) WT (black) and Rac2 KO (grey) BMMCs from 2 - 4.5 weeks post isolation were stained with trypan blue. Viable cells were stained and counted with a hemacytometer. (C) BMMCs were live cell stained with 488-conjugated FcεRI antibody and FcεRI positive cells were detected by flow cytometry. Values represent an average of 5 independent experiments and a biological replicate of n=2. Unpaired Student's T-Test with WT and Rac2 KO give a P value of 0.0717. Therefore, since P >0.05, there is no significant statistical difference between samples. (D) BMMCs were cytospun onto glass microscopy slides, fixed and stained with toluidine blue. Images were acquired using a 40X immersion lens on a light microscope. Representative images are displayed. (E) WT (black) and Rac2 KO (grey) BMMCs were treated with 0.1% TX-100 and total β-hexosaminidase content was measured by fluorometric detection of β-hexosaminidase in the supernatant. Values represent an average of 10 independent experiments and a biological replicate of n=2. Unpaired Student's T-Test with WT and Rac2 KO give a P value of 0.2844. Therefore, since P >0.05, there is no significant statistical difference between samples.

A.

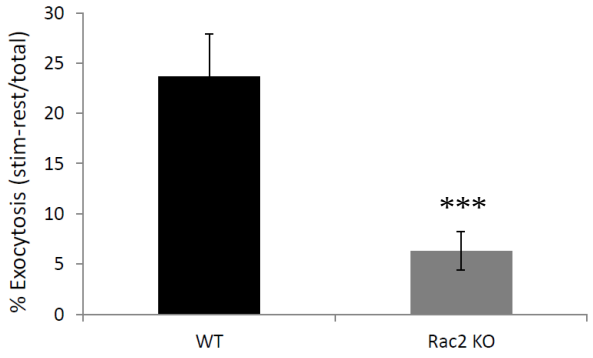


B.

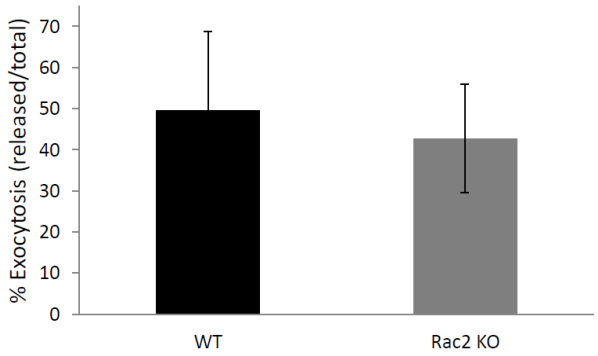


**Figure 3.2 Rac2 KO BMMCs exhibit decreased exocytosis**
(A) BMMCs were sensitized overnight with 60 ng/ml of anti-DNP IgE and then stimulated with 25 ng/ml of DNP-BSA for 30 min. Exocytosis of WT (black) and Rac2 KO (grey) BMMCs was measured by fluorometric detection of β-hexosaminidase released from the cells into the supernatant. Exocytosis is calculated as the percent of total after background subtraction. Values represent an average of five independent experiments per phenotype with a biological replicate of 2. Unpaired Student's T-Test with WT and Rac2 KO give a P value of 0.0001. Therefore, since P <0.05 there is a significant statistical difference between samples. (B) BMMCs were sensitized overnight with 60 ng/ml of anti-DNP IgE and stimulated with calcium ionophore at a final concentration of 500 nM. Values represent an average of 3 independent experiments. Unpaired Student's T-Test with WT and Rac2 KO give a P value of 0.2203. Therefore, since P >0.05 there is no significant statistical difference between samples.

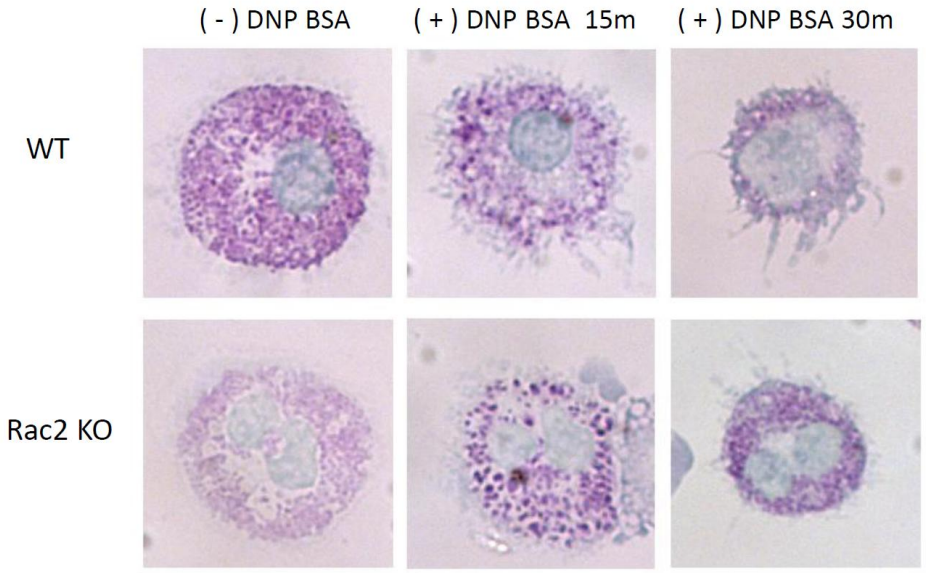


**Figure 3.3 Morphology of WT and Rac2 KO BMMCs**
Rac2 KO BMMCs exhibit altered granule density in response to antigen stimulus. BMMCs were sensitized overnight with 60 ng/ml of anti-DNP IgE and then stimulated with 25 ng/ml of DNP-BSA for 15 or 30 min. Cells were cytospun onto glass microscopy slides, fixed and stained with toluidine blue. Representative images are displayed. All images were acquired using a 40X immersion lens on a light microscope.

A.

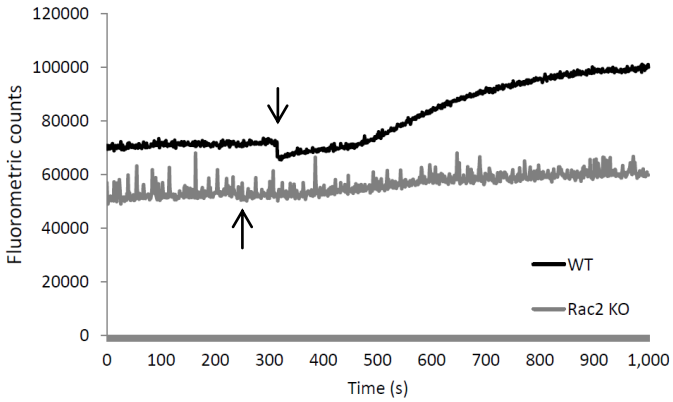


B.

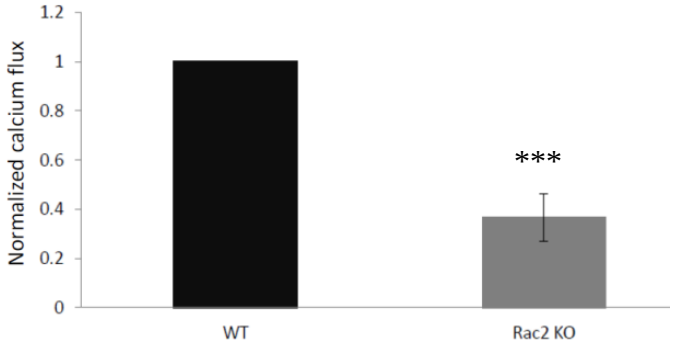


**Figure 3.4 Rac2 KO BMMCs exhibited decreased calcium flux**
BMMCs were sensitized overnight with 60 ng/ml of anti-DNP IgE. Cells were loaded with Fluo-3 and calcium influx into the cells was measured by fluorometry upon stimulation with 25 ng/ml DNP-BSA. Values represent an average of five independent experiments with a biological replicate n=2. (A) Calcium flux curves from WT (black) and Rac2 KO (grey) BMMCs stimulated with DNP-BSA (*arrow*) after approximately 300 s of baseline measurements were taken. Data is expressed in arbitrary units, fluorometric counts. (B) Average slopes from each curve were calculated using data points from 300 - 800 s and are represented as normalized calcium flux relative to WT BMMCs. Data shown is a representative of five independent experiments. Unpaired Student's T-Test with WT and Rac2 KO give a P value of 0.0001. Therefore, since P <0.05 there is a significant statistical difference between samples.

A.

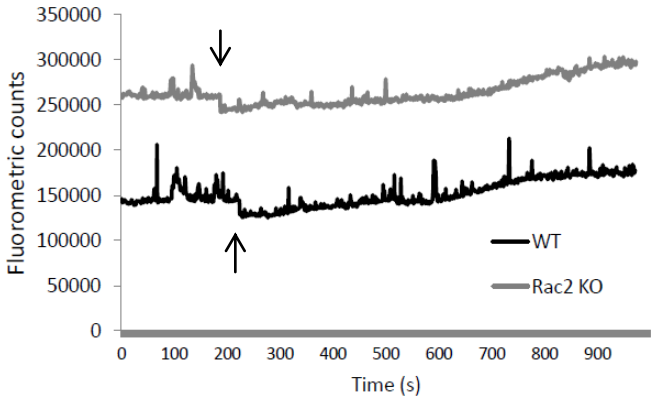


B.

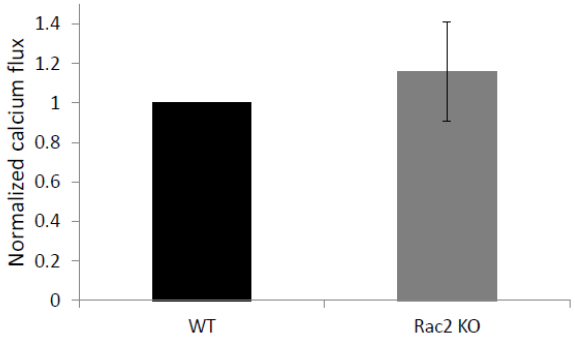


**Figure 3.5 Calcium ionophore restores calcium flux in Rac2 KO BMMCs**
BMMCs were sensitized overnight with 60 ng/ml of anti-DNP IgE. Cells were loaded with Fluo-3 and calcium influx into the cells was measured by fluorimetry upon stimulation with 500nM calcium ionophore. (A) Calcium flux curves from WT (black) and Rac2 KO (grey) BMMCs stimulated with 500 nM calcium ionophore (*arrow*) after approximately 300 s of baseline measurements were taken. Data is expressed in arbitrary units, fluorometric counts. (B) Average slopes from each curve were calculated using data points from 300 - 800 s and are represented as normalized calcium flux relative to WT BMMCs. Data shown in representative of three independent experiments with a biological replicate n=2. Unpaired Student's T-Test with WT and Rac2 KO give a P value of 0.4333. Therefore, since P >0.05, there is no significant statistical difference between samples.

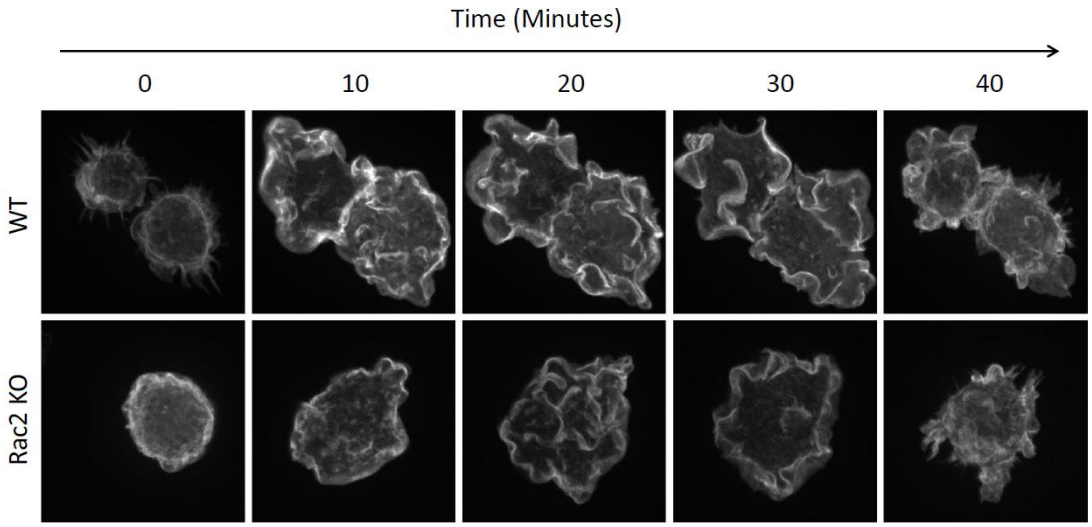


**Figure 3.6 F-actin rich membrane morphology in BMMCs**
Stimulated Rac2 KO BMMCs exhibit less prominent actin-rich membrane remodeling than WT BMMCs. BMMCs were sensitized overnight with 60 ng/ml of anti-DNP IgE and then stimulated with 25 ng/ml of DNP-BSA for 15 min. Cells shown have been stimulated for 15 min, fixed and cytospun onto glass microscopy slides. F-actin was stained with rhodamine-phalloidin. Representative images are displayed. All images were acquired using a 63X immersion lens on a spinning disk confocal microscope (Perkin Elmer UltraVIEW VoX Confocal Imaging System equipped with Leica optics).

A.

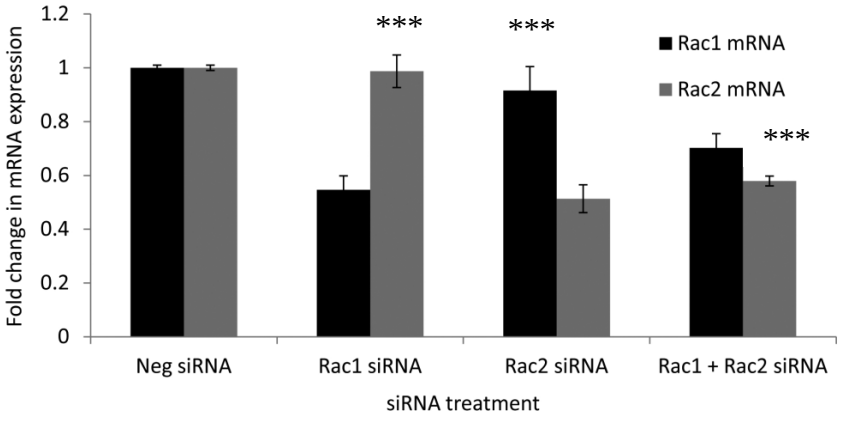


B.

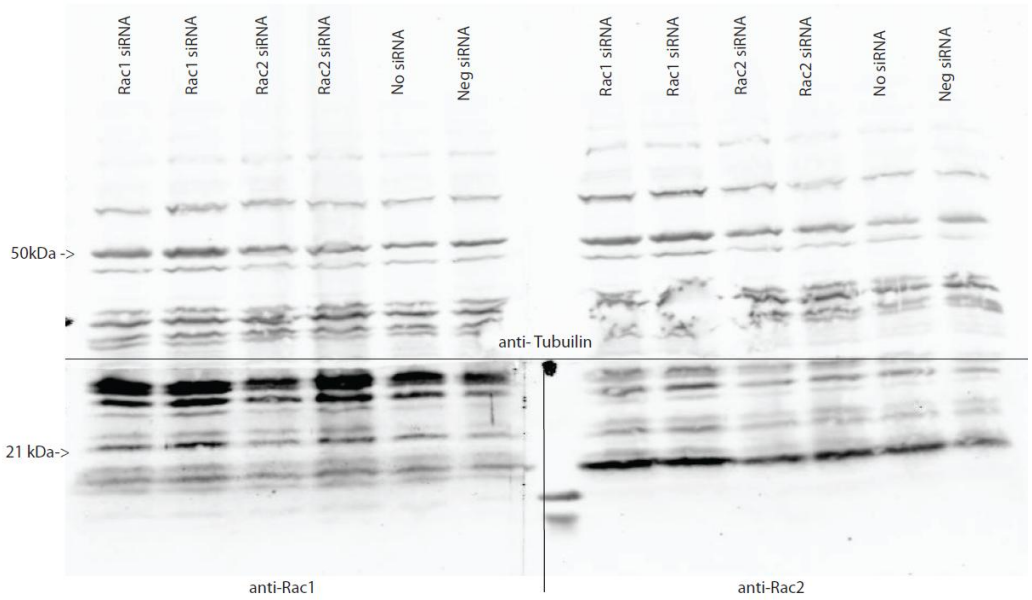


**Figure 3.7 Analysis of Rac1 and Rac2 expression after siRNA knock-down**
Expression of Rac1 and Rac2 in RBL-2H3 cells treated with negative, Rac1 or Rac2 siRNA were quantified by qRT-PCR and immunoblot analysis. (A) mRNA was isolated from RBL-2H3 cells 48 hours post transfection. mRNA levels were detected using qRT-PCR and values obtained were corrected to primer efficiencies for each mRNA and then corrected to the mRNA of a housekeeping gene, GAPDH. Values were normalized to expression of either Rac1 or Rac2 in cells treated with negative siRNA. Values represent an average of four independent experiments. ANOVA analysis for all treatments gives a P value of 0.0001. Individual T-tests for each treatment versus negative siRNA gives a P value of 0.0001. Therefore, since $P < 0.05$ in both tests, there is a significant statistical difference between samples. (B) Lysates were derived from RBL-2H3 cells 48 h post transfection and probed for expression of Rac1 or Rac2 protein. Tubulin was used as a loading control (50 kDa). Representative image is displayed.

A.

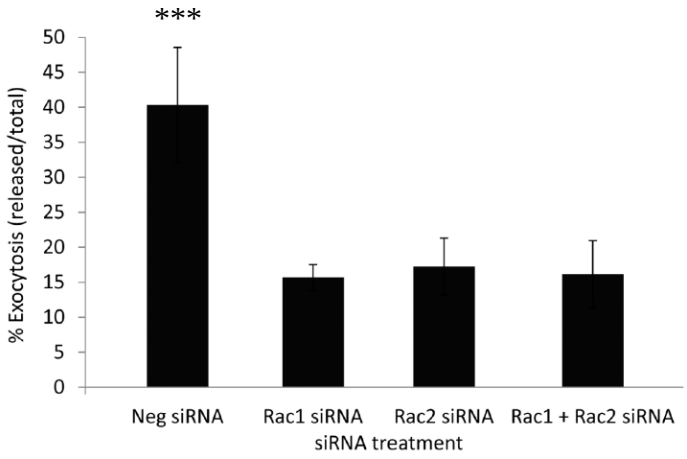
***
% Exocytosis (released/total)
50
45
40
35
30
25
20
15
10
5
0
Neg siRNA
Rac1 siRNA
Rac2 siRNA
Rac1 + Rac2 siRNA
siRNA treatment

B.

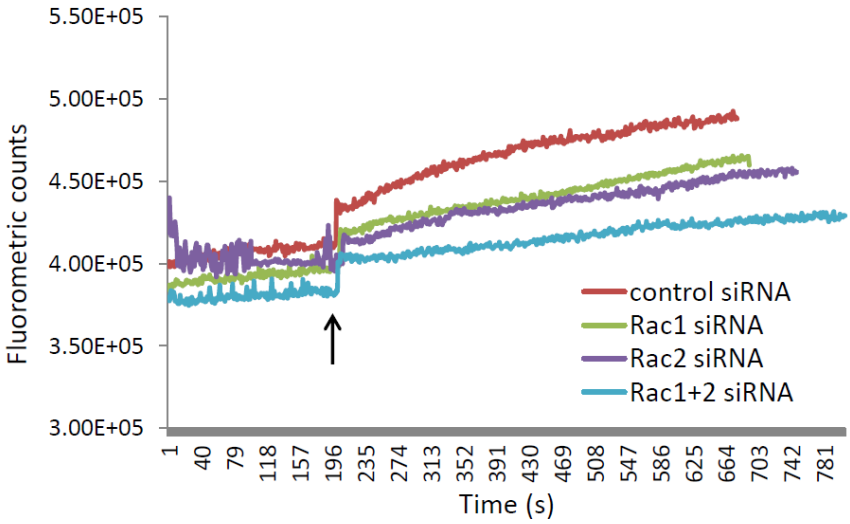
5.50E+05
5.00E+05
4.50E+05
4.00E+05
3.50E+05
3.00E+05
Fluorometric counts
1
40
79
118
157
196
235
274
313
352
391
430
469
508
547
586
625
664
703
742
781
Time (s)
control siRNA
Rac1 siRNA
Rac2 siRNA
Rac1+2 siRNA

C.

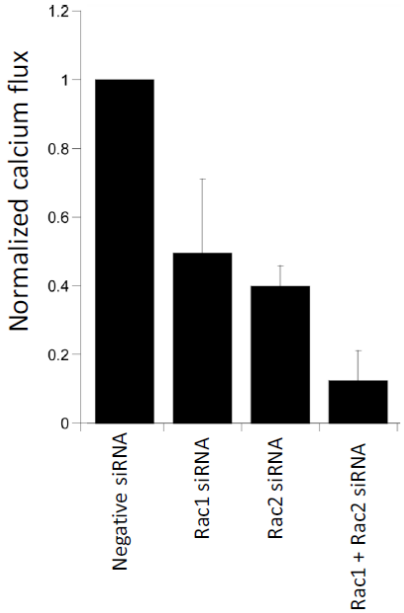
Normalized calcium flux
1.2
1
0.8
0.6
0.4
0.2
0
Negative siRNA
Rac1 siRNA
Rac2 siRNA
Rac1 + Rac2 siRNA

**Figure 3.8 Analysis of calcium flux and exocytosis after Rac1 and Rac2 knock-down**

Rac1 and Rac2 siRNA were used to knock-down their expression in RBL-2H3 cells which resulted in decreased exocytosis and calcium flux. (A) RBL-2H3 cells were sensitized for 2 h with 60 ng/ml of anti-DNP IgE and subsequently stimulated for 30 min. Exocytosis was measured as the release of β-hexosaminidase into the cell supernatant. Exocytosis is expressed as a percentage of total enzyme. Values represent an average of five independent experiments. ANOVA analysis of all treatments gives a P value of 0.0001. Individual T-tests for each treatment versus negative siRNA gives a P value of 0.0001. Therefore, since $P < 0.05$ in both tests, there is a significant statistical difference between samples. (B) Anti-DNP IgE-sensitized cells were loaded with Fluo-3 and calcium influx was measured by fluorometry upon stimulation with 125 ng/ml DNP-BSA (*arrow*) after approximately 200 s of baseline measurements were taken (calcium flux data contributed by M. Cruz-Tleugabulova, Eitzen lab). Values represent an average of two independent experiments. (C) Quantification of calcium flux using the average slope from curves, as shown in *panel B*. Values are normalized relative to negative siRNA.

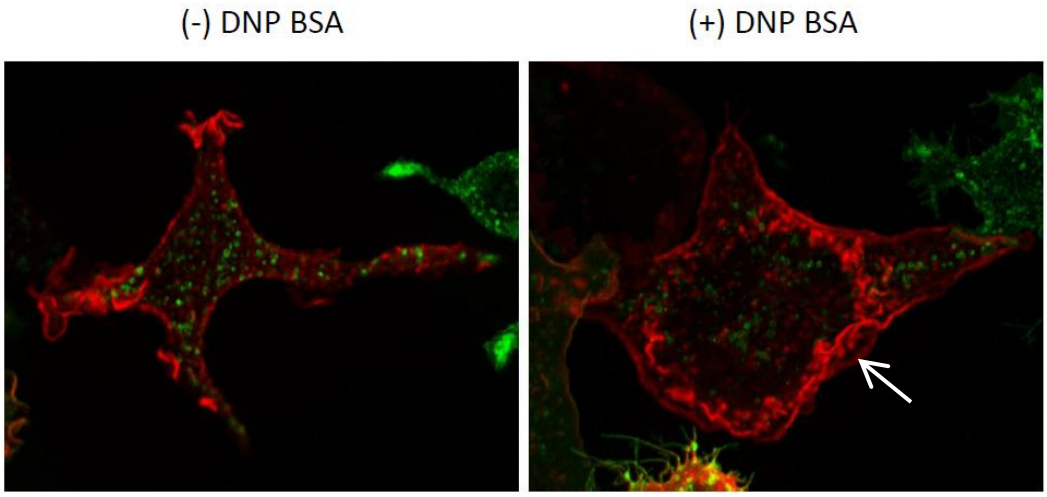


**Figure 3.9 Morphology of F-actin-rich membrane ruffles in stimulated mast cells**

Live cell confocal spinning disc microscopy was used to capture this transient and dynamic F-actin rich membrane formation. RBL-2H3 cells were doubly transfected with Lifeact- mRuby, to visualize F-actin (red) and CD63-GFP to visualize CD63 granules (green) in real time. Polymerized F-actin localizes to antigen induced membrane ruffles in RBL-2H3 cells. Image is of a representative cell exhibiting stimulated morphology of cell spreading and membrane ruffling *(arrow*). The image is a maximum intensity projection of 40 z-slices, each of which is 0.26 μm thick. All images were acquired using a 63X immersion lens on a spinning disk confocal microscope (Perkin Elmer UltraVIEW VoX Confocal Imaging System equipped with Leica optics).

A.

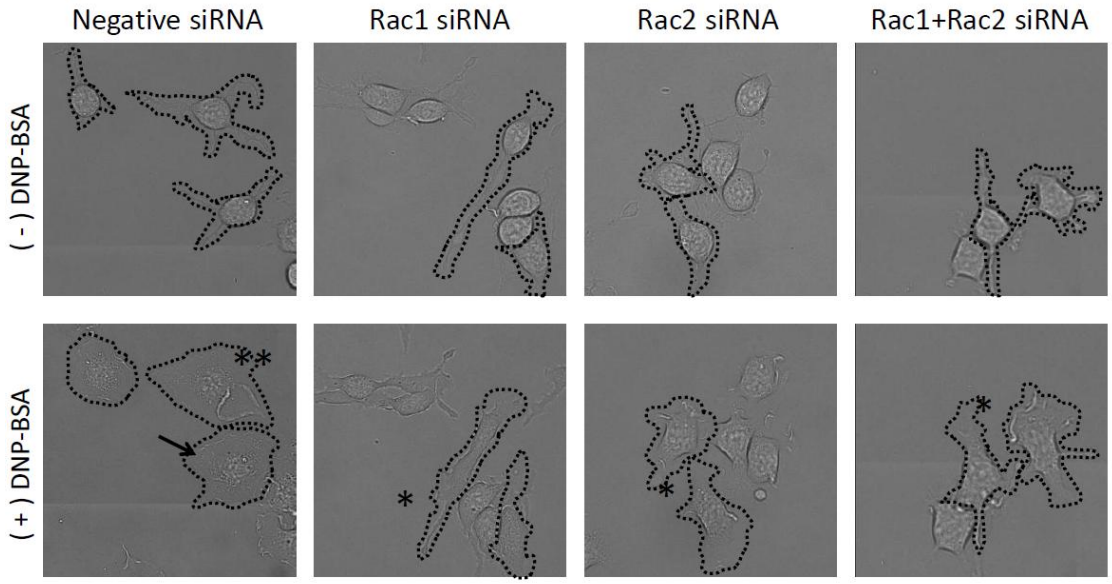


B.

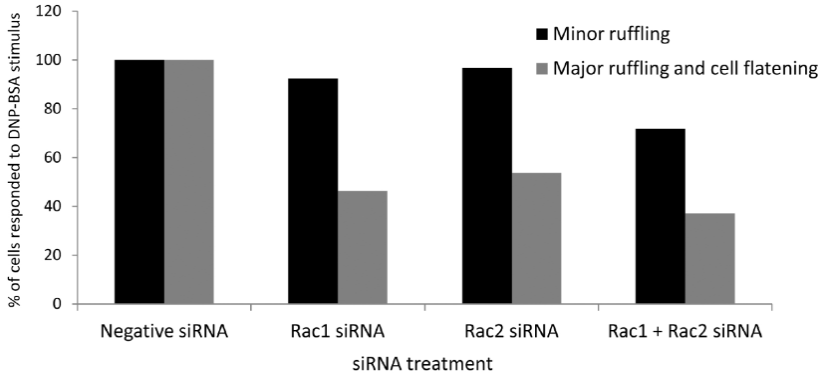


**Figure 3.10 Characterization of membrane ruffling after Rac1 and Rac2 knock-down**

Widefield/brightfield microscopy was used to observe dynamic membrane remodeling events. Rac1 and Rac2 siRNA was used to knock-down expression in RBL-2H3 cells, which resulted in reduced major membrane ruffling and cell flattening in response to stimulus. (A) Images from Cells were treated with the siRNA indicated, then either unstimulated (*upper panels*, (-) DNP-BSA) or stimulated for 15 min (*lower panels*, (+) DNP-BSA). A s*ingle* a*sterisk* indicates minor ruffling, A *double* a*sterisk* indicates major ruffling, and an *arrow* indicates cell flattening. Representative images are displayed. (B) 500 cells of each siRNA treatment were analyzed based on the following morphological criteria: 1. partially stimulated cells that form small ruffles and slightly spread; 2. fully stimulated cells that form large membrane ruffles and completely flatten. Data is represented as % of cells responded to DNP-BSA stimulus according to each morphological criteria. Images are representative of one field of view, acquired by widefield brightfield microscopy with a 40X oil immersion lens (Zeiss Observer Z1 widefield system).

A.

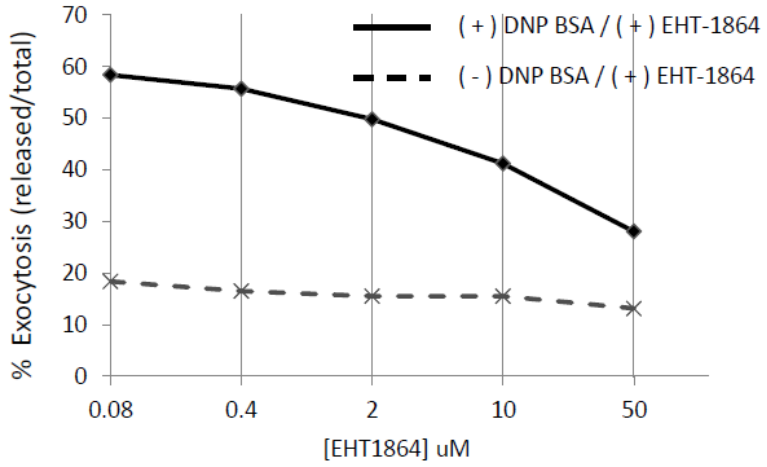


B.

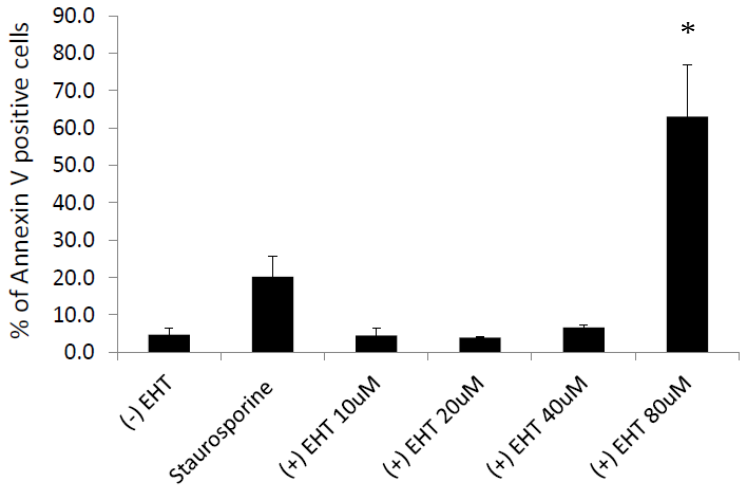


**Figure 3.11 Characterization of the Rac inhibitor, EHT-1864, on exocytosis and apoptosis**

Mast cells were pre-treated with EHT-1864 and examine for effect on exocytosis and apoptosis. (A) Following sensitization RBL-2H3 cells were incubated with 20 μM of EHT-1864 for 10 min prior to stimulation with 25 ng/ml of DNP-BSA for 30 min (data contributed by M. Cruz-Tleugabulova, Eitzen lab). Exocytosis was measured as the release of β-hexosaminidase into the cell supernatant. Exocytosis is expressed as the percentage of total after background subtraction. (B) BMMC cells were treated with various concentrations of EHT-1864 and staurosporine, which is known to induce apoptosis. After 5 h of incubation cells were live-stained with FITC-Annexin V. Annexin V positive cells were detected by flow cytometry. Values represent an average of 5 independent experiments. ANOVA analysis gives a P value of 0.0001. Individual T-tests between (-) EHT and other treatments show (+) EHT 80uM is the only treatment that has statistical significance, $P < 0.05$ ($P=0.016$).

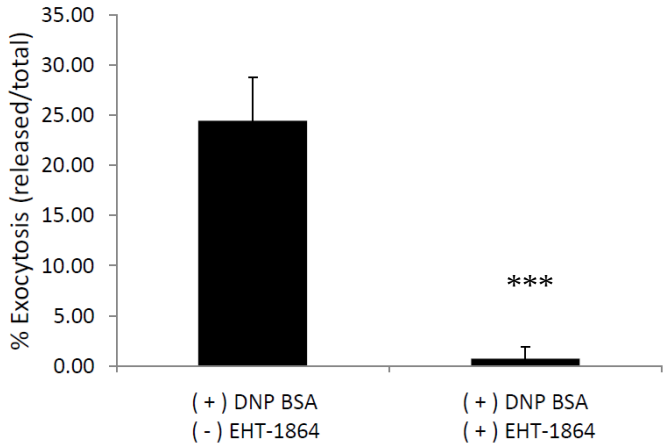


**Figure 3.12 The Rac inhibitor, EHT-1864, inhibits BMMC exocytosis**
BMMCs were sensitized overnight with 60 ng/ml of anti-DNP IgE. Following sensitization, cells were incubated with 40 μM of EHT-1864 for 10 min prior to stimulation with 25 ng/ml of DNP-BSA for 30 min. Exocytosis was measured as the release of β-hexosaminidase into the cell supernatant. Exocytosis is expressed as the percentage of total after background subtraction. Values represent an average of six independent experiments, with a biological replicate of n=2. Unpaired Student's T-Test with (-) EHT and (+) EHT treated BMMCs give a P value of 0.0001. Therefore, since $P<0.05$, there is a statistical difference between samples.

A.

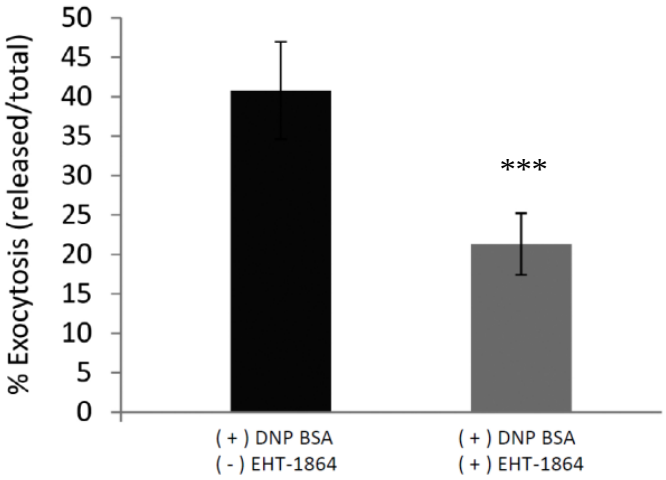


B.

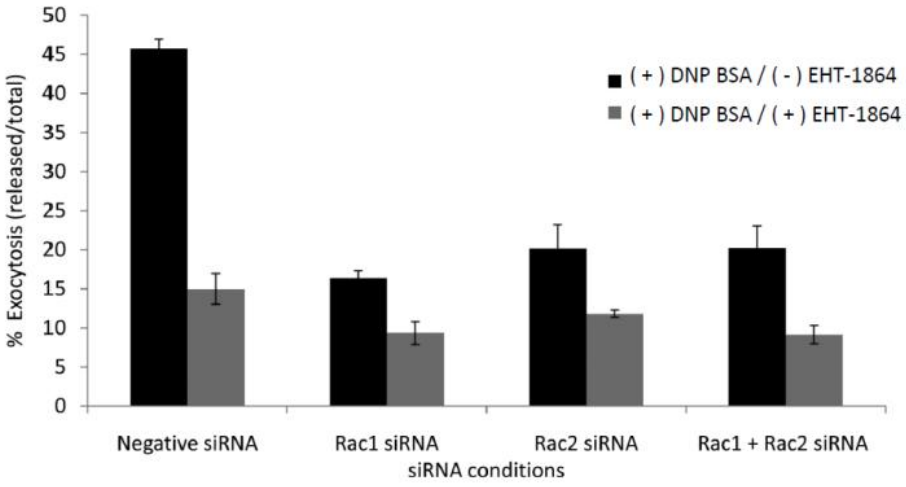


**Figure 3.13 The Rac inhibitor, EHT-1864, partially inhibits RBL-2H3 cell exocytosis**

(A) RBL-2H3 cells and (B) Rac1 and Rac2 siRNA treated RBL-2H3 cells were sensitized for 2 h with 60 ng/ml of anti-DNP IgE. Following sensitization, cells were incubated with 40 μM of EHT-1864 for 10 min prior to stimulation with 125 ng/ml of DNP-BSA for 30 min. Exocytosis was measured as the release of β-hexosaminidase into the cell supernatant. Exocytosis is expressed as the percentage of total after background subtraction. Values represent an average of six independent experiments. Unpaired Student's T-Test with (-) EHT and (+) EHT treated RBL-2H3 cells give a P value of 0.0001. Therefore, since $P<0.05$, there is a statistical difference between samples.

A.

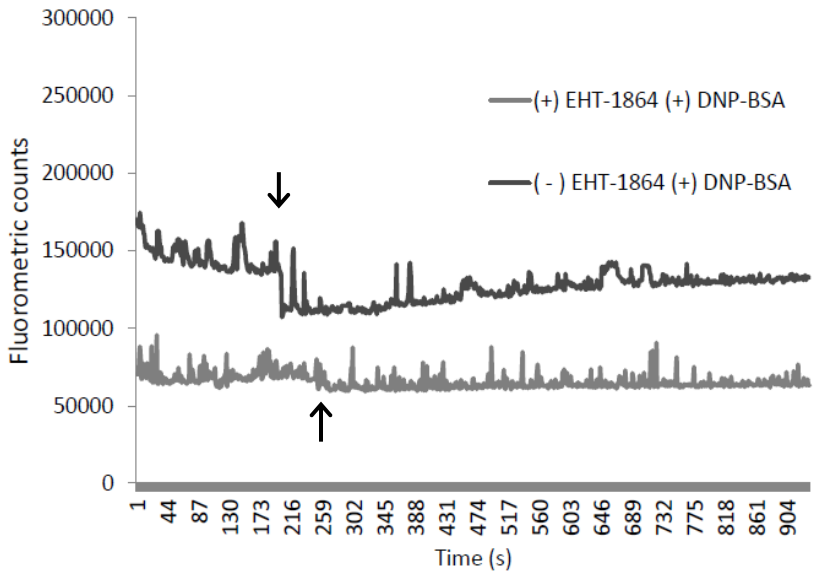
300000
250000
200000
150000
100000
50000
0
Fluorometric counts
(+) EHT-1864 (+) DNP-BSA
( - ) EHT-1864 (+) DNP-BSA
1
44
87
130
173
216
259
302
345
388
431
474
517
560
603
646
689
732
775
818
861
904
Time (s)

B.

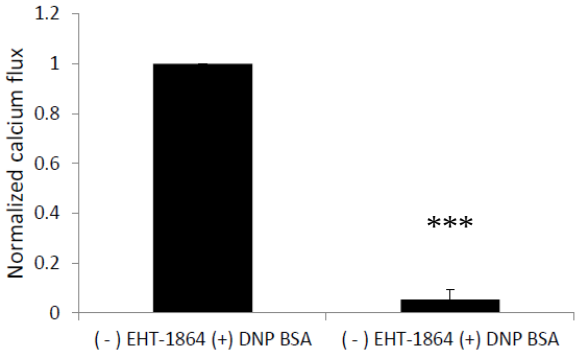
1.2
1
0.8
0.6
0.4
0.2
0
Normalized calcium flux
***
( - ) EHT-1864 (+) DNP BSA
( - ) EHT-1864 (+) DNP BSA

C.

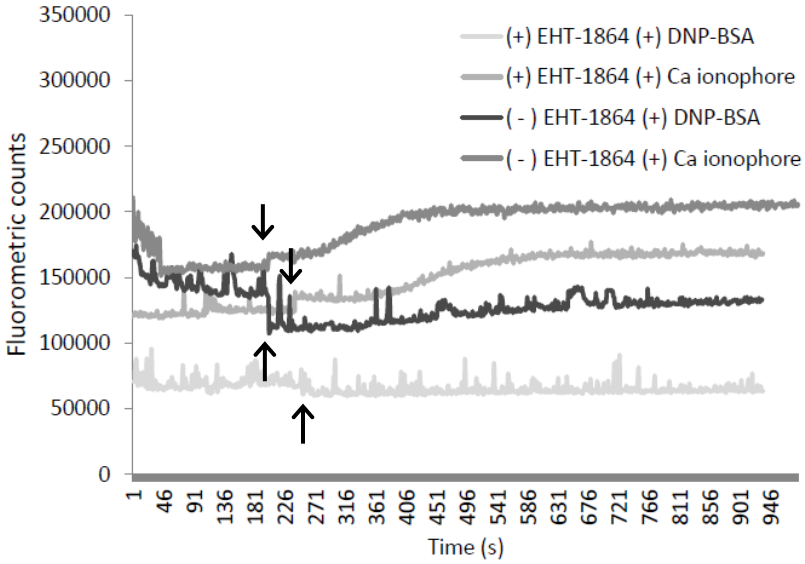
350000
300000
250000
200000
150000
100000
50000
0
Fluorometric counts
(+) EHT-1864 (+) DNP-BSA
(+) EHT-1864 (+) Ca ionophore
( - ) EHT-1864 (+) DNP-BSA
( - ) EHT-1864 (+) Ca ionophore
1
46
91
136
181
226
271
316
361
406
451
496
541
586
631
676
721
766
811
856
901
946
Time (s)

D.


E.

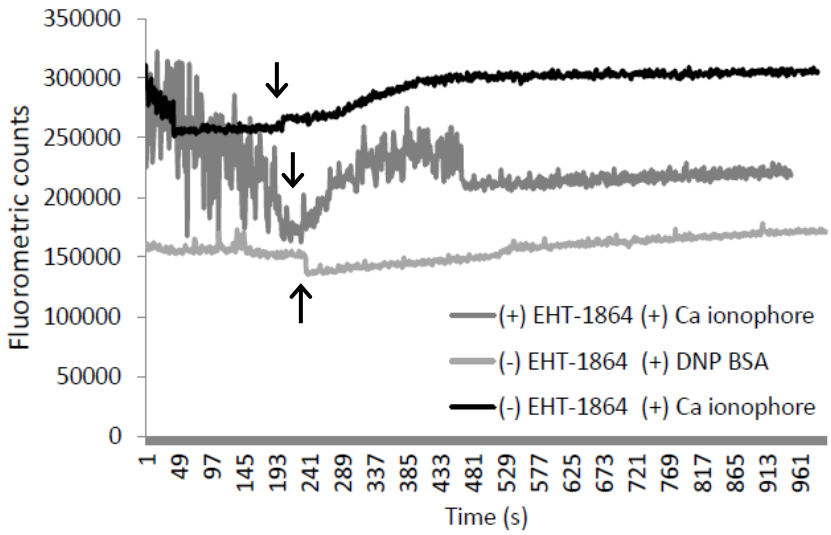


**Figure 3.14 Effect of DNP-BSA and calcium ionophore on EHT-1864 treated BMMCs**

BMMCs were sensitized overnight with 60 ng/ml of anti-DNP IgE. Following sensitization and Fluoro-3 loading, cells were incubated with 40 μM of EHT-1864 for 10 min prior to stimulation. Calcium influx was measured by fluorometry upon stimulation with (A, B) 125 ng/ml of DNP-BSA and (C, D, E) 500 nM calcium ionophore. Data is expressed in arbitrary units, fluorometric counts at emission 516nm. (B, D) Slopes of each curve were calculated (using data points from 300-800 s) and are expressed as a fold change in calcium flux with respect to (-) EHT treatment. (E) Representative calcium flux plot showing inconsistent and variable results obtained for this set of experiments. n=5 for (A) and (B). Results obtained in (B) are statistically significant; Unpaired Student's T-Test with (-) EHT and (+) EHT treated BMMCs give a P value of 0.0001 ($P<0.05$).

A.

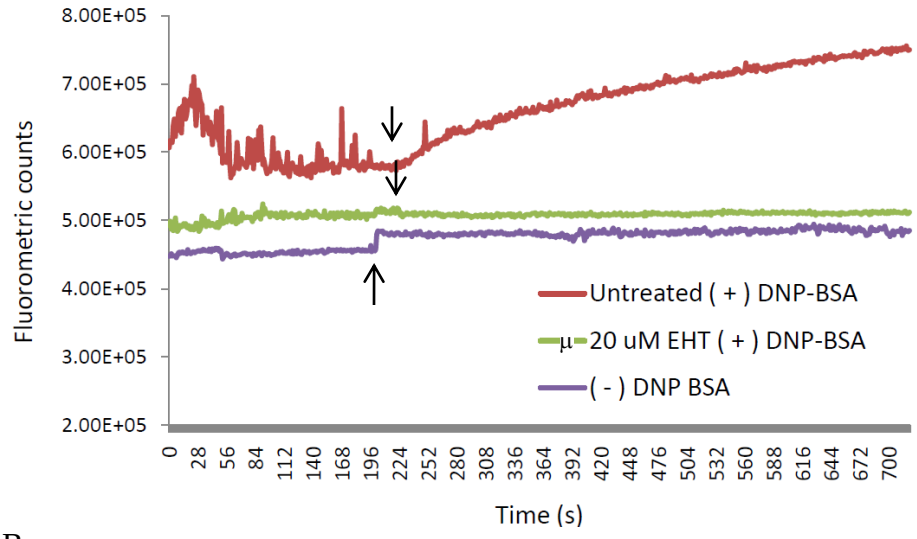
8.00E+05
7.00E+05
6.00E+05
5.00E+05
4.00E+05
3.00E+05
2.00E+05
Fluorometric counts
0
28
56
84
112
140
168
196
224
252
280
308
336
364
392
420
448
476
504
532
560
588
616
644
672
700
Time (s)
Untreated ( + ) DNP-BSA
20 uM EHT ( + ) DNP-BSA
( - ) DNP BSA

B.

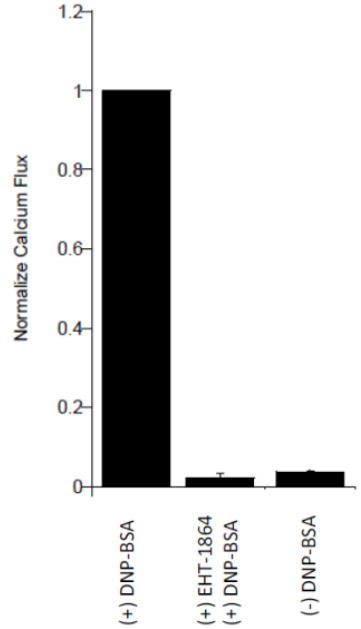
1.2
1
0.8
0.6
0.4
0.2
0
Normalize Calcium Flux
(+) DNP-BSA
(+) EHT-1864 (+) DNP-BSA
(-) DNP-BSA

C.

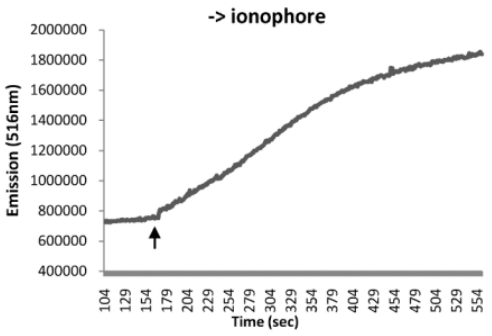
-> ionophore
2000000
1800000
1600000
1400000
1200000
1000000
800000
600000
400000
Emission (516nm)
104
129
154
179
204
229
254
279
304
329
354
379
404
429
454
479
504
529
554
Time (sec)

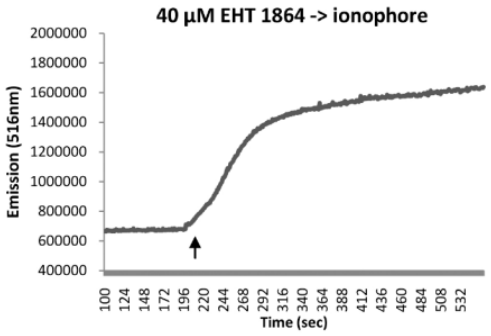
40 µM EHT 1864 -> ionophore
2000000
1800000
1600000
1400000
1200000
1000000
800000
600000
400000
Emission (516nm)
100
124
148
172
196
220
244
268
292
316
340
364
388
412
436
460
484
508
532
Time (sec)

**Figure 3.15 Effect of DNP-BSA and calcium ionophore on EHT-1864 treated RBL-2H3s**

RBL-2H3 cells were sensitized for 2 h with 60 ng/ml of anti-DNP IgE and then pre-treated with 40 μM of EHT-1864 for 10 min prior to stimulation. EHT-1864 pre-treated RBL-2H3 cells were loaded with Fluo-3 and calcium influx was measured by fluorometry upon stimulation with (A) 125 ng/ml DNP-BSA (*arrow*) or (C) calcium ionophore (*arrow*) after approximately 200 s of baseline measurements were taken. (B) Quantification of calcium flux using the average slope from curves. Values are normalized relative to negative siRNA. Data is expressed in arbitrary units, fluorometric counts at emission 516 nm. (n=2). Data contributed by M. Cruz-Tleugabulova, Eitzen lab.

A.

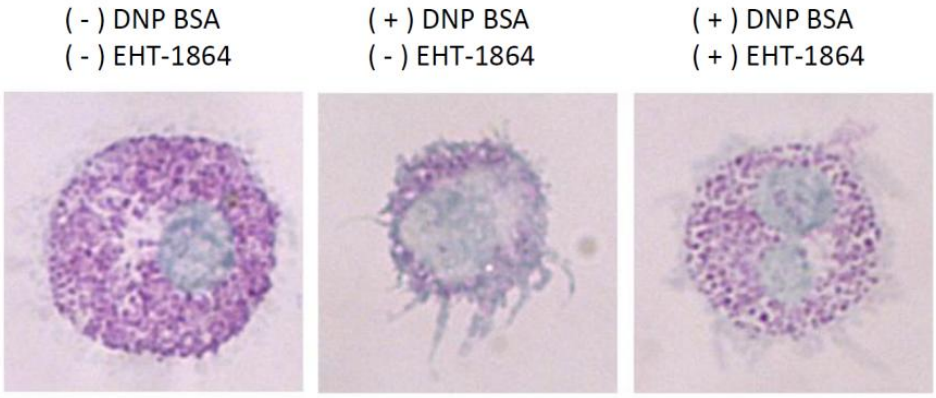


B.

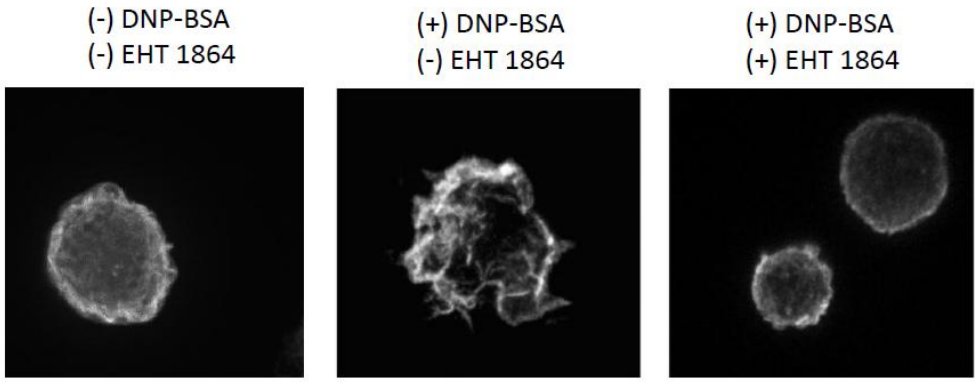


**Figure 3.16 EHT-1864 perturbs antigen induced membrane remodeling in BMMCs**

BMMCs were sensitized overnight with 60 ng/ml of anti-DNP IgE, pretreated with 40μM EHT-1864 for 10 min and then stimulated with 25 ng/ml of DNP-BSA for 15 or 30 min. Cells were cytospun onto glass microscopy slides and fixed. (A) BMMCs were stained with toluidine blue. Image set for each condition shows a representative sampling of various morphologies and staining darkness observed. All images were acquired using a 40X immersion lens on a light microscope. (B) BMMCs were stimulated for 15 m prior to fixation, cytospun and stained with rhodamine phaloidin-546. Images were acquired with a spinning disk confocal microscope with a 63X oil immersion lens (Perkin Elmer UltraVIEW VoX Confocal Imaging System equipped with Leica optics). Images are maximum intensity projections compiled from 20 z-slices, each of which is 0.26 μm thick.

A.

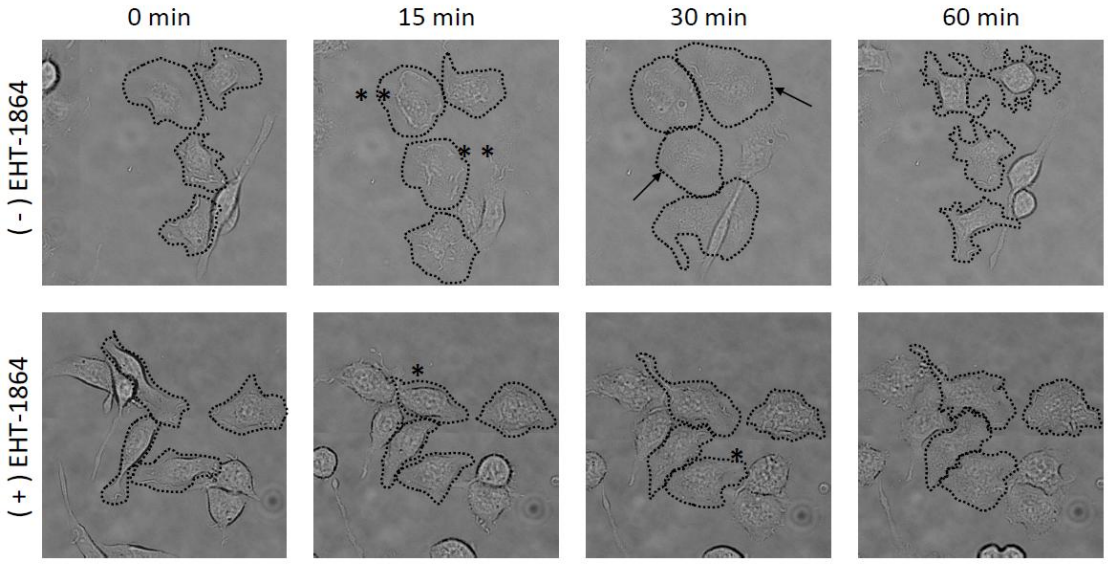


B.

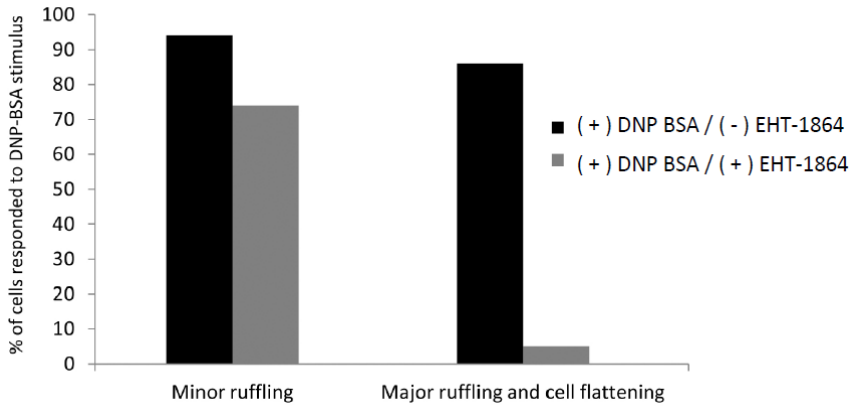


**Figure 3.17 EHT-1864 perturbs antigen induced membrane remodeling in RBL-2H3 cells**

Widefield/brightfield microscopy was used to observe dynamic membrane remodeling events. (A) Cells were sensitized for 2 h with 60 ng/ml of anti-DNP IgE, incubated with 40 μM EHT-1864 for 10 min and then stimulated with 125 ng/ml of DNP-BSA, then imaged. All images from untreated and EHT-1864 treated were time matched at T = 0, 15, 30 and 60 min post stimulation. Images are representative of one field of view, acquired by widefield/brightfield microscopy (Zeiss Observer Z1 widefield system) (B) A s*ingle* a*sterisk* indicates minor ruffling; a *double* a*sterisk* indicates major ruffling; an *arrow* indicates cell flattening. Representative images are displayed. (C) 150 cells of untreated or EHT-1864 were analyzed based on the following morphological criteria: 1. partially stimulated cells that form small ruffles and slightly spread; 2. fully stimulated cells that form large membrane ruffles and completely flatten. Data is represented as % of cells responded to DNP-BSA stimulus according to each morphological criteria.

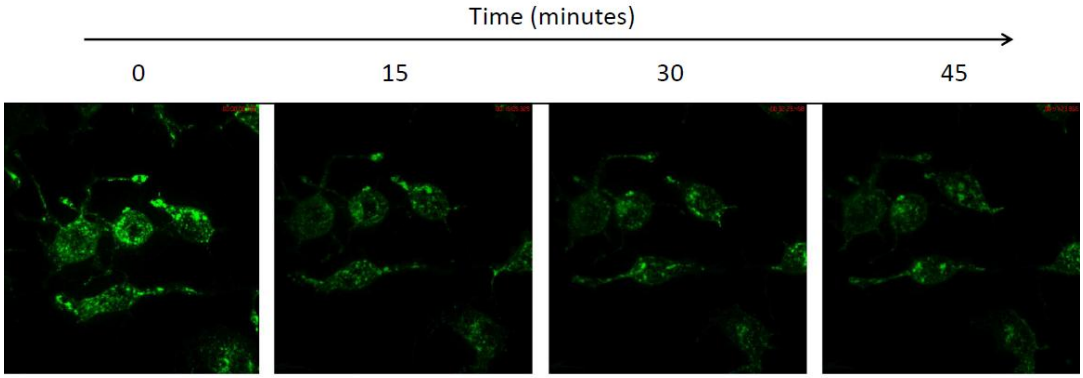


**Figure 3.18 Dynamics of CD63-GFP granules in RBL-2H3 cells**
RBL-2H3 cells were transfected with CD63-GFP to visualize CD63 granules (green) in real time. Cells were sensitized for 2 h with 60 ng/ml of anti-DNP IgE and then stimulated with 125 ng/ml of DNP-BSA upon acquisition. Images are maximum intensity projections of 40 z-slices, each of which is 0.26 μm thick. Live cell confocal spinning disc microscopy was used to capture the granule movements of this cell (Perkin Elmer UltraVIEW VoX Confocal Imaging System equipped with Leica optics).Frames correspond to the specified time post stimulation.

A.

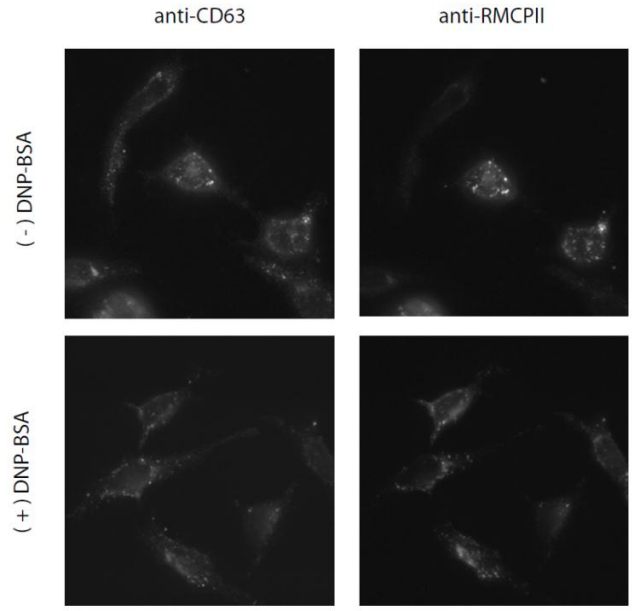


B.

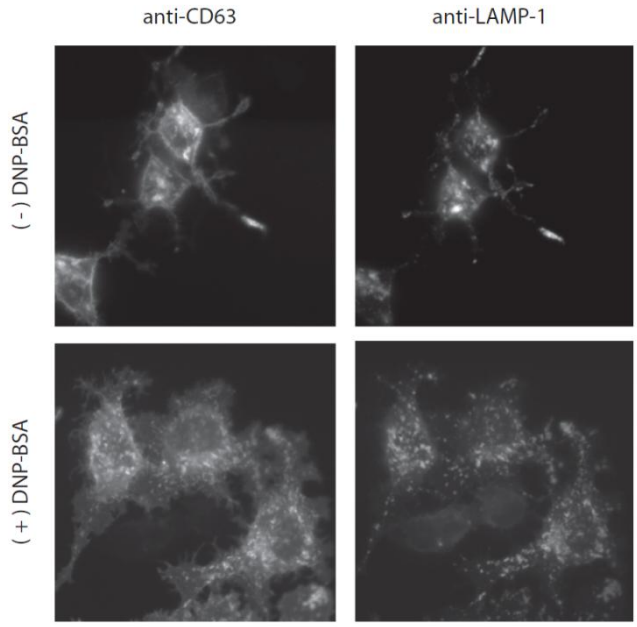


**Figure 3.19 Localization of RMCPII and Lamp1 positive granules in RBL-2H3 cells**

Images are maximum intensity projections of 40 z-slices, each of which is 0.26 μm thick. Cells were sensitized for 2 h with 60 ng/ml of anti-DNP IgE and stimulated with 125 ng/ml of DNP-BSA. Cells were fixed and stained with (A) anti-CD63 and anti-RMCPII or (B) anti-CD63 and anti-Lamp-1. Live cell confocal spinning disc microscopy was used to acquire images (Perkin Elmer UltraVIEW VoX Confocal Imaging System equipped with Leica optics).

A.

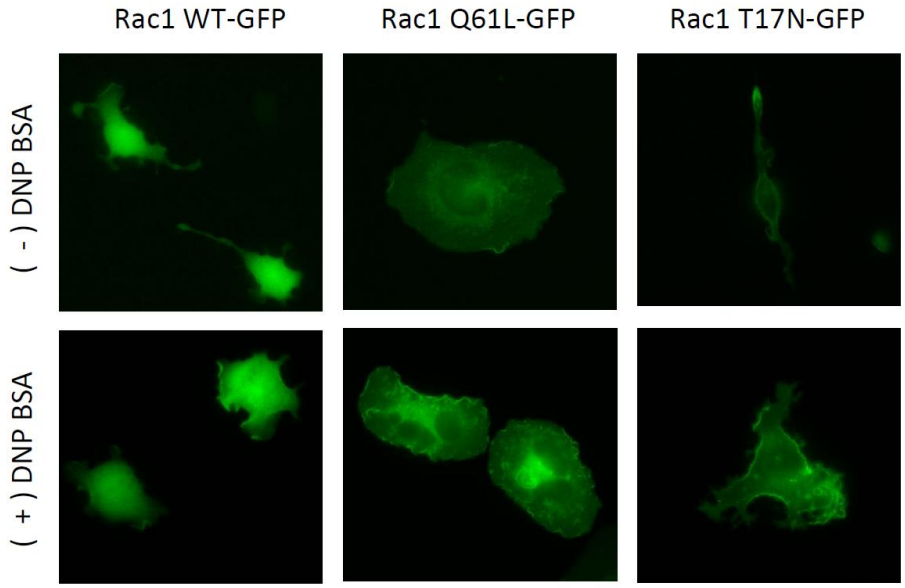
Rac1 WT-GFP
Rac1 Q61L-GFP
Rac1 T17N-GFP
( - ) DNP BSA
( + ) DNP BSA

B.

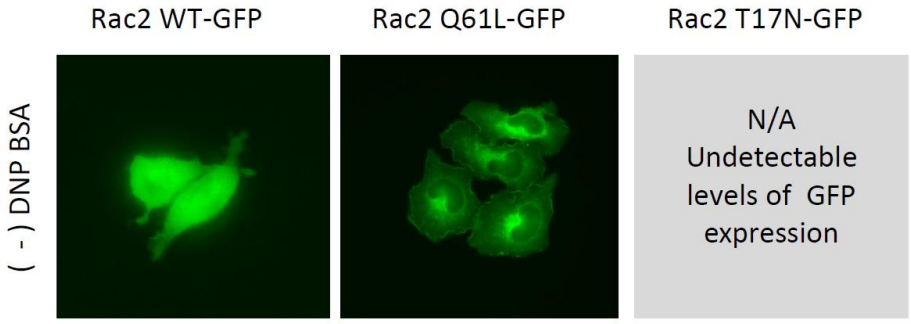
Rac2 WT-GFP
Rac2 Q61L-GFP
Rac2 T17N-GFP
( - ) DNP BSA
N/A
Undetectable
levels of GFP
expression

C.

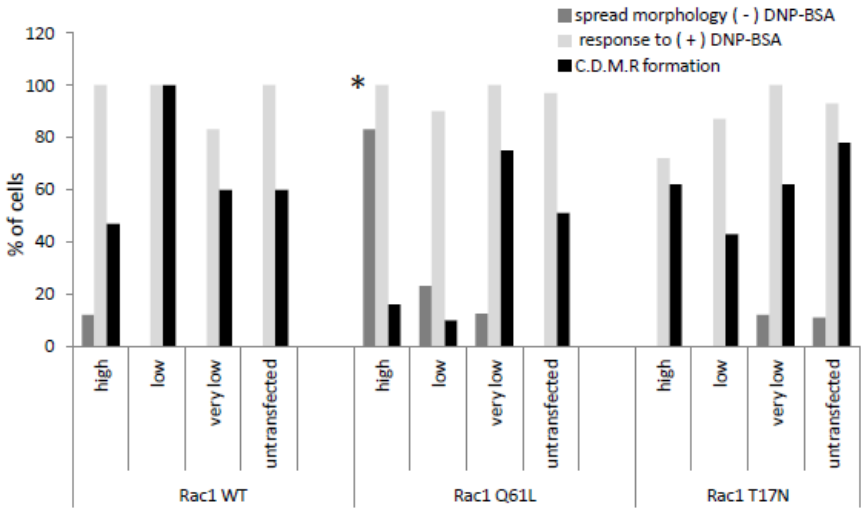
spread morphology ( - ) DNP-BSA
response to ( + ) DNP-BSA
C.D.M.R formation
% of cells
120
100
80
60
40
20
0
*
high
low
very low
untransfected
Rac1 WT
Rac1 Q61L
Rac1 T17N

D.

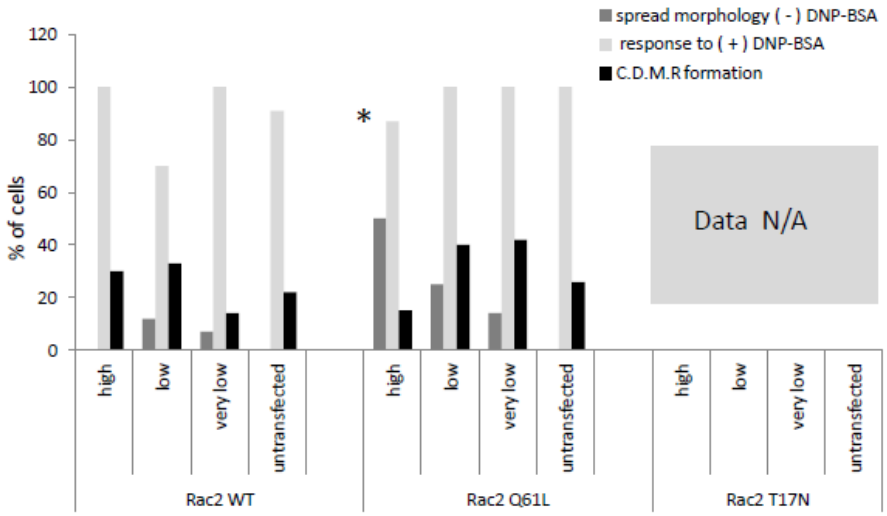


**Figure 3.20 Characterization of Rac1-GFP and Rac2-GFP expression**
WT, constitutively active (Q61L) and dominant negative (T17N) Rac1 (A) or Rac2 (B) mutants were expressed in RBL-2H3 cells. Cells were sensitized for 2 h with 60 ng/ml of anti-DNP IgE and then stimulated with 125 ng/ml of DNP-BSA upon acquisition. Representative images are shown. Images are maximum intensity projections of 40 z-slices, each of which is 0.26 μm thick. Live cell confocal spinning disc microscopy was used to acquire images (Perkin Elmer UltraVIEW VoX Confocal Imaging System equipped with Leica optics). Rac1-GFP (C) and Rac2-GFP (D) WT, Q61L, and T17N mutants were morphologically characterized by examining a series of live cell images. Varying levels of GFP expression was observed in the population of transiently transfected cells classified as very low, low and high expression levels. Cells were morphologically characterized by the presence of a spread or flattened morphology in the absence of DNP-BSA, response to DNP-BSA (presence of membrane ruffles and cell flattening) and the formation of circular dorsal membrane ruffles (CDMRs) (prominent, major dorsal ruffles).

A.

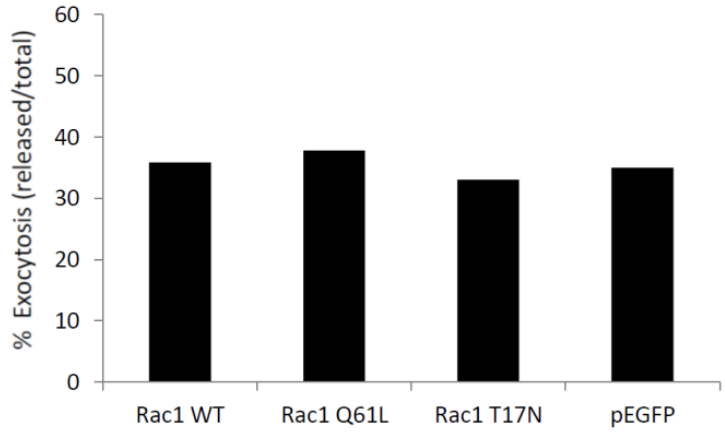


B.

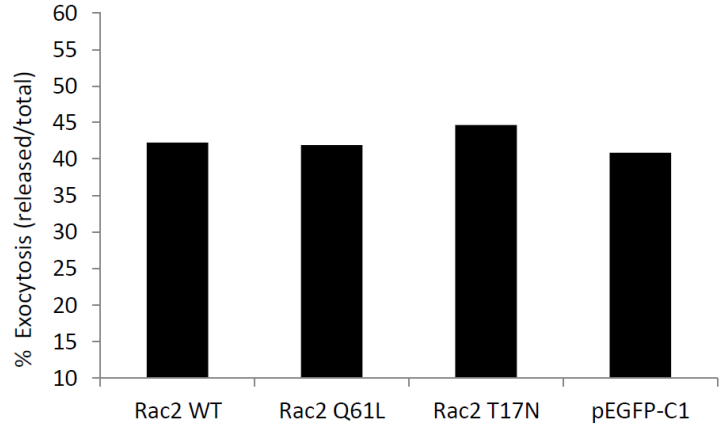


**Figure 3.21 Transiently transfected RBL-2H3 cells expressing Rac1 and Rac2 GFP mutants exhibit no reduction in exocytosis**

RBL-2H3 cells were transfected with pEGFP-C1 vectors containing WT, Q61L or T17N mutant Rac1 (A) or Rac2 (B). Cells were sensitized for two hours with 60 ng/ml of anti-DNP IgE and then stimulated with 125 ng/ml of DNP-BSA for 30min. Exocytosis was measured as the release of β-hexosaminidase into the cell supernatant. Exocytosis is expressed as the percentage of total after background subtraction.

A.

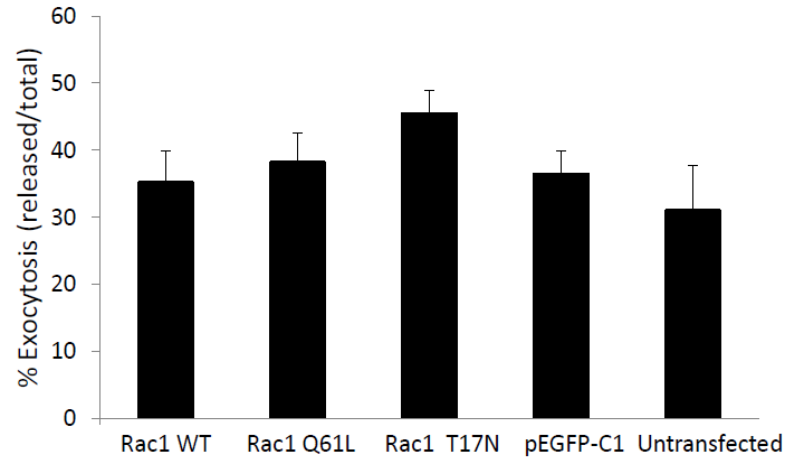


B.

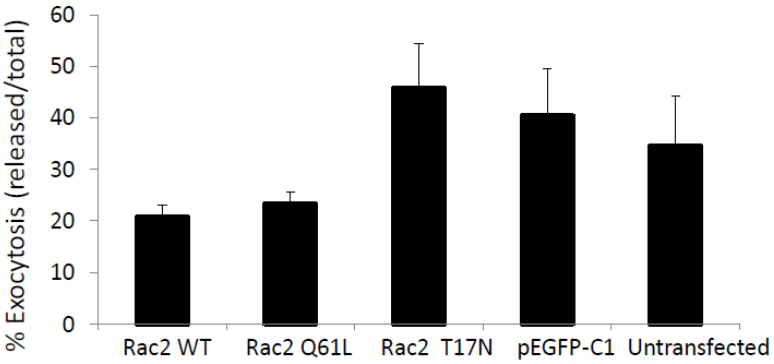


**Figure 3.22 Stable RBL-2H3 cells expressing Rac1 and Rac2 GFP mutants exhibit no reduction in exocytosis**

RBL-2H3 cells were transfected with pEGFP-C1 vectors containing WT, Q61L or T17N mutant Rac1 or Rac2, grown under neomycin resistant conditions and sorted to produce cultures stably expressing Rac1 (A) and Rac2 (B). Cells were sensitized for two hours with 60 ng/ml of anti-DNP IgE and then stimulated with 125 ng/ml of DNP-BSA for 30 m. Exocytosis was measured as the release of β-hexosaminidase into the cell supernatant. Exocytosis is expressed as the percentage of total after background subtraction. Values represent an average of two independent experiments.

# CHAPTER 4

# DISCUSSION

Mast cells are tissue-resident immune cells involved in initiating inflammatory responses via antigen-induced exocytosis of pro-inflammatory molecules such as histamine and cytokines. Mast cell activation via FcεRI-mediated signaling results in several cellular events; increase in cytosolic levels of calcium, exocytosis of preformed mediators contained within intracellular granules (a.k.a. degranulation), generation of lipid-derived mediators and the synthesis and secretion of cytokines and chemokines (reviewed in Metcalfe et al., 1997). Rho GTPases may act as central regulators of several of these processes in immune cells. Studies in neutrophils have demonstrated roles for Rho GTPases, Rac1 and Rac2 in the regulation of exocytosis in conjunction with actin remodelling in neutrophils (Li et al., 2002; Abdel-Latif et al., 2004; Sun et al., 2007). Our hypothesis is that signal transduction events that trigger exocytosis converge through a Rac GTPase-mediated pathway. Of particular interest to this study is to further define the function of Rac2, which is an immune cell-specific Rho GTPase.

## 4.1 Exocytosis and calcium flux are Rac2 dependent processes in bone marrow-derived mast cells

Rac2 is known to be required for primary granule exocytosis in neutrophils and c-kit induced exocytosis in mast cells (Abdel-Latif et al., 2004; Yang et al., 2000). In light of these findings, we hypothesized that Rac2 regulates calcium flux for exocytosis. My findings show that Rac2 is required for FcεRI-mediated exocytosis and calcium flux (Figures 3.2, 3.4). Rac2 KO BMMCs

exhibited a 72% reduction in exocytosis and a 63% reduction in calcium, when compared to WT BMMCs. These findings are consistent with the findings of Yang et al. (2000) as they also observed a decrease in c-kit activated exocytosis in Rac2 KO BMMCs. That a complete abrogation was not observed was not surprising, since other studies using BMMC KO cells have reported comparable levels of reduction in exocytosis, regardless of the Rac gene that was knocked out (Manetz et al., 2001; Alvarex-Errico et al., 2010; Suzuki et al., 2010). Taken together, these results suggest that Rac2 regulates FcεRI-mediated exocytosis and calcium flux. Furthermore, these findings suggest that Rac2 may regulate pathway components that are common to both c-kit and FcεRI signaling pathways.

Two of the most proximal tyrosine kinases in the FcεRI pathway, Fyn and Lyn, exhibit differential regulation on calcium flux and exocytosis pathways (Figure 1.1). Fyn kinase KO BMMCs exhibited decreased exocytosis and PI3K activity, but maintained normal levels of calcium flux (Parravicini et al., 2002; Suzuki et al., 2010). Conversely, Lyn kinase KO BMMCs exhibited decreased calcium flux, while exocytosis was enhanced (Alvarex-Errico et al., 2010). Moreover, in Syk KO BMMCs, both calcium flux and exocytosis was reduced (Costello et al., 1996), suggesting that Syk is a proximal regulator of both the calcium and exocytosis regulatory pathways. Taken together, these results suggest that divergent proximal pathways regulate calcium flux and exocytosis within the FcεRI pathway, and that these pathways may be convergently regulated.

In light of previous studies, my findings that Rac2 KO BMMCs did not exhibit exocytosis and calcium flux suggests a role for Rac2 in regulating these

distinct pathways at a point of convergence in the FcεRI pathway. Rac2 KO BMMCs exhibited similar cellular defects to the Syk KO BMMCs, as both calcium flux and exocytosis were decreased. Rac2 could regulate the distinct pathways of calcium flux and exocytosis or alternatively act on a point of convergence in the pathway that regulates both the calcium flux and exocytosis pathways. Baba et al. (2008) and Vig et al. (2008) showed increases in intracellular calcium are required to trigger exocytosis in mast cells. These studies showed that exocytosis and calcium flux was abrogated in BMMCs deficient in CRAC plasma membrane channel proteins. This suggests that exocytosis cannot occur without functional store-operated calcium entry (SOCE), which requires CRAC plasma membrane channel proteins. Therefore, it may be possible that Rac2 regulates these processes at the level of the plasma membrane CRAC channels, which are responsible for regulating intracellular calcium during exocytosis.

### 4.2 FcεRI-mediated actin rich membrane ruffling is not Rac2 dependent in BMMCs

Rac2 is the predominant Rho GTPase involved in actin remodelling in neutrophils (Li et al., 2002 and Sun et al., 2007). Therefore, we hypothesized that Rac2 would have a similar role in regulating actin remodelling events in mast cells. While it was found that Rac2 KO BMMCs exhibited reduced exocytosis and calcium flux (Figure 3.2, 3.4), there was no effect on actin rich membrane remodelling (Figure 3.6, Supplementary Movie1). However, substantial evidence

from work in neutrophils suggests that Rac2 has a function in actin remodelling, which contrasts with my findings in mast cells. Li et al. (2002) showed that Rac2 KO mouse neutrophils exhibited drastically reduced F-actin formation and migration in response to stimulus. Moreover, studies in neutrophils have shown that Rac2 is responsible for nucleating the majority of the free barbed ends of F-actin in the cell via interaction with Arp2/3 (Sun et al., 2007). Rac is a known regulator of Arp2/3 – WAVE dependent actin branching and nucleation, a process that is required for the formation of actin-rich membrane ruffling and cell spreading (Suetsugu et al., 2003). However, it remains unclear as to whether Rac1 and Rac2 differentially regulate the WAVE family members in this process. Therefore, one possible explanation for this discrepancy is that although Rac2 is the dominant regulator of actin remodelling, Rac1 may have compensatory functions in Rac2 KO BMMCs. When protein lystates were compared by western blot analysis, I found that, in contrast to WT BMMCs, which express Rac1 and Rac2 proteins at equal levels, Rac2 KO BMMCs exhibited elevated protein expression of Rac1 in the absence of Rac2 (Figure 3.1 A). This is different from Rac2 KO neutrophils which do not exhibit elevated expression of Rac1 in comparison to WT BMMCs and therefore may not exhibit compensatory functions (Roberts et al., 1999). This suggests that Rac1 expression is elevated in the absence of Rac2 only in mast cells. This aligns with previous studies which showed a 3 fold increase in Rac1 expression in Rac2 KO BMMCs (Yang et al., 2000).

An alternative explanation for the lack of an effect on actin remodelling is that unlike neutrophils, the primary regulator of actin remodelling in mast cells is Rac1. Neutrophils are highly motile cells, whereas mast cells are sedentary cells that reside in tissues. Therefore, due to the different motility functions of these cells, Rac1 and Rac2 may exhibit different regulatory roles within each cell type to accommodate distinct functional requirements. Furthermore, studies in RBL-2H3 mast cells suggest that Rac1 is the predominant regulator of actin-rich membrane remodelling. Guillemot et al. (1997) found that expression of a Rac1 dominant negative mutant resulted in the failure to display actin-rich membrane remodelling.

My finding that Rac2 KO BMMCs did not exhibit defects in actin remodelling does not fully agree with the work of Yang et al. (2002). They showed that Rac2 KO BMMCs exhibited decreased actin-mediated migration in response to c-kit activation. The fact that Rac2 KO BMMCs did not exhibit defects in membrane ruffling, but did exhibit migrational defects (Yang et al., 2000), could suggest a differential role for Rac1 and Rac2 in mast cells. In light of the results from Yang et al. (2000), Rac2 may regulate actin remodelling via interaction with WAVE2, which is known to regulate actin remodelling for cell motility, lamellipodia formation and peripheral membrane ruffling in fibroblasts (Yamazaki et al., 2003; Yan et al., 2003). Initially, we hypothesized that Rac1 and Rac2 differentially regulate actin remodelling, possibly through differential regulation of the actin modifying WAVE family members, specifically WAVE1 and WAVE2. Studies in fibroblasts have shown that WAVE1 is responsible for

dorsal membrane ruffling (Suetsugu et al., 2003), while WAVE2 is responsible for peripheral membrane ruffling and lamellipodia formation (Yamazaki et al., 2003; Yan et al., 2003). That the loss of Rac2 did not affect dorsal membrane ruffling in my study, suggests that Rac1 may be responsible for regulating WAVE1-mediated dorsal membrane ruffling in mast cells.

Taken together, the examination of Rac2 KO BMMCs revealed that Rac2 regulates calcium flux and exocytosis, but not actin remodelling, downstream in the FcεRI signaling pathway. The exact mechanism by which Rac2 exerts regulation of exocytosis and calcium flux remains to be further deduced.

### 4.3 Rac1 and Rac2 are required for calcium flux and exocytosis in the mast cell line, RBL-2H3

While Rac2 KO mice are viable and have been used in several significant studies, similar studies investigating Rac1 have not been done because Rac1 KO mice are embryonic lethal (Sugihara et al., 1998) and inducible KO systems are not feasible for mast cells studies (***See Section 5.5***). To overcome this limitation, I used siRNAi methodology in combination with the mast cell line RBL-2H3 to examine the differential functions of Rac1 and Rac2. Studies in neutrophils have defined distinct roles for Rac1 and Rac2 (Sun et al., 2007); therefore, we hypothesized that they may have differential functions in regulating mast cell function.

RBL-2H3 cells were treated with siRNA targeting Rac1, Rac2 or both mRNAs to study the effect of Rac1 and Rac2 deficiency on mast cell function

(Figure 3.7 A). Both Rac1 and Rac2 siRNA knock-down RBL-2H3 cells exhibited similar decreases in both exocytosis and calcium flux. Rac1 and Rac2 siRNA double knock-down in RBL-2H3 cells did not result in a further reduction in exocytosis, but did result in a further reduction in calcium flux. These results suggest that both Rac1 and Rac2 are required in regulating exocytosis, calcium flux and actin remodelling. That double knock-down of Rac1 and Rac2 results in a further decrease in calcium flux, but no change in exocytosis, suggests that Rac1 and Rac2 may regulate calcium flux pathways independent of exocytosis pathways. Moreover, these results suggest that Rac1 and Rac2 do not compensate for the deficiency of their respective paralogous GTPase. In contrast to our original hypothesis, differential regulation by Rac1 and Rac2 on these cellular processes was not observed.

### 4.4 Rac1 and Rac2 are required for actin-dependent membrane remodelling in the mast cell line RBL-2H3

It has been previously shown that Rac1 and Rac2 exhibit differential regulation of actin remodelling in neutrophils (Sun et al., 2007). Therefore, we hypothesized that Rac1 and Rac2 would exhibit differential regulation of actin remodelling in mast cells. I observed that both Rac1 and Rac2 regulate the formation of transient major ruffles and cell spreading in stimulated RBL-2H3 cells (Figure 3.10, 3.16). Interestingly, minor and peripheral ruffle formation and cell spreading in response to stimulation did not appear to be Rac-dependent, as these ruffles still formed in cells depleted of both Rac1 and Rac2. These

observations suggest that Rac1 and Rac2 are both needed to induce the formation of large membrane ruffles and cell spreading, but may have compensatory abilities for formation of small minor membrane ruffles. Alternatively, the formation of minor ruffles may neither be a Rac1- or Rac2-mediated process. These findings in RBL-2H3 cells contradict my findings in BMMCs, as Rac2 appears to regulate actin-rich membrane remodeling in RBL-2H3 cells, but not in BMMCs (Figure 3.6). However, it is important to note that these conflicting results were observed in different cell lines and were obtained by different molecular manipulations. Depletion of Rac1 and Rac2 protein expression in the Rac2 KO mice and Rac1 and Rac2 siRNA-treated RBL-2H3 cells ultimately resulted in very different levels of Rac2 protein expression. In summary, examination of Rac1 and Rac2 depletion in RBL-2H3 cells revealed that Rac1 and Rac2 regulate prominent membrane remodelling in addition to exocytosis and calcium flux to a comparable degree.

### 4.5 Characterization of a Rac-specific inhibitory drug, EHT-1864, in mast cell exocytosis, calcium flux and actin-dependent membrane remodeling

I used the Rac inhibitory drug, EHT-1864, as an alternative to genetic manipulation to study the function of Rac1 and Rac2. We hypothesized that treatment of mast cells with the Rac inhibitory drug EHT-1864 would yield similar findings to those observed in molecular manipulation of Rac depletion experiments in mast cells. I observed that EHT-1864 treatment resulted in slightly different effects on BMMCs versus RBL-2H3 mast cells. Both cell models

exhibited reduced exocytosis, calcium flux and dysfunctional actin remodeling to varying degrees when treated with EHT-1864. EHT-1864 treatment of BMMCs resulted in a complete abrogation of exocytosis, calcium flux and actin-rich membrane remodelling (Figure 3.12; 3.14 A, B; 3.16). This suggests that in BMMC mast cells, both Rac1 and Rac2 are absolutely essential for functional exocytosis, calcium flux and actin remodelling. EHT-1864 treatment of RBL-2H3 cells resulted in a 50% decrease in exocytosis (Figure 3.13), with a complete loss of calcium flux (Figure 3.15 A, B). EHT-1864 may have been a more potent inhibitor of BMMC function as these cells are physiologically more similar to mast cells and less robust than the immortalized RBL-2H3 mast cell line.

These results support my findings from the siRNA knock-down experiments which showed that when both Rac1 and Rac2 were depleted a further reduction in calcium flux was observed (Figure 3.8). Hence in RBL-2H3 mast cells, both Rac1 and Rac2 regulate calcium flux to a greater degree than exocytosis, perhaps through direct regulation of the plasma membrane CRAC calcium channels. Moreover, EHT-1864 treatment of cells resulted in the abrogation of large dorsal membrane ruffling while small ruffle formation was not affected (Figure 3.17). This suggests that while both Rac1 and Rac2 are required for the formation of large dorsal membrane ruffles, they are not required for the formation of minor membrane ruffling.

Overall, EHT-1864 appears to be an excellent regulator of Rac-specific activity as shown by its potency for inhibiting Rac-mediated exocytosis, calcium

flux and actin remodelling. Further structural analysis of EHT-1864 is required to elucidate the exact mechanism by which it inhibits Rac GTPase function.

### 4.6 Use of CD63, a lysosomal secretory granule marker, to visualize mast cell granules

CD63 was found to be a poor marker for observing granule dynamics in BMMCs and RBL-2H3 mast cells (Figure 18, Supplementary Movie 2 and 4). There are a few possible explanations for a lack of observable granule dynamics using GFP-CD63. The first is that mast cells possess distinct sub-populations of granules and lysosomes (Puri and Roche, 2008) that are all marked by CD63, but may not actually be exocytosed in the same fashion as β-hexosaminidase containing granules. An alternative explanation is that granule translocation to the plasma membrane occurs rapidly and may be under the resolving power of the microscope or the imaging technique. Previous work on granule dynamics has shown these events occur very rapidly on the scale of milliseconds to seconds (Allersma et al., 2004; Williams and Webb, 2000; Allersma et al., 2006). Moreover, the dynamics of granule exocytosis varies significantly between model organisms and cell lines, as some mast cells exocytose in a compound manner, while other mast cells exocytose in a piecemeal or kiss-and-run manner (Williams et al., 1999; personal communication: Dr, Ulrich Blank, Université Paris, France; personal communication: Dr. Juan Rivera, National Institute of Health, USA). Allersma et al. (2006) suggest that translocation and pre-fusion behaviour of some granules is heterogeneous and may not occur as the classical model predicts them

to, in that there may not be extensive interaction of granules with the plasma membrane prior to fusion but instead it may be a transient process that occurs within milliseconds as suggested by the kiss-and-run model.

Despite these issues, several studies have used CD63 as a granule marker in RBL-2H3 exocytosis (Amano et al., 2001; Vincent-Schneider et al., 2000; Grutzkau et al., 2004). However, all of these studies are centered on the kinetics of a single CD63 granule translocation event. These studies used specialized microscopy techniques such as total internal reflection fluorescence (TIRF) microscopy, followed by extensive computational analysis. These techniques were outside of the scope of this project and therefore, CD63 could not be used as a marker for qualitative analysis of exocytosis and actin-granule dynamics.

## 4.7 Rac1 and Rac2 localization, morphological and functional studies using constitutively active and dominant negative mutant proteins

### Localization analysis

Studies in neutrophils have shown that Rac1 and Rac2 localize to membranes of different intracellular structures, primarily as a result of the differences in amino acids that compose the C-terminal tails (Filippi et al., 2004). Rac1 localizes to the plasma membrane whereas Rac2 localizes to granule membranes (Filippi et al., 2004; Magalhaus and Glogauer, 2010). In light of these findings, we hypothesized that Rac1 and Rac2 may exhibit differential cellular localization. Using GFP-tagged N-terminal fusions of both Rac1 and

Rac2, I observed no obvious differential localization, as they both localized to membrane ruffles and to a lesser extent, the cytoplasm (Figure 20 A, B).

The non-specific localization of Rac1 and Rac2 may be due to either the presence of a GFP-tag attached to the proteins, or the expression level of the proteins. The GFP-vector that was used to transfect the cells contained a CMV promoter that was used to direct expression of the Rac GTPase. A vector containing a CMV promoter was used, as the mutant Rac proteins needed to be overexpressed to ensure that mutant forms were in excess so a phenotype could be observed. However, this overexpression may have resulted in off-target effects through overloading regulatory proteins GEFs and GAPs, or possibly other downstream effectors. Use of an inducible system could have enabled controlled protein overexpression of Rac1 and Rac2 mutants, however, an inducible system for a mast cell line does not exist.

**Morphological analysis**

To determine if the expression of mutant Rac1 and Rac2 proteins affected cell morphology, I characterized cells under resting and stimulated conditions (Figure 20 C, D). Wild-type Rac1-GFP and Rac2-GFP expressing RBL-2H3 cells exhibited unaltered morphology when compared to untransfected cells, which shows that the GFP-tag or overexpression of WT did not affect morphology. Moreover, expression of Rac1 and Rac2 dominant negative (T17N) mutants in RBL-2H3 cells did not result in morphological defects in the resting state (unstimulated). However, expression of Rac1 and Rac2 constitutively active (Q61L) mutants resulted in cells with a flattened morphology in the resting state.

Rac is known to be the GTPase responsible for regulating lamellipodia formation (Tapon and Hall, 1997; Kurokawa et al., 2004) and therefore, a fully spread morphology when constitutively active Rac1 and Rac2 were overexpressed is not surprising.

**Functional analysis**

Numerous studies in RBL-2H3 cells have used mutant protein analysis to determine functions of specific Rho GTPases. Therefore, I sought to determine if Rac1 and Rac2 constitutively active and dominant negative mutants affected exocytosis and actin remodelling. RBL-2H3 cells transfected with mutant Rac1 or Rac2 exhibited no defects in exocytosis (Figure 3.21, 3.22) which is in contrast to the findings of Hong Geller et al. (2000; 2001), who found that expression of constitutively active Rac1 mutants augment exocytosis, while dominant negative mutants slightly inhibit exocytosis. That Rac1 and Rac2 mutants had no effect on exocytosis may be a result of the low transfection efficiency and variability in mutant protein expression, contributing to the inability to detect changes in β-hexosaminidase exocytosis between mutants.

To overcome the issue of low transfection efficiency and variability in mutant protein expression, stable cell lines were created using RBL-2H3 cells transfected with GFP tagged wild-type, Q61L or T17N mutant versions of either Rac1 or Rac2. However, there was no observable effect of these mutants on exocytosis (Figure 3.22). One possible explanation for this finding would be that a variety of phenotypes may have been sustained in the polyclonal culture, as monoclonal cultures were not made due to time and laboratory limitations. During

the selection process, cells that could compensate for dysfunctional Rac1 or Rac2 may have dominated the culture, resulting in a GFP-positive population that exhibited no defects in exocytosis.

# CHAPTER 5

# FUTURE DIRECTIONS

## 5.1 Delineation of the mechanism of regulation by Rac1 and Rac2 on the FcεRI pathway

To further delineate the role of Rac1 and Rac2 in the regulation of the FcεRI signaling pathway, investigation of both upstream and downstream components could reveal the specific mechanism of regulation of these GTPases. Tyrosine phosphorylation assays of a proximal pathway component, PLC-γ1 and PLC-γ2 could be investigated in similar fashion to previous studies in BMMCs (Manetz et al., 2001). For PLC-γ to become activated and propagate downstream effects, it must first be phosphorylated and form a complex with other signaling molecules on the adaptor protein LAT (Figure 1.1). This assay could potentially reveal if Rac directly regulates calcium flux, exocytosis and actin remodeling at the level of proximal pathway components, such as PLC-γ. The rational for this approach is that PLC-γ is responsible for the activation of IP3 and DAG production, which are key proximal events that modulate calcium flux and exocytosis (Figure 1.1). Since I observed decreased exocytosis and calcium flux in Rac2 KO BMMCs and in Rac1 and Rac2 siRNA treated RBL-2H3 cells, investigation of proximal components in this pathway such as PLC-γ and others, may reveal if these GTPases regulate these functions at a point of convergence in the pathway. This assay would involve immunoblotting lystates of activated WT or Rac2 KO BMMCs for PLC-γ1 or PLC-γ2 alone and with a phospho-tyrosine antibody.

## 5.2 Delineation of the mechanism of Rac-dependent regulation of calcium mobilization

Through this study I observed that Rac1 and Rac2 regulate calcium mobilization in mast cells. However, I was unable to identify the mechanism by which it exerts this regulation. To distinguish if Rac1 or Rac2 regulates calcium flux at the level of ER calcium stores or the store-operated calcium entry pathway (SOCE) channels (e.g. CRAC calcium channels), calcium depletion-repletion assays could be conducted, in accordance with other studies (Baba et al., 2008; Suzuki et al., 2010). Microscopic assays using sensitive calcium dye indicators (e.g. Fura-2) to detect changes in intracellular calcium at the single cell level could also be done, which would enable the detection of relatively small changes in intracellular calcium concentration resulting from ER store depletion (Baba et al., 2008; Suzuki et al., 2010). In accordance with previous studies, conducting additional experiments using thapsigargin could also reveal the mechanisms by which calcium flux is defective in Rac mutants (Suzuki et al., 2010; Manetz et al., 2001). Thapsigargin raises cytoslic calcium concentrations by blocking calcium from being pumped into the ER, thereby depleting ER stores (Rogers et al., 1995). Furthermore, investigation of SOCE could reveal if Rac1 and Rac2 directly regulates plasma membrane CRAC channels.

## 5.3 Delineation of the mechanism of Rac dependent regulation of actin remodeling

In this study, I found that Rac1 and Rac2 regulates actin-rich membrane remodeling in siRNA treated and EHT-1864 treated RBL-2H3 cells, but that Rac2 does not regulate actin-rich membrane remodeling in BMMCs. Therefore, it is of great interest to further investigate the relationship between Rac1 and Rac2 and the predominant actin nucleation promoting factors (NPFs), WAVE1 and WAVE2. Studies have previously shown that Rac interacts with these NPFs (Kirosu and Takenawa, 2009) and that WAVE1 and WAVE2 differentially regulate actin remodeling events (Suetsugu et al, 2003; Yamazaki et al., 2003; Yan et al., 2003). To further investigate NPFs, fluorescently-tagged versions could be expressed in WT and Rac2 KO mast cells and dynamic localization to ruffles during cell stimulation could be examined by live cell microscopy.

## 5.4 Differentiating Rac1 and Rac2 regulation of mast cell function

In this study, I used the mast cell line, RBL-2H3 and siRNA knock-down, to examine the differential functions of Rac1 and Rac2 in mast cells due to the lack of Rac1 KO cell availability. However, my interpretation of the results from this study is limited as the expression of Rac1 and Rac2 were only knocked down by half via siRNA, therefore leaving functional GTPases remaining in the cell. Use of an inducible Rac1 KO system would provide an alternative method to determine if Rac1 and Rac2 exhibit differential functions. Researchers have created inducible systems for Rac1 KO in hematopoietic cells using a conditional

floxed allele of rac1 and a mouse expressing Cre recombinase under the control of a neutrophil/monocyte specific promoter, lysozyme-M (Mizukawa et al., 2011; Mollers et al., 1992). Unfortunately, expression of lysozyme-M in mast cells is quite variable relative to neutrophils or macrophages, and is therefore not a viable system for generating Rac1 KO mast cells (Mollers et al., 1992; personal communication: Dr. Juan Rivera, National Institute of Health, USA). Alternatively, use of lentiviral shRNA for knockdown experiments in BMMCs has been found to work well and could be used to achieve a significant knockdown of Rac1 expression in BMMCs (personal communication: Dr. Juan Rivera, National Institute of Health, USA).

### 5.5 Characterization of EHT-1864 and Rac interaction

To further characterize the molecular structure of EHT-1864 and elucidate its binding site to both Rac1 and Rac2, NMR spectroscopy will be conducted in collaboration with Dr. Bryan Sykes (Department of Biochemistry, U of A). Molecular NMR assignments have already been done for Rac1 and Rac2 (Bouguet-Bonnet and Buck, 2006; Thapar et al., 2003) and we have been able to successfully purify recombinant Rac1 and Rac2 protein. This NMR study will resolve the mechanism of inhibition of EHT-1864, including whether EHT-1864 is inhibitory via competitive or noncompetitive binding with the nucleotide binding pocket, the activating GEF domain or downstream effector recruitment domain. By further characterizing this molecular inhibitor of the Rac GTPases,

we can contribute to the growing body of literature by further describing this potentially significant inhibitory molecule.

# CHAPTER 6

# CONCLUSION

Three molecular approaches were used to investigate the roles of Rac1 and Rac2 in mast cell function; bone marrow mast cells derived from wild-type and Rac2 knockout mice, Rac1 and Rac2 siRNA-mediated knockdown in the RBL-2H3 mast cell line and a novel Rac-specific inhibitory drug, EHT-1864. My results suggest that Rac1 and Rac2 regulate multiple stages of FcεRI-mediated response in mast cells (Figure 6.1). I found that both Rac1 and Rac2 are required for calcium flux and exocytosis. My data suggests that Rac1 and Rac2 regulate exocytosis through a convergent pathway since inhibition of either Rac1 or Rac2, or both, resulted in a similar decrease in exocytosis. However, my data suggests that Rac1 and Rac2 regulate calcium flux through alternate pathways since inhibition of Rac1 and Rac2 resulted in different decreases in calcium flux, while inhibition of both Rac1 and Rac2 resulted in a further decrease in calcium flux (Figure 6.2). Moreover, I found that Rac2 does not regulate actin remodelling, thereby suggesting this may be a Rac1-mediated process (Figure 6.2).

The distinct mechanism of Rac1 and Rac2-mediated regulation of events required for exocytosis remains unknown, however, the GTPases may exhibit regulation either through multiple pathway components or through a single point of convergence in the pathway, as shown in the final model (Figure 6.1). Further characterization of the roles that the Rho GTPases, Rac1 and Rac2, play in mast cell exocytosis is required to determine the exact mechanism by which they exert their regulation. This will not only increase the understanding of the biological process of exocytosis in mast cells, but also provide useful insight for future

studies aimed at targeting regulatory molecules involved in allergic inflammation and asthmatic disease.

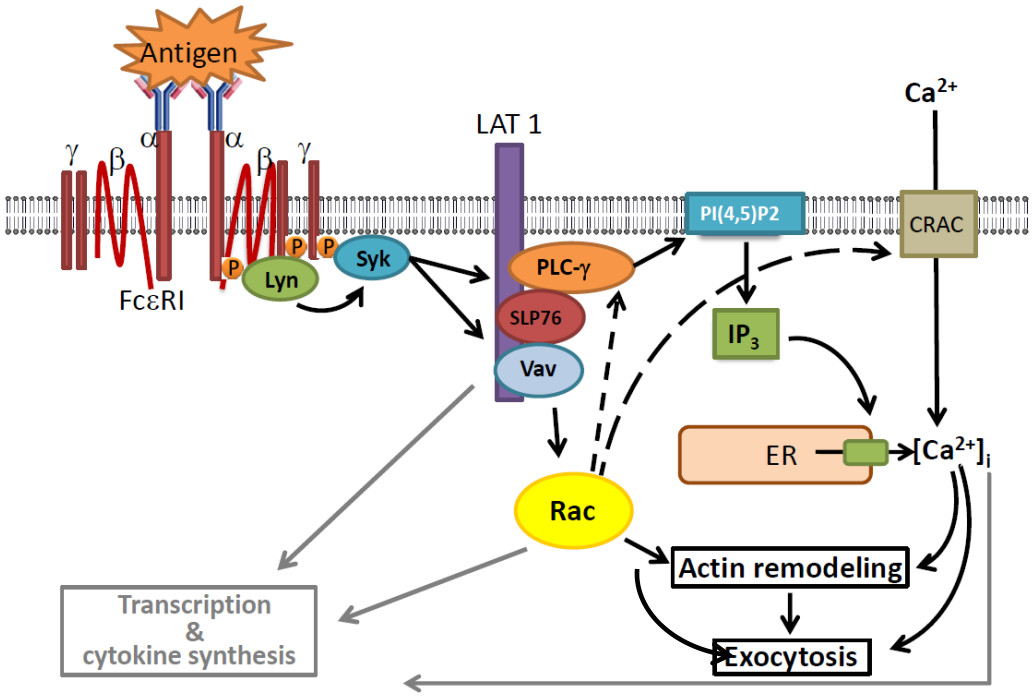


**Figure 6.1 Final model for the role of Rac1 and Rac2 in regulating FcεRI-mediated activation of mast cells**

The findings from this study support a role for Rac in regulating actin remodelling, calcium flux and exocytosis. However, the precise mechanism of Rac1 and Rac2-mediated regulation of events required for exocytosis remains unknown. We hypothesize that Rac1 and Rac2 may exhibit regulation either through multiple pathway components (actin remodeling, calcium flux and other signaling molecules) or through a single point of convergence in the pathway, such as PLC-γ or plasma membrane CRAC channels (*dashed arrows*) which would affect calcium flux, an obligate requirement for exocytosis.

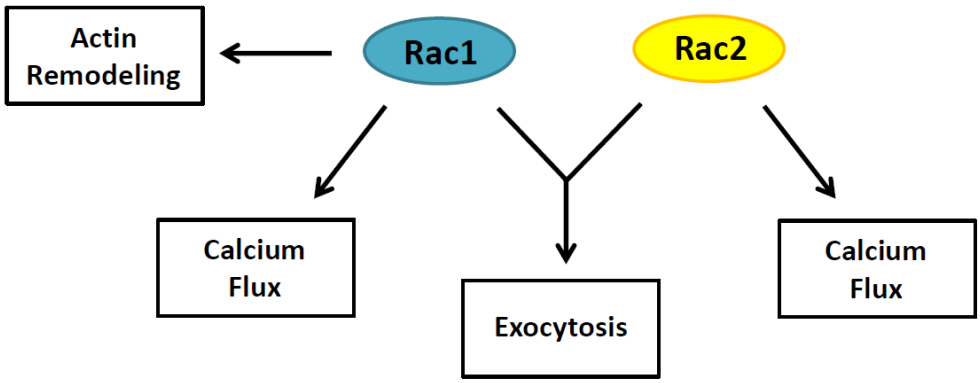


**Figure 6.2 Model for Rac1 and Rac2 regulation of actin remodelling, exocytosis and calcium flux in FcεRI-mediated activation of mast cells**
The findings from this study suggest that actin remodelling, calcium flux and exocytosis are Rac-mediated processes. It was found that Rac2 does not regulate actin remodelling, but does regulate calcium flux and exocytosis. In contrast, Rac1 was found to regulate calcium flux, exocytosis and possibly actin remodelling.

## REFERENCES


Abdel-Latif, D., Steward, M., Macdonald, D.L., Francis, G.A., Dinauer, M.C., and Lacy, P. (2004). Rac2 is critical for neutrophil primary granule exocytosis. Blood 104, 832-839.

Advani, R.J., Bae, H.R., Bock, J.B., Chao, D.S., Doung, Y.C., Prekeris, R., Yoo, J.S., and Scheller, R.H. (1998). Seven novel mammalian SNARE proteins localize to distinct membrane compartments. J Biol Chem 273, 10317-10324.

Allersma, M.W., Bittner, M.A., Axelrod, D., and Holz, R.W. (2006). Motion matters: secretory granule motion adjacent to the plasma membrane and exocytosis. Mol Biol Cell 17, 2424-2438.

Allersma, M.W., Wang, L., Axelrod, D., and Holz, R.W. (2004). Visualization of regulated exocytosis with a granule-membrane probe using total internal reflection microscopy. Mol Biol Cell 15, 4658-4668.

Alvarez-Errico, D., Lessmann, E., and Rivera, J. (2009). Adapters in the organization of mast cell signaling. Immunol Rev 232, 195-217.

Alvarez-Errico, D., Yamashita, Y., Suzuki, R., Odom, S., Furumoto, Y., Yamashita, T., and Rivera, J. (2010). Functional analysis of Lyn kinase A and B isoforms reveals redundant and distinct roles in Fc epsilon RI-dependent mast cell activation. J Immunol 184, 5000-5008.

Amano, T., Furuno, T., Hirashima, N., Ohyama, N., and Nakanishi, M. (2001). Dynamics of intracellular granules with CD63-GFP in rat basophilic leukemia cells. J Biochem 129, 739-744.

Andrews, N.W. (2000). Regulated secretion of conventional lysosomes. Trends Cell Biol 10, 316-321.

Aronson, N.N., Jr., and Kuranda, M.J. (1989). Lysosomal degradation of Asn-linked glycoproteins. FASEB J 3, 2615-2622.

Baba, Y., Nishida, K., Fujii, Y., Hirano, T., Hikida, M., and Kurosaki, T. (2008). Essential function for the calcium sensor STIM1 in mast cell activation and anaphylactic responses. Nat Immunol 9, 81-88.

Bader, M.F., Doussau, F., Chasserot-Golaz, S., Vitale, N., and Gasman, S. (2004). Coupling actin and membrane dynamics during calcium-regulated exocytosis: a role for Rho and ARF GTPases. Biochim Biophys Acta 1742, 37-49.

Baram, D., Mekori, Y.A., and Sagi-Eisenberg, R. (2001). Synaptotagmin regulates mast cell functions. Immunol Rev 179, 25-34.

Barsumian, E.L., Isersky, C., Petrino, M.G., and Siraganian, R.P. (1981). IgE-induced histamine release from rat basophilic leukemia cell lines: isolation of releasing and nonreleasing clones. Eur J Immunol 11, 317-323.

Beckers, C.J., and Balch, W.E. (1989). Calcium and GTP: essential components in vesicular trafficking between the endoplasmic reticulum and Golgi apparatus. J Cell Biol 108, 1245-1256.

Belmokhtar, C.A., Hillion, J., and Segal-Bendirdjian, E. (2001). Staurosporine induces apoptosis through both caspase-dependent and caspase-independent mechanisms. Oncogene 20, 3354-3362.

Bement, W.M., Miller, A.L., and von Dassow, G. (2006). Rho GTPase activity zones and transient contractile arrays. Bioessays 28, 983-993.

Blank, U., Ra, C., Miller, L., White, K., Metzger, H., and Kinet, J.P. (1989). Complete structure and expression in transfected cells of high affinity IgE receptor. Nature 337, 187-189.

Blank, U., and Rivera, J. (2004). The ins and outs of IgE-dependent mast-cell exocytosis. Trends Immunol 25, 266-273.

Blank, U., and Rivera, J. (2006). Assays for regulated exocytosis of mast cell granules. Curr Protoc Cell Biol Chapter 15, Unit 15 11.

Blott, E.J., and Griffiths, G.M. (2002). Secretory lysosomes. Nat Rev Mol Cell Biol 3, 122-131.

Boettner, B., and Van Aelst, L. (2002). The role of Rho GTPases in disease development. Gene 286, 155-174.

Boguski, M.S., and McCormick, F. (1993). Proteins regulating Ras and its relatives. Nature 366, 643-654.

Bohn, A., and Konig, W. (1982). Generation of monoclonal murine anti-DNP-IgE, IgM and IgG1 antibodies: biochemical and biological characterization. Immunology 47, 297-311.

Bonnefoy-Berard, N., Munshi, A., Yron, I., Wu, S., Collins, T.L., Deckert, M., Shalom-Barak, T., Giampa, L., Herbert, E., Hernandez, J., et al. (1996). Vav: function and regulation in hematopoietic cell signaling. Stem Cells 14, 250-268.

Bouguet-Bonnet, S., and Buck, M. (2006). 1H, 15N, 13C assignments for the activated form of the small Rho-GTPase Rac1. J Biomol NMR 36 Suppl 1, 51.

Brumell, J.H., and Grinstein, S. (2004). Salmonella redirects phagosomal maturation. Curr Opin Microbiol 7, 78-84.

Burwen, S.J., and Satir, B.H. (1977). Plasma membrane folds on the mast cell surface and their relationship to secretory activity. J Cell Biol 74, 690-697.

Campellone, K.G., and Welch, M.D. (2010). A nucleator arms race: cellular control of actin assembly. Nat Rev Mol Cell Biol 11, 237-251.

Chapman, E.R. (2002). Synaptotagmin: a Ca(2+) sensor that triggers exocytosis? Nat Rev Mol Cell Biol 3, 498-508.

Chavrier, P., and Goud, B. (1999). The role of ARF and Rab GTPases in membrane transport. Curr Opin Cell Biol 11, 466-475.

Chen, Y.A., and Scheller, R.H. (2001). SNARE-mediated membrane fusion. Nat Rev Mol Cell Biol 2, 98-106.

Chrencik, J.E., Brooun, A., Zhang, H., Mathews, II, Hura, G.L., Foster, S.A., Perry, J.J., Streiff, M., Ramage, P., Widmer, H., et al. (2008). Structural basis of guanine nucleotide exchange mediated by the T-cell essential Vav1. J Mol Biol 380, 828-843.

Costello, P.S., Turner, M., Walters, A.E., Cunningham, C.N., Bauer, P.H., Downward, J., and Tybulewicz, V.L. (1996). Critical role for the tyrosine kinase Syk in signaling through the high affinity IgE receptor of mast cells. Oncogene 13, 2595-2605.

Crespo, P., Schuebel, K.E., Ostrom, A.A., Gutkind, J.S., and Bustelo, X.R. (1997). Phosphotyrosine-dependent activation of Rac-1 GDP/GTP exchange by the vav proto-oncogene product. Nature 385, 169-172.

Croker, B.A., Tarlinton, D.M., Cluse, L.A., Tuxen, A.J., Light, A., Yang, F.C., Williams, D.A., and Roberts, A.W. (2002). The Rac2 guanosine triphosphatase regulates B lymphocyte antigen receptor responses and chemotaxis and is required for establishment of B-1a and marginal zone B lymphocytes. J Immunol 168, 3376-3386.

Deng, Z., Zink, T., Chen, H.Y., Walters, D., Liu, F.T., and Liu, G.Y. (2009). Impact of actin rearrangement and degranulation on the membrane structure of primary mast cells: a combined atomic force and laser scanning confocal microscopy investigation. Biophys J 96, 1629-1639.

Didsbury, J., Weber, R.F., Bokoch, G.M., Evans, T., and Snyderman, R. (1989). rac, a novel ras-related family of proteins that are botulinum toxin substrates. J Biol Chem 264, 16378-16382.

Dong, X., Mo, Z., Bokoch, G., Guo, C., Li, Z., and Wu, D. (2005). P-Rex1 is a primary Rac2 guanine nucleotide exchange factor in mouse neutrophils. Curr Biol 15, 1874-1879.

Doussau, F., Gasman, S., Humeau, Y., Vitiello, F., Popoff, M., Boquet, P., Bader, M.F., and Poulain, B. (2000). A Rho-related GTPase is involved in Ca(2+)-dependent neurotransmitter exocytosis. J Biol Chem 275, 7764-7770.

Dowrick, P., Kenworthy, P., McCann, B., and Warn, R. (1993). Circular ruffle formation and closure lead to macropinocytosis in hepatocyte growth factor/scatter factor-treated cells. Eur J Cell Biol 61, 44-53.

Edgar, A.J., and Bennett, J.P. (1997). Circular ruffle formation in rat basophilic leukemia cells in response to antigen stimulation. Eur J Cell Biol 73, 132-140.

Ehre, C., Rossi, A.H., Abdullah, L.H., De Pestel, K., Hill, S., Olsen, J.C., and Davis, C.W. (2005). Barrier role of actin filaments in regulated mucin secretion from airway goblet cells. Am J Physiol Cell Physiol 288, C46-56.

Eitzen, G. (2003). Actin remodeling to facilitate membrane fusion. Biochim Biophys Acta 1641, 175-181.

Erdei, A., Andrasfalvy, M., Peterfy, H., Toth, G., and Pecht, I. (2004). Regulation of mast cell activation by complement-derived peptides. Immunol Lett 92, 39-42.

Etienne-Manneville, S., and Hall, A. (2002). Rho GTPases in cell biology. Nature 420, 629-635.

Filippi, M.D., Harris, C.E., Meller, J., Gu, Y., Zheng, Y., and Williams, D.A. (2004). Localization of Rac2 via the C terminus and aspartic acid 150 specifies superoxide generation, actin polarity and chemotaxis in neutrophils. Nat Immunol 5, 744-751.

Galli, S.J., Maurer, M., and Lantz, C.S. (1999). Mast cells as sentinels of innate immunity. Curr Opin Immunol 11, 53-59.

Galli, S.J., Wershil, B.K., Costa, J.J., and Tsai, M. (1994). For better or for worse: does stem cell factor importantly regulate mast cell function in pulmonary physiology and pathology? Am J Respir Cell Mol Biol 11, 644-645.

Gasman, S., Chasserot-Golaz, S., Malacombe, M., Way, M., and Bader, M.F. (2004). Regulated exocytosis in neuroendocrine cells: a role for subplasmalemmal Cdc42/N-WASP-induced actin filaments. Mol Biol Cell 15, 520-531.

Gasman, S., Chasserot-Golaz, S., Popoff, M.R., Aunis, D., and Bader, M.F. (1997). Trimeric G proteins control exocytosis in chromaffin cells. Go regulates the peripheral actin network and catecholamine secretion by a mechanism involving the small GTP-binding protein Rho. J Biol Chem 272, 20564-20571.

Gasman, S., Chasserot-Golaz, S., Popoff, M.R., Aunis, D., and Bader, M.F. (1999). Involvement of Rho GTPases in calcium-regulated exocytosis from adrenal chromaffin cells. J Cell Sci 112 ( Pt 24), 4763-4771.

Gaudenzio, N., Espagnolle, N., Mars, L.T., Liblau, R., Valitutti, S., and Espinosa, E. (2009). Cell-cell cooperation at the T helper cell/mast cell immunological synapse. Blood 114, 4979-4988.

Ghosh, M., Song, X., Mouneimne, G., Sidani, M., Lawrence, D.S., and Condeelis, J.S. (2004). Cofilin promotes actin polymerization and defines the direction of cell motility. Science 304, 743-746.

Giner, D., Neco, P., Frances Mdel, M., Lopez, I., Viniegra, S., and Gutierrez, L.M. (2005). Real-time dynamics of the F-actin cytoskeleton during secretion from chromaffin cells. J Cell Sci 118, 2871-2880.

Glogauer, M., Marchal, C.C., Zhu, F., Worku, A., Clausen, B.E., Foerster, I., Marks, P., Downey, G.P., Dinauer, M., and Kwiatkowski, D.J. (2003). Rac1 deletion in mouse neutrophils has selective effects on neutrophil functions. J Immunol 170, 5652-5657.

Goley, E.D., and Welch, M.D. (2006). The ARP2/3 complex: an actin nucleator comes of age. Nat Rev Mol Cell Biol 7, 713-726.

Grutzkau, A., Smorodchenko, A., Lippert, U., Kirchhof, L., Artuc, M., and Henz, B.M. (2004). LAMP-1 and LAMP-2, but not LAMP-3, are reliable markers for activation-induced secretion of human mast cells. Cytometry A 61, 62-68.

Gu, Y., Byrne, M.C., Paranavitana, N.C., Aronow, B., Siefring, J.E., D'Souza, M., Horton, H.F., Quilliam, L.A., and Williams, D.A. (2002). Rac2, a hematopoiesis-specific Rho GTPase, specifically regulates mast cell protease gene expression in bone marrow-derived mast cells. Mol Cell Biol 22, 7645-7657.

Gu, Y., Jia, B., Yang, F.C., D'Souza, M., Harris, C.E., Derrow, C.W., Zheng, Y., and Williams, D.A. (2001). Biochemical and biological characterization of a

human Rac2 GTPase mutant associated with phagocytic immunodeficiency. J Biol Chem 276, 15929-15938.

Guillemot, J.C., Montcourrier, P., Vivier, E., Davoust, J., and Chavrier, P. (1997). Selective control of membrane ruffling and actin plaque assembly by the Rho GTPases Rac1 and CDC42 in FcepsilonRI-activated rat basophilic leukemia (RBL-2H3) cells. J Cell Sci 110 ( Pt 18), 2215-2225.

Haataja, L., Groffen, J., and Heisterkamp, N. (1997). Characterization of RAC3, a novel member of the Rho family. J Biol Chem 272, 20384-20388.

Heidelberger, R., Heinemann, C., Neher, E., and Matthews, G. (1994). Calcium dependence of the rate of exocytosis in a synaptic terminal. Nature 371, 513-515.

Hibi, T., Hirashima, N., and Nakanishi, M. (2000). Rat basophilic leukemia cells express syntaxin-3 and VAMP-7 in granule membranes. Biochem Biophys Res Commun 271, 36-41.

Hong-Geller, E., and Cerione, R.A. (2000). Cdc42 and Rac stimulate exocytosis of secretory granules by activating the IP(3)/calcium pathway in RBL-2H3 mast cells. J Cell Biol 148, 481-494.

Hong-Geller, E., Holowka, D., Siraganian, R.P., Baird, B., and Cerione, R.A. (2001). Activated Cdc42/Rac reconstitutes Fcepsilon RI-mediated Ca2+ mobilization and degranulation in mutant RBL mast cells. Proc Natl Acad Sci U S A 98, 1154-1159.

Jaffe, A.B., and Hall, A. (2005). Rho GTPases: biochemistry and biology. Annu Rev Cell Dev Biol 21, 247-269.

Jahn, R., and Sudhof, T.C. (1999). Membrane fusion and exocytosis. Annu Rev Biochem 68, 863-911.

Jaiswal, J.K., Andrews, N.W., and Simon, S.M. (2002). Membrane proximal lysosomes are the major vesicles responsible for calcium-dependent exocytosis in nonsecretory cells. J Cell Biol 159, 625-635.

Jensen, B.M., Swindle, E.J., Iwaki, S., and Gilfillan, A.M. (2006). Generation, isolation, and maintenance of rodent mast cells and mast cell lines. Curr Protoc Immunol Chapter 3, Unit 3 23.

Kalesnikoff, J., and Galli, S.J. (2008). New developments in mast cell biology. Nat Immunol 9, 1215-1223.

Kambayashi, T., Allenspach, E.J., Chang, J.T., Zou, T., Shoag, J.E., Reiner, S.L., Caton, A.J., and Koretzky, G.A. (2009). Inducible MHC class II expression by mast cells supports effector and regulatory T cell activation. J Immunol 182, 4686-4695.

Kim, C., Marchal, C.C., Penninger, J., and Dinauer, M.C. (2003). The hemopoietic Rho/Rac guanine nucleotide exchange factor Vav1 regulates N-formyl-methionyl-leucyl-phenylalanine-activated neutrophil functions. J Immunol 171, 4425-4430.

Kinet, J.P. (1999). The high-affinity IgE receptor (Fc epsilon RI): from physiology to pathology. Annu Rev Immunol 17, 931-972.

Kirshenbaum, A.S., Kessler, S.W., Goff, J.P., and Metcalfe, D.D. (1991). Demonstration of the origin of human mast cells from CD34+ bone marrow progenitor cells. J Immunol 146, 1410-1415.

Kitamura, Y., and Fujita, J. (1989). Regulation of mast cell differentiation. Bioessays 10, 193-196.

Klenchin, V.A., and Martin, T.F. (2000). Priming in exocytosis: attaining fusion-competence after vesicle docking. Biochimie 82, 399-407.

Kohler, G., and Milstein, C. (1976). Derivation of specific antibody-producing tissue culture and tumor lines by cell fusion. Eur J Immunol 6, 511-519.

Kowluru, A., Li, G., Rabaglia, M.E., Segu, V.B., Hofmann, F., Aktories, K., and Metz, S.A. (1997). Evidence for differential roles of the Rho subfamily of GTP-binding proteins in glucose- and calcium-induced insulin secretion from pancreatic beta cells. Biochem Pharmacol 54, 1097-1108.

Krueger, E.W., Orth, J.D., Cao, H., and McNiven, M.A. (2003). A dynamin-cortactin-Arp2/3 complex mediates actin reorganization in growth factor-stimulated cells. Mol Biol Cell 14, 1085-1096.

Kulczycki, A., Jr., and Metzger, H. (1974). The interaction of IgE with rat basophilic leukemia cells. II. Quantitative aspects of the binding reaction. J Exp Med 140, 1676-1695.

Kurisu, S., and Takenawa, T. (2009). The WASP and WAVE family proteins. Genome Biol 10, 226.

Kurokawa, K., Itoh, R.E., Yoshizaki, H., Nakamura, Y.O., and Matsuda, M. (2004). Coactivation of Rac1 and Cdc42 at lamellipodia and membrane ruffles induced by epidermal growth factor. Mol Biol Cell 15, 1003-1010.

Lagunoff, D., Martin, T.W., and Read, G. (1983). Agents that release histamine from mast cells. Annu Rev Pharmacol Toxicol 23, 331-351.

Lawson, C.D., Donald, S., Anderson, K.E., Patton, D.T., and Welch, H.C. (2011). P-Rex1 and Vav1 cooperate in the regulation of formyl-methionyl-leucyl-phenylalanine-dependent neutrophil responses. J Immunol 186, 1467-1476.

Lee, T.D., Swieter, M., Bienenstock, J., and Befus, A.D. (1985). Heterogeneity in mast cell populations. Clin Immunol Rev 4, 143-199.

Legg, J.A., Bompard, G., Dawson, J., Morris, H.L., Andrew, N., Cooper, L., Johnston, S.A., Tramountanis, G., and Machesky, L.M. (2007). N-WASP involvement in dorsal ruffle formation in mouse embryonic fibroblasts. Mol Biol Cell 18, 678-687.

Lerm, M., Holm, A., Seiron, A., Sarndahl, E., Magnusson, K.E., and Rasmusson, B. (2006). Leishmania donovani requires functional Cdc42 and Rac1 to prevent phagosomal maturation. Infect Immun 74, 2613-2618.

Li, B., Yu, H., Zheng, W., Voll, R., Na, S., Roberts, A.W., Williams, D.A., Davis, R.J., Ghosh, S., and Flavell, R.A. (2000). Role of the guanosine triphosphatase Rac2 in T helper 1 cell differentiation. Science 288, 2219-2222.

Li, S., Yamauchi, A., Marchal, C.C., Molitoris, J.K., Quilliam, L.A., and Dinauer, M.C. (2002). Chemoattractant-stimulated Rac activation in wild-type and Rac2-deficient murine neutrophils: preferential activation of Rac2 and Rac2 gene dosage effect on neutrophil functions. J Immunol 169, 5043-5051.

Livak, K.J., and Schmittgen, T.D. (2001). Analysis of relative gene expression data using real-time quantitative PCR and the 2(-Delta Delta C(T)) Method. Methods 25, 402-408.

Magalhaes, M.A., and Glogauer, M. (2010). Pivotal Advance: Phospholipids determine net membrane surface charge resulting in differential localization of active Rac1 and Rac2. J Leukoc Biol 87, 545-555.

Malacombe, M., Bader, M.F., and Gasman, S. (2006). Exocytosis in neuroendocrine cells: new tasks for actin. Biochim Biophys Acta 1763, 1175-1183.

Manetz, T.S., Gonzalez-Espinosa, C., Arudchandran, R., Xirasagar, S., Tybulewicz, V., and Rivera, J. (2001). Vav1 regulates phospholipase cgamma activation and calcium responses in mast cells. Mol Cell Biol 21, 3763-3774.

Marshall, J.S. (2004). Mast-cell responses to pathogens. Nat Rev Immunol 4, 787-799.

Mekori, Y.A., and Galli, S.J. (1990). [125I]fibrin deposition occurs at both early and late intervals of IgE-dependent or contact sensitivity reactions elicited in mouse skin. Mast cell-dependent augmentation of fibrin deposition at early intervals in combined IgE-dependent and contact sensitivity reactions. J Immunol 145, 3719-3727.

Mellor, H., and Parker, P.J. (1998). The extended protein kinase C superfamily. Biochem J 332 ( Pt 2), 281-292.

Metcalfe, D.D., Baram, D., and Mekori, Y.A. (1997). Mast cells. Physiol Rev 77, 1033-1079.

Michaelson, D., Silletti, J., Murphy, G., D'Eustachio, P., Rush, M., and Philips, M.R. (2001). Differential localization of Rho GTPases in live cells: regulation by hypervariable regions and RhoGDI binding. J Cell Biol 152, 111-126.

Millard, T.H., Sharp, S.J., and Machesky, L.M. (2004). Signaling to actin assembly via the WASP (Wiskott-Aldrich syndrome protein)-family proteins and the Arp2/3 complex. Biochem J 380, 1-17.

Mitchell, T., Lo, A., Logan, M.R., Lacy, P., and Eitzen, G. (2008). Primary granule exocytosis in human neutrophils is regulated by Rac-dependent actin remodeling. Am J Physiol Cell Physiol 295, C1354-1365.

Mizukawa, B., Wei, J., Shrestha, M., Wunderlich, M., Chou, F.S., Griesinger, A., Harris, C.E., Kumar, A.R., Zheng, Y., Williams, D.A., et al. (2011). Inhibition of Rac GTPase signaling and downstream prosurvival Bcl-2 proteins as combination targeted therapy in MLL-AF9 leukemia. Blood 118, 5235-5245.

Moll, J., Sansig, G., Fattori, E., and van der Putten, H. (1991). The murine rac1 gene: cDNA cloning, tissue distribution and regulated expression of rac1 mRNA by disassembly of actin microfilaments. Oncogene 6, 863-866.

Mollers, B., Klages, S., Wedel, A., Cross, M., Spooncer, E., Dexter, T.M., and Renkawitz, R. (1992). The mouse M-lysozyme gene domain: identification of myeloid and differentiation specific DNasel hypersensitive sites and of a 3'-cis acting regulatory element. Nucleic Acids Res 20, 1917-1924.

Moon, T.C., St Laurent, C.D., Morris, K.E., Marcet, C., Yoshimura, T., Sekar, Y., and Befus, A.D. (2010). Advances in mast cell biology: new understanding of heterogeneity and function. Mucosal Immunol 3, 111-128.

Munson, M., and Novick, P. (2006). The exocyst defrocked, a framework of rods revealed. Nat Struct Mol Biol 13, 577-581.

Naal, R.M., Tabb, J., Holowka, D., and Baird, B. (2004). In situ measurement of degranulation as a biosensor based on RBL-2H3 mast cells. Biosens Bioelectron 20, 791-796.

Nimnual, A.S., Taylor, L.J., and Bar-Sagi, D. (2003). Redox-dependent downregulation of Rho by Rac. Nat Cell Biol 5, 236-241.

Nishida, K., Yamasaki, S., Ito, Y., Kabu, K., Hattori, K., Tezuka, T., Nishizumi, H., Kitamura, D., Goitsuka, R., Geha, R.S., et al. (2005). Fc{epsilon}RI-mediated mast cell degranulation requires calcium-independent microtubule-dependent translocation of granules to the plasma membrane. J Cell Biol 170, 115-126.

Nishizuka, Y. (1995). Protein kinase C and lipid signaling for sustained cellular responses. FASEB J 9, 484-496.

Noli, C., and Miolo, A. (2001). The mast cell in wound healing. Vet Dermatol 12, 303-313.

Norman, J.C., Price, L.S., Ridley, A.J., and Koffer, A. (1996). The small GTP-binding proteins, Rac and Rho, regulate cytoskeletal organization and exocytosis in mast cells by parallel pathways. Mol Biol Cell 7, 1429-1442.

Ohta, Y., Hartwig, J.H., and Stossel, T.P. (2006). FilGAP, a Rho- and ROCK-regulated GAP for Rac binds filamin A to control actin remodelling. Nat Cell Biol 8, 803-814.

Onesto, C., Shutes, A., Picard, V., Schweighoffer, F., and Der, C.J. (2008). Characterization of EHT 1864, a novel small molecule inhibitor of Rac family small GTPases. Methods Enzymol 439, 111-129.

Orth, J.D., and McNiven, M.A. (2006). Get off my back! Rapid receptor internalization through circular dorsal ruffles. Cancer Res 66, 11094-11096.

Ory, S., and Gasman, S. (2011). Rho GTPases and exocytosis: what are the molecular links? Semin Cell Dev Biol 22, 27-32.

Parravicini, V., Gadina, M., Kovarova, M., Odom, S., Gonzalez-Espinosa, C., Furumoto, Y., Saitoh, S., Samelson, L.E., O'Shea, J.J., and Rivera, J. (2002). Fyn kinase initiates complementary signals required for IgE-dependent mast cell degranulation. Nat Immunol 3, 741-748.

Parsons, J.T., Horwitz, A.R., and Schwartz, M.A. (2010). Cell adhesion: integrating cytoskeletal dynamics and cellular tension. Nat Rev Mol Cell Biol 11, 633-643.

Passante, E., and Frankish, N. (2009). The RBL-2H3 cell line: its provenance and suitability as a model for the mast cell. Inflamm Res 58, 737-745.

Peters, C., and Mayer, A. (1998). Ca2+/calmodulin signals the completion of docking and triggers a late step of vacuole fusion. Nature 396, 575-580.

Pfeffer, S.R. (1999). Transport-vesicle targeting: tethers before SNAREs. Nat Cell Biol 1, E17-22.

Pfeiffer, J.R., Seagrave, J.C., Davis, B.H., Deanin, G.G., and Oliver, J.M. (1985). Membrane and cytoskeletal changes associated with IgE-mediated serotonin release from rat basophilic leukemia cells. J Cell Biol 101, 2145-2155.

Piper, P.J., and Seale, J.P. (1979). Non-immunological release of slow-reacting substance from guinea-pig lungs. Br J Pharmacol 67, 67-72.

Pollard, T.D., and Borisy, G.G. (2003). Cellular motility driven by assembly and disassembly of actin filaments. Cell 112, 453-465.

Pujol, C., and Bliska, J.B. (2005). Turning Yersinia pathogenesis outside in: subversion of macrophage function by intracellular yersiniae. Clin Immunol 114, 216-226.

Puri, N., and Roche, P.A. (2008). Mast cells possess distinct secretory granule subsets whose exocytosis is regulated by different SNARE isoforms. Proc Natl Acad Sci U S A 105, 2580-2585.

Repke, H., and Bienert, M. (1987). Mast cell activation--a receptor-independent mode of substance P action? FEBS Lett 221, 236-240.

Ridley, A.J. (2001). Rho family proteins: coordinating cell responses. Trends Cell Biol 11, 471-477.

Riedl, J., Crevenna, A.H., Kessenbrock, K., Yu, J.H., Neukirchen, D., Bista, M., Bradke, F., Jenne, D., Holak, T.A., Werb, Z., et al. (2008). Lifeact: a versatile marker to visualize F-actin. Nat Methods 5, 605-607.

Roberts, A.W., Kim, C., Zhen, L., Lowe, J.B., Kapur, R., Petryniak, B., Spaetti, A., Pollock, J.D., Borneo, J.B., Bradford, G.B., et al. (1999). Deficiency of the hematopoietic cell-specific Rho family GTPase Rac2 is characterized by abnormalities in neutrophil function and host defense. Immunity 10, 183-196.

Rogers, T.B., Inesi, G., Wade, R., and Lederer, W.J. (1995). Use of thapsigargin to study Ca2+ homeostasis in cardiac cells. Biosci Rep 15, 341-349.

Rottem, M., Goff, J.P., Albert, J.P., and Metcalfe, D.D. (1993). The effects of stem cell factor on the ultrastructure of Fc epsilon RI+ cells developing in IL-3-dependent murine bone marrow-derived cell cultures. J Immunol 151, 4950-4963.

Schwartz, L.B., Austen, K.F., and Wasserman, S.I. (1979). Immunologic release of beta-hexosaminidase and beta-glucuronidase from purified rat serosal mast cells. J Immunol 123, 1445-1450.

Seldin, D.C., Adelman, S., Austen, K.F., Stevens, R.L., Hein, A., Caulfield, J.P., and Woodbury, R.G. (1985). Homology of the rat basophilic leukemia cell and the rat mucosal mast cell. Proc Natl Acad Sci U S A 82, 3871-3875.

Shutes, A., Onesto, C., Picard, V., Leblond, B., Schweighoffer, F., and Der, C.J. (2007). Specificity and mechanism of action of EHT 1864, a novel small molecule inhibitor of Rac family small GTPases. J Biol Chem 282, 35666-35678.

Stevens, R.L., and Austen, K.F. (1989). Recent advances in the cellular and molecular biology of mast cells. Immunol Today 10, 381-386.

Stipp, C.S., Kolesnikova, T.V., and Hemler, M.E. (2003). Functional domains in tetraspanin proteins. Trends Biochem Sci 28, 106-112.

Suetsugu, S., Yamazaki, D., Kurisu, S., and Takenawa, T. (2003). Differential roles of WAVE1 and WAVE2 in dorsal and peripheral ruffle formation for fibroblast cell migration. Dev Cell 5, 595-609.

Sugihara, K., Nakatsuji, N., Nakamura, K., Nakao, K., Hashimoto, R., Otani, H., Sakagami, H., Kondo, H., Nozawa, S., Aiba, A., et al. (1998). Rac1 is required for the formation of three germ layers during gastrulation. Oncogene 17, 3427-3433.

Sun, C.X., Magalhaes, M.A., and Glogauer, M. (2007). Rac1 and Rac2 differentially regulate actin free barbed end formation downstream of the fMLP receptor. J Cell Biol 179, 239-245.

Suzuki, R., Liu, X., Olivera, A., Aguiniga, L., Yamashita, Y., Blank, U., Ambudkar, I., and Rivera, J. (2010). Loss of TRPC1-mediated Ca2+ influx contributes to impaired degranulation in Fyn-deficient mouse bone marrow-derived mast cells. J Leukoc Biol 88, 863-875.

Symons, M., and Rusk, N. (2003). Control of vesicular trafficking by Rho GTPases. Curr Biol 13, R409-418.

Tapon, N., and Hall, A. (1997). Rho, Rac and Cdc42 GTPases regulate the organization of the actin cytoskeleton. Curr Opin Cell Biol 9, 86-92.

Thapar, R., Moore, C.D., and Campbell, S.L. (2003). Backbone 1H, 13C, and 15N resonance assignments for the 21 kDa GTPase Rac1 complexed to GDP and Mg2+. J Biomol NMR 27, 87-88.

Tsai, M., Shih, L.S., Newlands, G.F., Takeishi, T., Langley, K.E., Zsebo, K.M., Miller, H.R., Geissler, E.N., and Galli, S.J. (1991). The rat c-kit ligand, stem cell factor, induces the development of connective tissue-type and mucosal mast cells in vivo. Analysis by anatomical distribution, histochemistry, and protease phenotype. J Exp Med 174, 125-131.

Tsicopoulos, A., Hamid, Q., Haczku, A., Jacobson, M.R., Durham, S.R., North, J., Barkans, J., Corrigan, C.J., Meng, Q., Moqbel, R., et al. (1994). Kinetics of cell infiltration and cytokine messenger RNA expression after intradermal challenge with allergen and tuberculin in the same atopic individuals. J Allergy Clin Immunol 94, 764-772.

Ungermann, C., Sato, K., and Wickner, W. (1998). Defining the functions of trans-SNARE pairs. Nature 396, 543-548.

Vig, M., DeHaven, W.I., Bird, G.S., Billingsley, J.M., Wang, H., Rao, P.E., Hutchings, A.B., Jouvin, M.H., Putney, J.W., and Kinet, J.P. (2008). Defective mast cell effector functions in mice lacking the CRACM1 pore subunit of store-operated calcium release-activated calcium channels. Nat Immunol 9, 89-96.

Vincent-Schneider, H., Thery, C., Mazzeo, D., Tenza, D., Raposo, G., and Bonnerot, C. (2001). Secretory granules of mast cells accumulate mature and immature MHC class II molecules. J Cell Sci 114, 323-334.

Wedemeyer, J., Tsai, M., and Galli, S.J. (2000). Roles of mast cells and basophils in innate and acquired immunity. Curr Opin Immunol 12, 624-631.

Wickner, W. (2002). Yeast vacuoles and membrane fusion pathways. EMBO J 21, 1241-1247.

Williams, R.M., Shear, J.B., Zipfel, W.R., Maiti, S., and Webb, W.W. (1999). Mucosal mast cell secretion processes imaged using three-photon microscopy of 5-hydroxytryptamine autofluorescence. Biophys J 76, 1835-1846.

Williams, R.M., and Webb, W.W. (2000). Single granule pH cycling in antigen-induced mast cell secretion. J Cell Sci 113 Pt 21, 3839-3850.

Yamazaki, D., Suetsugu, S., Miki, H., Kataoka, Y., Nishikawa, S., Fujiwara, T., Yoshida, N., and Takenawa, T. (2003). WAVE2 is required for directed cell migration and cardiovascular development. Nature 424, 452-456.

Yan, C., Martinez-Quiles, N., Eden, S., Shibata, T., Takeshima, F., Shinkura, R., Fujiwara, Y., Bronson, R., Snapper, S.B., Kirschner, M.W., et al. (2003). WAVE2 deficiency reveals distinct roles in embryogenesis and Rac-mediated actin-based motility. EMBO J 22, 3602-3612.

Yang, F.C., Kapur, R., King, A.J., Tao, W., Kim, C., Borneo, J., Breese, R., Marshall, M., Dinauer, M.C., and Williams, D.A. (2000). Rac2 stimulates Akt activation affecting BAD/Bcl-XL expression while mediating survival and actin function in primary mast cells. Immunity 12, 557-568.

Zerial, M., and McBride, H. (2001). Rab proteins as membrane organizers. Nat Rev Mol Cell Biol 2, 107-117.

Zigmond, S.H. (2004). Formin-induced nucleation of actin filaments. Curr Opin Cell Biol 16, 99-105.

Zink, T., Deng, Z., Chen, H., Yu, L., Liu, F.T., and Liu, G.Y. (2008). High-resolution three-dimensional imaging of the rich membrane structures of bone marrow-derived mast cells. Ultramicroscopy 109, 22-31.